NUCLEAR PHYSICS INSTITUTE OF THE SIBERIAN
SECTION OF THE USSR ACADEMY OF SCIENCES

Report IYaF 40-70

IRON-FREE AND IRON-PLUS CONDUCTOR MAGNETS AND LENSES WITH THICK WINDINGS FOR ACCELERATORS

V.G. Davidovskij

Novosibirsk 1970

Translated at CERN by B. Hodge
(Original: Russian)
Not revised by the Translation Service

(CERN Trans. 71-35)

Geneva
October 1971

BH/st
15.2.1971

V.G. Davidovskij

IRONLESS AND IRON-CONDUCTOR MAGNETS AND LENSES WITH THICK WINDINGS FOR ACCELERATORS

A b s t r a c t

The author examines the formation of stationary two-dimensional magnetic fields by ironless and iron-conductor magnets and lenses with windings of an arbitrary thickness which closely surround the domain of formation. The current density remains constant over the cross-section of the winding. Analytical expressions are found for the magnetic fields in the metal of the windings of magnets with a circular and elliptical domain, according to a given field produced in the domain. A numerical solution of boundary equations at the outer boundary of the conductors of the winding enables the shape of this boundary to be determined. A detailed examination is made of the case of iron-free (shielded or non-shielded by iron or current) and iron-conductor magnets.

The proposed method is applied to the calculation of iron-free and iron-conductor magnets with a circular domain. The author gives the results of calculations which provide a picture of the shapes of windings of various "thicknesses", the size and distribution of the field energy in the case of

magnets producing dipole and quadrupole fields and constant gradient fields with horizontal and vertical planes of symmetry.

A calculation method is indicated for magnets with a rectangular domain and the methods of producing quadrupole fields are reviewed.

List of Contents

		Page
	Introduction	1
I.	Forming two-dimensional magnetic fields by the iron-free method in a circular domain	6
	§ 1. Formulation of the problem and breakdown of the fields	6
	§ 2. The "thin" winding of "iron-free" unshielded magnets	8
	§ 3. The "thick" winding of "iron-free" unshielded magnets	11
	§ 4. Shielding	15
	4.1. Current shielding	17
	4.2. Iron shielding	21
	§ 5. Equations for "thin" windings and nodal points for the superposition of dipole and quadrupole fields	23
	§ 6. "Centres" of the windings, and maximum possible fields that can be obtained for a given current density	28
	§ 7. Numerical method for solving "thick" winding equations	30
II.	Results of a numerical calculation for a circular domain	33
	§ 1. Iron-free unshielded magnets	
	1.1. Dipole field	34
	1.2. Quadrupole field	36
	1.3. Constant gradient field with a horizontal plane of symmetry	38
	1.4. Constant gradient field with a vertical plane of symmetry	40

		page
§ 2.	Iron-free magnets with a co-axial iron cylinder as shielding	42
	2.1. Dipole field	42
	2.2. Quadrupole field	47
§ 3.	Iron-free magnets with co-axial current shielding	51
	3.1. Dipole field	51
	3.2. Quadrupole field	55
§ 4.	Points of the winding where the maximum field value is achieved	60
III.	Forming two-dimensional magnetic fields by the iron-free method in the elliptical domain	62
§ 1.	Formulation of the problem and breakdown of the fields	63
§ 2.	The "thin" winding of unshielded magnets	65
§ 3.	The "thick" winding of unshielded magnets	68
§ 4.	Shielding	72
	4.1. Current shielding	73
	4.2. Iron shielding	79
§ 5.	Equations for "thin" windings and nodal points for the superposition of dipole and quadrupole fields	82
§ 6.	The position of the centre of the windings and maximum achievable fields for a given current density	88
IV.	The rectangular domain	94
V.	Iron-conductor magnets	99
§ 1.	Iron-conductor magnets for producing fields in a circular domain	100
	1.1. Dipole field	102
	1.2. Quadrupole field	103

		page
	1.3. Constant gradient field with a horizontal plane of symmetry	104
§ 2.	Iron-conductor magnets for producing fields in an elliptical domain	107
§ 3.	Iron-conductor magnets for producing a quadrupole field in a rectangular domain	110
	3.1. The Hand-Panofsky lattice	110
	3.2. The iron-conductor surface, and three types of lenses	115
	3.3. The Lublov-Morpurgo-Steffen lens	118
	3.4. The Blewett lens	121
	3.5. The Hand-Panofsky lens	122
	3.6. Comparison of iron-conductor lenses with rectangular and circular domains of formation	123
Appendix		127

N.B. For полн please read tot.
For экр please read shield.
For мет please read met.
For пр please read cond.
For нар please read ext.
For уз please read nod.

I N T R O D U C T I O N

In accelerator technology wide use is made of various types of two-dimensional magnetic fields*. The method by which fields are formed with a skin-layer /2/ are valid only if the duration of the field used is much shorter than that of substantial field penetration into the metal conductor. The following methods may be used for forming longer pulsed and time-constant magnetic fields of a given configuration:

1. The iron method: the field is formed by iron poles of the appropriate shape. The size of the field obtained is, in principle, restricted by the requirement that the iron must not be saturated.

---

* If we follow the accepted terminology /1/, we shall refer to a field which is constant in the domain of formation as a "dipole" field, since when this type of field is formed inside the circle of the "thin" winding, the field outside is a dipole. We shall refer to the super - position of a dipole and quadrupole field as:
1) A field having a constant gradient with a horizontal plane of symmetry, if the axes of the quadrupole field are at an angle of 45° to the dipole field (fields of this type are used in cyclic accelerator magnets, where the magnet system is of the non-separated function type),
2) a field having a constant gradient with a vertical plane of symmetry if one of the axes of the quadrupole field is oriented along the dipole field.

2. The iron-free method: the field is formed by a certain distribution of the currents in space. The size of the field obtained when using a winding made of a normal conductor, is limited for purely technical reasons: the power of the supply sources, the possibility of cooling, mechanical rigidity, etc. Iron is sometimes used for the additional purpose of screening and reducing the overall energy of the magnetic field produced. In examining these systems we shall confine ourselves to those cases in which the iron is not saturated, i.e. when $\mu = \infty$.

3. The iron-conductor method: the field is formed by both the shape of the iron and a certain arrangement of the conductors in space. The size of the field obtained is, generally speaking, also restricted by the requirement that the iron should not be saturated.

The above sub-divisions are not entirely accurate. For example, if the iron screen of an iron-free magnet is close to the winding which forms the field, then it participates to a marked degree in the forming of the field; this type of magnet can also be assimilated to the iron-conductor type. In order, therefore, to make our terminology precise we shall use the term "iron-conductor magnets" only for those in which the iron and conductor have sections of a common boundary. Magnets having an indeterminate pole /3/ for the circular domain are those of the iron-conductor type in the infinitely-"thin" winding range.

The iron method is the one that is most widely used at present in accelerator technology. Even if the normal conductors are used, it is quite possible to produce iron-free magnets for accelerators, which have magnetic fields several times greater than the field in the iron type magnets. In view of the development of superconductor technology and the trend toward very high energy accelerators, the manufacture of iron-free magnets has become a matter of special interest. A detailed study was made in /4,5,6,7/ of the forming of the magnetic field in the circular and elliptical domains by the "iron-free" method by using an infinitely-thin current layer on the surface of the domain. In practice, however, even when super-conductors are used, the creation of strong magnetic fields can be achieved only by using coils of a finite thickness. In /8/ a winding having a finite thickness for the forming of the dipole field in a circle was considered to be the superposition of a number of infinitely thin windings /4,5/, of increasing radii. In a winding of this type, however, the current density varies with the azimuth. From the design point of view, the use of varying current densities is not always convenient. In the case, however, of windings with a finite thickness and a constant current density the solutions known relate only to certain specific cases . In this way, a dipole field is formed, for example, in the elliptical area produced when two long circular parallel conductors are made to overlap and in which currents of the same density flow in

opposite directions. In a similar way, if we use long conductors which are not circular but elliptical in shape and their cross-sections are mutually oriented in the appropriate manner, a dipole or quadrupole field, or a constant gradient field with a horizontal plane of symmetry will form in the area of the overlap /7,9/. This was, in fact, the method used when designing the Australian iron-free synchrotron /10/. The shapes of the ellipses formed, however, are not suitable for practical use and are not economical with regard to utilization of the magnetic field produced, which is particularly important in the case of pulsed magnetic systems.

Basically, the present work gives the results of calculations for iron-free and iron-conductor magnets, which form a given magnetic field, constant in time, in a cylindrical domain by means of windings in which the current density remains at a constant value. As each actual design is only an approximation to an ideal theoretical design, and the purpose of the present work was to obtain a general picture, we did not aim at a high degree of numerical accuracy. The shapes obtained for the windings can, from the design point of view, sometimes be approximated to step functions which vary with the azimuth, as has been proposed in /5,7/ for thin windings. For the sake of completeness, we have given the calculation methods for iron-free magnets used for producing a field in the elliptical and rectangular domains and for iron-conductor magnets used for the

production of a quadrupole field in a rectangular domain by means of windings which have a current density whose value remains constant.

The results obtained can be used also for magnetic fields which are variable in time, provided that the predominant currents in the windings vary slowly in comparison with the speeds at which the field is produced. To increase the speed at which the field is produced, reduce the field distortions which arise as a result, and reduce the dissipation of energy by Foucault currents, it is necessary to choose the appropriate combination and switching for the winding's conductors(as well as the normal choice of the correct grade of iron, if applicable); These questions, however, fall outside the scope of the present work.

1. FORMING TWO-DIMENSIONAL MAGNETIC FIELDS BY THE IRON-FREE METHOD IN A CIRCULAR DOMAIN

§1. Formulation of the Problem and Breakdown of the Fields

In a circular domain having a radius r_0 (fig. 1) a two-dimensional magnetic field $\vec{H}_0(r,\varphi)$ must be produced by means of infinitely long conductors, perpendicular to the plane of the circle and lying closely around it (this is the forming winding). A constant-density current j flows through the conductors, but its direction is dependent on the angle φ In this case, the current density in the cross-section of the winding is an alternating step-function $j(\varphi)$ of the angle φ . The problem is to determine $j(\varphi)$ and the external boundary of the winding $r(\varphi)$. By virtue of the linearity of the Maxwell equation with regard to field and current density, the amplitude of the field formed is proportional to the current density in the winding. In this document we shall consider the current density to have a specified fixed value.

It is also possible, of course, to pose the problem of when the external boundary of the conductors which produce a given field constitute the periphery, whilst the internal boundary of the conductors, and consequently the domains of formation, is determined as the problem is being solved. To this formulation of the problem correspond the shapes of conductor

given in /11/ for the case of the quadrupole field.

Let us break down the magnetic field formed in a circle and the corresponding vector magnetic potential into a series in multipoles:

$$H_{oz}(z,\varphi)=\sum_{n=1}^{\infty} b_n \left(\frac{z}{z_0}\right)^{n-1}\sin(n\varphi+\psi_n),$$
$$H_{o\varphi}(z,\varphi)=\sum_{n=1}^{\infty} b_n \left(\frac{z}{z_0}\right)^{n-1}\cos(n\varphi+\psi_n), \qquad (1)$$
$$A_o(z,\varphi)=\sum_{n=1}^{\infty} \frac{b_n z_0}{n}\left(\frac{z}{z_0}\right)^{n}\cos(n\varphi+\psi_n).$$

In practice, the formed field is usually already set in the form of this expansion. Let b_A be any non-vanishing expansion co-efficient (1); it is preferable that this should be the co-efficient of the most significant multipole in the formed field and we shall place it behind the sign of the sums in (1). We shall consider that the value b_A characterizes the amplitude of the formed field, whilst the combination of the relations of the co-efficients of all the other multipoles to b_A (b_K/b_A) is its configuration. It is clearly important in practice that the field should fall off outside the system as soon as possible. We shall therefore consider only the case in which the integral of the current density over the total cross-section of the winding is 0, i.e. the case in which the total forward and return currents in the cross-section are equal. Then the

expansion of the vector potential outside the system in multipoles will not contain a term with $\ln r$, whilst the expansion of the magnetic field outside the system will not contain a term which is proportional to $1/r$:

$$A_H(r,\varphi) = -\sum_{n=1}^{\infty} \frac{d_n}{n} \cdot \left(\frac{r_0^{n+1}}{r^n}\right) \cdot \cos(n\varphi + \psi_n),$$
$$H_{Hr}(r,\varphi) = \sum_{n=1}^{\infty} d_n \cdot \left(\frac{r_0}{r}\right)^n \cdot \sin(n\varphi + \psi_n), \qquad (2)$$
$$H_{H\varphi}(r,\varphi) = \sum_{n=1}^{\infty} d_n \cdot \left(\frac{r_0}{r}\right)^n \cdot \cos(n\varphi + \psi_n).$$

We shall call the function $\Delta(\varphi) = r(\varphi) - r_0$, where $r(\varphi)$ is the external boundary of the winding, the thickness function of the winding, and similarly $\Delta(\varphi)/r_0$, the relative thickness function. If $\Delta(\varphi) \ll r_0$ for all φ , we shall consider the winding "thin", and if this condition is not fulfilled we shall consider the winding "thick". Let us first examine the case of the "thin" winding.

§2. The "thin" winding of"iron-free" unshielded magnets

The "thin" winding can be considered as a current layer, and the boundary conditions on the boundary of the domain of

formation, i.e. on the periphery of the radius r_0 , are of the form:

$$H_{Hz}(r_0,\varphi) = H_{0z}(r_0,\varphi),$$
$$H_{H\varphi}(r_0,\varphi) - H_{0\varphi}(r_0,\varphi) = \frac{4\pi}{c} j(\varphi)\cdot\Delta(\varphi). \qquad (3)$$

By using expansions (1) and (2) we obtain:

$$d_n = b_n ,$$
$$-\frac{j(\varphi)}{j}\cdot\frac{\Delta(\varphi)}{r_0} = \frac{1}{\frac{2\pi}{c} j r_0}\cdot\sum_{n=1}^{\infty} b_n\cdot\cos(n\varphi+\psi_n) = \qquad (4)$$
$$= \frac{b_A}{\frac{2\pi}{c} j r_0}\cdot\sum_{n=1}^{\infty}\frac{b_n}{b_A}\cdot\cos(n\varphi+\psi_n).$$

This is the equation for the "thin" winding according to the known combination of coefficients b_n it defines the function $j(\varphi)/j$, whilst for a given j it also defines the thickness function of the winding $\Delta(\varphi)$, i.e. the shape of the winding. The function $j(\varphi)/j$ changes its sign at those points of φ , where the sum in the first part of (4) changes sign; at these points $\Delta(\varphi) = 0$ and, as can be seen from (1) and (4), $H_{0\varphi}(r,\varphi)$ also changes sign. Below, we shall refer to these points as "nodal". We determine the position (φ_{yz}) of these points on the circumference r_0 by equating the sum in (4) to 0, on the condition that it changes sign when it passes through this point. Consequently their

position is determined exclusively by the configuration of the field formed and does not depend on its amplitude.

It follows from (4) that the total thickness-function of the winding is the sum of individual multipole"thicknesses", the amplitude of the relative "multipole thickness" of the number n being

$$t_n = b_n / \left(\frac{2\pi}{c} j r_0\right).$$

Thus, for example, the amplitude of the relative dipole thickness is $H_0 / \left(\frac{2\pi}{c} j r_0\right)$, the amplitude of the relative quadripole is $- \nabla H / \left(\frac{2\pi}{c} j\right)$. The required conditions for the "thinness" of the winding $(\Delta(\varphi) \ll r_0)$ are $t_n \ll 1$ for all multipoles of the expansion (1); these conditions are sufficient if the formed field contains a finite number of multipoles. For a given field configuration, i.e. for a given combination of b_K / b_A ($K = 1,2,\ldots$), the value $\alpha = b_A / \left(\frac{2\pi}{c} j r_0\right)$ - we shall call it the thickness parameter - determines unambiguously the relative thickness function $\Delta(\varphi)/r_0$, and consequently we will write the latter as a function of α, φ: $\Delta(\alpha, \varphi)/r_0$. $(\Delta(\alpha, \varphi) \sim \alpha)$ As the multipole co-efficient chosen as the amplitude is more substantial in the formed field, it is natural to consider that the size of all b_K / b_A does not exceed unity, in order of magnitude. Then, as can be seen from (4), the "thinness" condition of the winding is $\alpha \ll 1$. In the case, however, of forming the field of a pure multipole, the thickness parameter α is simply the amplitude of the relative thickness

function.

For example, for a dipole (fig. 2a):

$$-\frac{j(\varphi)}{j}\cdot\frac{\Delta(\alpha,\varphi)}{r_0}=\alpha\cdot\cos(\varphi+\psi_1),\quad\text{where}\quad\alpha=H_0\Big/\left(\frac{2\pi}{c}jr_0\right).$$

for a quadrupole (fig.2e):

$$-\frac{j(\varphi)}{j}\cdot\frac{\Delta(\alpha,\varphi)}{r_0}=\alpha\cdot\cos(2\varphi+\psi_2),\ \text{where}\ \alpha=\nabla H\Big/\left(\frac{2\pi}{c}j\right).$$

for constant gradient fields

$$-\frac{j(\varphi)}{j}\cdot\frac{\Delta(\alpha,\varphi)}{r_0}=\alpha\cdot\left(\cos(\varphi+\psi_1)+\frac{r_0\nabla H}{H_0}\cdot\cos(2\varphi+\psi_1+\psi_2)\right).$$

where $\alpha=H_0\Big/\left(\frac{2\pi}{c}jr_0\right)$

$\psi_1=0$, $\psi_2=0$ - with a horizontal plane of symmetry (fig. 2 b,c,d)

$\psi_1=0$, $\psi_2=\pi/2$ - with a vertical plane of symmetry (fig. 2 B,C,D).

§3. The "Thick" winding of iron-free non-shielded magnets.

On the basis of the results given in paragraph 2 the following conclusions can be drawm:

1. The external limits of windings which, in a circular domain with a radius r_0 form a two-dimensional field of a given configuration, form a single-parameter family of lines

$$r(\alpha, \varphi)/r_0 = 1 + \Delta(\alpha, \varphi)/r_0$$

having nodal points which lie on the boundary of the domain of formation, i.e. on the circumference of r_0 ;

2. The parameter of the family is the parameter of the winding thickness $\alpha = b_A/\left(\frac{2\pi}{C} j r_0\right)$, where b_A is the co-efficient of the multipole in the expansion (1), chosen as the field amplitude;

3. The position of the nodal points of φ_{yz} on the circumference of r_0 is determined exclusively by the configuration of the field formed;

4. The thickness-function $\Delta(\alpha, \varphi)$ is proportional to α

These conclusions are shown to be correct only for the case of the "thin" winding ($\Delta(\alpha,\varphi) \ll r_0$ i.e. $\alpha \ll 1$). As the thickness parameter α increases, the winding finally ceases to be thin, and $\Delta(\alpha, \varphi)$ becomes a non-linear function of α , i.e. conclusion 4 is violated. We consider, however, that conclusions 1, 2 and 3 are correct for windings of any thickness, i.e. for any permissible sizes of the parameter α . When α varies within any permissible limits, the thickness function of the winding $\Delta(\alpha, \varphi)$ varies, whilst the

nodal points φ_{ij} remain stationary; their position is determined by the field configuration and does not depend on its amplitude, i.e. the parameter α . This is confirmed by considerations of symmetry in those cases where the formed field is a pure multipole (fig. 2a,e) or such a superposition of multipoles that all the nodal points coincide with the nodal points of the multipole of the lowest order of this superposition (fig. 2B, C). The grounds which support this in the general case will be given below. Consequently, we may find the position of the nodal points from the equation (4) for the "thin" winding.

The nodal points break the winding down into a number of separate elementary parts, each of which has only one common nodal point with its neighbour. The current density is constant over the entire cross-section of the winding ($|j(\varphi)| = j = \text{const.}$), but changes its sign as it passes through each nodal point. In other words, in each two neighbouring elementary parts of the winding, currents having an identical density j flow in opposite directions. Consequently, the vector potential of the magnetic field inside each elementary part of the winding is described by the equation (the sign of $j(\varphi)$ is not of any consequence and we shall therefore simply write j):

$$\Delta A_{mer}(z, \varphi) = -\frac{4\pi}{c} j.$$

It can easily be seen that the potential

$$A_{мет}(r,\varphi)=A_0(r,\varphi)-\frac{\pi}{c}j\left[r^2-r_0^2-2r_0^2\ln(r/r_0)\right], \quad (5)$$

where $A_0(r,\varphi)$ - the potential of the field formed in the circle $\vec{H_0}(r,\varphi)$, satisfies equation (7). The potential $A_{мет}(r,\varphi)$ corresponds to the field $\vec{H}_{мет}(r,\varphi)$:

$$\begin{aligned} H_{мет\,r}(r,\varphi) &= H_{0r}(r,\varphi), \\ H_{мет\,\varphi}(r,\varphi) &= H_{0\varphi}(r,\varphi)+\frac{2\pi}{c}j\left(r-\frac{r_0^2}{r}\right). \end{aligned} \quad (6)$$

It is obvious that $\vec{H}_{мет}(r_0,\varphi)=\vec{H}_{0r}(r,\varphi)$

i.e. the boundary conditions on the boundary of the domain of formation and the metal of the elementary part of the winding under consideration (the corresponding section of the circumference of r_0) are satisfied. Consequently $A_{мет}(r,\varphi)$ and $\vec{H}_{мет}(r,\varphi)$ are the desired vector potential and magnetic field in the metal of the conductor. As the elementary section of the winding under consideration is in a way separated and during the transition from one such part to another there is only a change in the sign of $j(\varphi)$ (i.e. the sign in front of j) and in the domain of the change in r and φ , we know the potential and field throughout the winding. It follows from expressions (5,6) that the field configuration in the metal of the winding is determined entirely by the configuration of the formed field $\vec{H}_0(r,\varphi)$.

Using (2) and (6) we shall write out the boundary conditions on the external boundary of the winding $r(\varphi)$:

$$H_{0r}(r(\varphi),\varphi)=\sum_{n=1}^{\infty}{}' a_n\left(\frac{r_0}{r(\varphi)}\right)^{n+1}\sin(n\varphi+\psi_n),$$

$$H_{0\varphi}(r(\varphi),\varphi)=-\sum_{n=1}^{\infty}{}' a_n\left(\frac{r_0}{r(\varphi)}\right)^{n+1}\cos(n\varphi+\psi_n)-\frac{2\pi}{c}j(\varphi)\left(r(\varphi)-\frac{r_0^2}{r(\varphi)}\right). \quad (7)$$

These are the equations for "thick" windings; they define the field outside the system (i.e. the combination of a_n and ψ_n) and the external boundary of the winding $r(\varphi)$. Within the limit of $r(\varphi)-r_0 \ll r_0$, expansion of the equations(7) results in the equation for a "thin winding" (4). In the case of the "thick" winding, a similar expansion can be made in the region of each nodal point, i.e. the equations of (7) in the vicinity of the nodal points coincide formally with the equations for the "thin" winding, but the size of the thickness parameter is now arbitrary. Consequently the equation which determines the position of the nodal points of the "thick" windings corresponds with the similar equation for "thin" windings, and consequently the position of the nodal points does not depend on the "thickness" of the winding. This argument is applicable also when various types of screens are used and also when a field is formed in the elliptical domain.

§4. Shielding

It is, however clear that unshielded iron-free magnets are impractical to use because the magnetic fields extend beyond

the system. It is possible to shield the system by surrounding it either with iron shielding or by means of a special system for screening the currents -"current screening" - as was proposed in /5,6/ in the case of "thin" windings. Here, we shall consider only the case in which the inner boundary of the shielding (iron or current screening system) is a cylinder having a radius r_3, which is co-axial with the field-forming domain (fig. 3 and 4). We shall call the winding which directly surrounds the forming domain the forming winding. This is, of course, an arbitrary designation because if the shielding (current or iron) is close to the forming winding then it will make a substantial contribution to the field formed.

As in unshielded systems, when a shield is used it is important from the energy view-point that the field should fall off as quickly as possible in the gap between the forming winding and the shielding (current or iron). We shall therefore consider only those systems in which the integral of the current density over the total cross section of the forming winding is 0,(in the case of current shielding the requirement for a rapid fall-off in the field outside the system means that the integral of the current density of the shielding winding over its total cross section also becomes 0). In such systems the expansion of the vector potential of the magnetic field $A_{np}(r,\varphi)$ in the gap between the forming winding and the screen does not contain a term with $\ln r$, and correspondingly the expansion of the magnetic field $\vec{H}_{np}(r,\varphi)$ does not contain a term which

is proportional to $1/z$:

$$A_{np}(z,\varphi)=-\sum_{n=1}^{\infty}\left\{\frac{d_n}{n}\left(\frac{z_0^{n+1}}{z^n}\right)+\frac{c_n}{n}\left(\frac{z^n}{z_э^{n-1}}\right)\right\}\cos(n\varphi+\psi_n),$$

$$H_{np\,z}(z,\varphi)=\sum_{n=1}^{\infty}\left\{d_n\left(\frac{z_0}{z}\right)^{n+1}+c_n\left(\frac{z}{z_э}\right)^{n-1}\right\}\cdot\sin(n\varphi+\psi_n), \qquad (8)$$

$$H_{np\,\varphi}(z,\varphi)=\sum_{n=1}^{\infty}\left\{-d_n\left(\frac{z_0}{z}\right)^{n+1}+c_n\left(\frac{z}{z_э}\right)^{n-1}\right\}\cdot\cos(n\varphi+\psi_n).$$

Before we can write out the equations for the "thin" winding for a shielded system we must, as in the case of the unshielded systems, first find the elementary parts of the winding. We shall consequently commence the study by finding equations for the "thin" winding and determining the position of the nodal points.

4.1. Current Shielding

Figure 3 is a qualitative illustration of dipole and quadrupole magnets with current shielding.

We shall consider only the case which is of most practical interest, when there is no field outside the winding which provides the shielding, i.e. the case of total shielding.

Having considered the "thin" forming and screening

windings as current layers, we shall write the boundary conditions on these:

$$H_{np\,z}(r_0,\varphi) = H_{0z}(r_0,\varphi),$$
$$H_{np\,\varphi}(r_0,\varphi) - H_{0\varphi}(r_0,\varphi) = \frac{4\pi}{c} j(\varphi)\cdot\Delta(\alpha,\varphi),$$
$$H_{np\,z}(r_э,\varphi) = 0,$$
$$H_{np\,\varphi}(r_э,\varphi) = \frac{4\pi}{c} j_э(\varphi)\cdot\Delta_э(\alpha_э,\varphi)$$

where $\Delta(\alpha,\varphi) = r(\alpha,\varphi) - r_0$, $\Delta_э(\alpha_э,\varphi) = r_э(\alpha_э,\varphi) - r_э$,

$r(\alpha,\varphi)$ - is the external boundary of the forming winding,

$r_э(\alpha,\varphi)$ - is the external boundary of the shielding winding.

The conditions or the "thinness" of the windings are:
$\Delta(\alpha,\varphi)/r_0 \ll 1$, $\Delta_э(\alpha,\varphi) \ll 1$. By using the expansions of (1) and (8) we obtain:

$$c_n = -\frac{(r_0/r_э)^{n+1}}{1-(r_0/r_э)^{2n}}\cdot b_n, \quad d_n = \frac{b_n}{1-(r_0/r_э)^{2n}}.$$

and the equations for a "thin" winding:

$$-\frac{j(\varphi)}{j}\cdot\frac{\Delta(\alpha,\varphi)}{r_0} = \frac{1}{\frac{2\pi}{c} j r_0}\cdot\sum_{n=1}^{\infty}\frac{1}{1-(r_0/r_э)^{2n}} b_n\cos(n\varphi+\psi_n),$$
$$\frac{j_э(\varphi)}{j_э 0}\cdot\frac{\Delta_э(\alpha_э,\varphi)}{r_0} = \frac{1}{\frac{2\pi}{c} j_э r_0}\cdot\sum_{n=1}^{\infty}\frac{(r_0/r_э)^{n+1}}{1-(r_0/r_э)^{2n}} b_n\cos(n\varphi+\psi_n). \qquad (9)$$

where b_n are the co-efficients for the multipoles of the field formed in the circle $\vec{H}_0(r_0, \varphi)$. These equations for a given combination of co-efficients of b_n determine the alternating step-functions $j(\varphi)/j$ and $j_э(\varphi)/j_э$ and if j and $j_э$ are given, also the thickness functions of the forming $\Delta(\alpha, \varphi)$ and shielding $\Delta_э(\alpha, \varphi)$ windings, and therefore their shape ("thin" windings). Having reduced the right-hand members of these equations to zero, we determine the position of the nodal points. Consequently we now know how the forming and shielding windings of an arbitrary thickness are broken down into their elementary parts. Now we can turn to an examination of "thick" windings.

The magnetic field $\vec{H}_{нем}(r, \varphi)$ in the metal of a random elementary part of the forming winding is determined as before by the expression (6) and the field $H_{нем\,э}(r, \varphi)$ in the metal of the elementary part of a shielding winding is similarly determined by the expressions:

$$\begin{aligned} H_{нем\,э,r}(r, \varphi) &= H_{пр,r}(r, \varphi), \\ H_{нем\,э,\varphi}(r, \varphi) &= H_{пр\varphi}(r, \varphi) + \frac{2\pi}{c} j_э(\varphi) \cdot \left(r - \frac{r_э^2}{2r}\right). \end{aligned} \tag{10}$$

The boundary conditions on the external boundaries of the forming $r(\varphi)$ and shielding $r_э(\varphi)$ windings are of the form:

$$\vec{H}_{нем}(r(\varphi), \varphi) = \vec{H}_{пр}(r(\varphi), \varphi),$$
$$\vec{H}_{нем\,э}(r_э(\varphi), \varphi) = 0.$$

Using expressions (1), (6), (8) and (10) we re-write these equations in the following form:

$$H_{0z}(z(\varphi),\varphi)=\sum_{n=1}^{\infty}\left\{d_n\cdot\left(\frac{z_0}{z(\varphi)}\right)^{n+1}+c_n\cdot\left(\frac{z(\varphi)}{z_э}\right)^{n-1}\right\}\cdot\sin(n\varphi+\psi_n), \tag{11.1.}$$

$$H_{0\varphi}(z(\varphi),\varphi)+\frac{2\pi}{c}j(\varphi)\cdot\left(z(\varphi)-\frac{z_0^2}{z(\varphi)}\right)= \tag{11.2.}$$

$$=\sum_{n=1}^{\infty}\left\{-d_n\left(\frac{z_0}{z(\varphi)}\right)^{n+1}+c_n\cdot\left(\frac{z(\varphi)}{z_э}\right)^{n-1}\right\}\cdot\cos(n\varphi+\psi_n),$$

$$0=\sum_{n=1}^{\infty}\left\{d_n\cdot\left(\frac{z_0}{z_э(\varphi)}\right)^{n+1}+c_n\cdot\left(\frac{z_э(\varphi)}{z_э}\right)^{n-1}\right\}\cdot\sin(n\varphi+\psi_n), \tag{11.3.}$$

$$\frac{2\pi}{c}j_э(\varphi)\cdot\left(z_э(\varphi)-\frac{z_{0э}^2}{z_э(\varphi)}\right)= \tag{11.4.}$$

$$=\sum_{n=1}^{\infty}\left\{-d_n\cdot\left(\frac{z_0}{z_э(\varphi)}\right)^{n+1}+c_n\left(\frac{z_э(\varphi)}{z_э}\right)^{n-1}\right\}.$$

These are the equations for the "thick" windings of iron-free magnets with current screening; they determine the field in the gap between the forming and shielding windings (i.e. the combination of c_n, d_n, ψ_n) and the external boundaries of the forming winding $z(\varphi)$ and of the shielding winding $z_э(\varphi)$. In the limits of $z(\varphi)-z_0 \ll z_0$ and $z_э(\varphi)-z_э \ll z_0$ the equations of (11) become equations for "thin" windings (9).

4.2. Iron Shielding

Figure 4 gives a qualitative illustration of a dipole and quadrupole magnet with iron shielding. We shall consider the magnetic permeability of the screen to be infinite ($\mu = \infty$). We shall write the boundary conditions on a "thin" forming winding and on iron shielding as follows:-

$$H_{np\,z}(z_0,\varphi) = H_{oz}(z_0,\varphi),$$
$$H_{np\,\varphi}(z_0,\varphi) - H_{o\varphi}(z_0,\varphi) = \frac{4\pi}{c} j(\varphi)\cdot\Delta(\alpha,\varphi),$$
$$H_{np\,\varphi}(z_э,\varphi) = 0$$

where $\Delta(\alpha,\varphi) = z(\alpha,\varphi) - z_0$, $z(\varphi)$ is the external boundary of the forming winding. The condition of the "thinness" of the winding is: $\Delta(\alpha,\varphi)/z_0 \ll 1$.

Using expansions (1) and (8) we obtain

$$c_n = \frac{(z_0/z_э)^{n+1}}{1+(z_0/z_э)^{2n}}\cdot b_n, \quad d_n = \frac{1}{1+(z_0/z_э)^{2n}}\cdot b_n.$$

and the equation for a "thin" winding;

$$-\frac{j(\varphi)}{j}\cdot\frac{\Delta(\alpha,\varphi)}{z_0} = \frac{1}{\frac{2\pi}{c} j z_0}\cdot\sum_{n=1}^{\infty}\frac{b_n}{1+(z_0/z_э)^{2n}}\cos(n\varphi+\psi_n) \qquad (12)$$

Having reduced to zero the right-hand side of this equation we determine the position of the nodal points. Consequently, we know how the forming winding of an arbitrary thickness is broken down into its elementary parts. We can now proceed to examine the "thick" winding.

The magnetic field $\vec{H}_{мет}(z, \varphi)$ in the metal of a random elementary part of a forming winding is determined as before by the equations of (6). The boundary conditions on the external boundary of the forming winding $z(\varphi)$ and on the boundary of the iron shielding $z_э$ are of the form:

$$\vec{H}_{мет}(z(\varphi), \varphi) = \vec{H}_{пр}(z(\varphi), \varphi),$$

$$H_{пр, \varphi}(z_э, \varphi) = 0.$$

By using expressions (6) and (8) we obtain

$$c_n = d_n \cdot (z_0/z_э)^{n+1}$$

$$H_{oz}(z(\varphi), \varphi) = \sum_{n=1}^{\infty} d_n \{(z_0/z(\varphi))^{n+1} + (z_0/z_э)^{2n} \cdot (z(\varphi)/z_0)^{n-1}\} \cdot \sin(n\varphi + \psi_n). \quad (13)$$

$$H_{o\varphi}(z(\varphi), \varphi) + \frac{2\pi}{c} j(\varphi) \cdot (z(\varphi) - z_0^2/z(\varphi)) =$$

$$= \sum_{n=1}^{\infty} d_n \cdot \{-(z_0/z(\varphi))^{n+1} + (z_0/z_э)^{2n} \cdot (z(\varphi)/z_0)^{n-1}\} \cos(n\varphi + \psi_n).$$

These are the equations for "thick" windings of iron-free magnets with iron shielding, they determine the field between the forming winding and the iron shielding (the combination of d_n) and the external boundaries of the forming winding $z(\varphi)$. In the limits of $z(\varphi) - z_0 << z_0$, the equations of (13) become the equation for a "thin" winding (12).

§ 5. Equations for "thin" windings and nodal points for the superposition of dipole and quadrupole fields.

Let us consider the equations for "thin" windings and determine the positions of the nodal points of iron-free magnets which produce in a circle a magnetic field of $\vec{H}_0(z, \varphi)$ with the components:

$$H_{0z}(z,\varphi) = H_0 \sin\varphi + z\nabla H \cdot \sin z(2\varphi + \psi),$$
$$H_{0\varphi}(z,\varphi) = H_0 \cos\varphi + z\nabla H \cdot \cos(2\varphi + \psi) \qquad (14)$$

and with a potential

$$A = -H_{0z}\cos\varphi - 0.5\, z^2\, \nabla H \cdot \cos(2\varphi + \psi).$$

A field of this type contains, as specific cases, the fields which are the most frequently used in accelerator technology.

Having compared the equations for the "thin" winding of unshielded magnets (4), and of magnets having current (9) and iron (12) shielding, provided that they produce the same field (i.e. the combination of the co-efficients b_n is identical), we see that these equations are all of the same type and differ only in the factors in the presence of the b_n co-efficients. In fact, having made a substitution by

in equation (4) we obtain the first equation of

(9), by $b_n \to \frac{(r_0/r_3)^{n+1}}{1-(r_0/r_3)^{2n}} \cdot b_n$ и $j(\varphi) \to -j_3(\varphi)$, we obtain the second equation of (9), and by $b_n \to \frac{1}{1+(r_0/r_3)^{2n}} \cdot b_n$ we obtain the equation (12). We shall therefore examine in detail only the case of unshielded magnets. The corresponding results for shielded magnets can be obtained from the results given below for unshielded magnets, after making the following substitutions in them:

1. Current shielding:

   Forming winding: $H_0 \to \frac{H_0}{1-(r_0/r_3)^2}$, $\nabla H \to \frac{\nabla H}{1-(r_0/r_3)^4}$,

   Shielding winding: $H_0 \to \frac{(r_0/r_3)^2 H_0}{1-(r_0/r_3)^2}$, $\nabla H \to \frac{(r_0/r_3)^3 \nabla H}{1-(r_0/r_3)^4}$,

   $j(\varphi) \to -j_3(\varphi)$

2. Iron shielding: $H_0 \to \frac{H_0}{1+(r_0/r_3)^2}$, $\nabla H \to \frac{\nabla H}{1+(r_0/r_3)^4}$.

Let us now consider the particular cases of the field (14) and at the same time make a qualitative study of the way in which the transition is made from one case to the other.

The equation for the "thin" winding for an unshielded iron-free magnet which produces in a circle with a radius of r_0 a field (14), is of the form:

$$-\frac{j(\varphi)}{j}\cdot\frac{\Delta}{r_0} = \frac{H_0}{\frac{2\pi}{c} j r_0}\cdot\cos\varphi + \frac{\nabla H}{\frac{2\pi}{c} j}\cos(2\varphi+\psi). \quad (15)$$

1. $H_0 \neq 0$; $\nabla H = 0$; $\psi = 0$; - is a dipole field having a value H_0, oriented along the axis η

(fig. 1). It can be seen from (15) that this field in the "thin" case is produced by a winding (fig. 2a) having a thickness $\Delta(\varphi)$:

$$-\frac{j(\varphi)}{j}\cdot\frac{\Delta(\varphi)}{z_0}=\frac{H_0}{\frac{2\pi}{c}jz_0}\cdot\cos(\varphi)$$

The nodal points are:

$$\varphi_{y3\,1,2}=\pm\pi/2.$$

It follows from field symmetry that in the breakdown of the field outside the forming winding (2) there are multipoles of the order of n = 1,3,5,7..., i.e. with n = 2k + 1 in which all $\psi_n = 0$.

2. $H_0 = 0;\ \nabla H \neq 0;\ \psi = 0;$ - is a quadrupole field. It can be seen from (15) that this field in the "thin" case is composed of a winding (2e) having a thickness $\Delta(\varphi)$:

$$-\frac{j(\varphi)}{j}\cdot\frac{\Delta(\varphi)}{z_0}=\frac{\nabla H}{\frac{2\pi}{c}j}\cdot\cos(2\varphi).$$

The nodal points are: $\varphi_{y3\,p}=\frac{\pi}{4}\cdot p$: = 1, 2, 3, 4.

It follows from field symmetry that in the breakdown of the field outside the forming winding (2) there are multipoles with n = 2,6,10,14..., i.e. n = 2 + 4k in which all $\psi_n = 0$.

3. $H_0 \neq 0;\ \nabla H \neq 0;\ \psi = 0;$ is the superposition of a dipole and quadrupole field with a horizontal plane of symmetry; these fields are used in cyclic accelerators in which the magnet system is of the non-separated function type.

It can be seen from (15) that this field in the "thin" case is produced by the winding (fig. 2 b,c,d)

$$-\frac{j(\varphi)}{j}\cdot\frac{\Delta(\varphi)}{r_0}=\frac{1}{\frac{2\pi}{c}jr_0}\cdot\left(H_0\cos\varphi+r_0\nabla H\cdot\cos 2\varphi\right).$$

Let us study the manner in which the winding varies during a gradual reduction in the $H_0/(r_0\nabla H)$ ratio.

When $H_0/(r_0\nabla H)\gg 1$ we have case 1 (fig. 2 a).

When $H_0/r_0\nabla H)>1$ is finite there are two nodal points (fig. 2 b):

$$\varphi_{y3\,1,2}=\pm\arccos\left(0.25\cdot\left(-\frac{H_0}{r_0\nabla H}+\sqrt{\left(\frac{H_0}{r_0\nabla H}\right)^2+8}\right)\right).$$

When $H_0/(r_0\nabla H)=1$, the external boundary of the conductor touches the circumference at a point $\varphi=\pi$ (fig.2c), but this is not a nodal point, i.e. $j(\varphi)$ does not change its sign in it.

When $H_0/(r_0\nabla H)<1$ there are already four nodal points (2 d): two of these are defined as before (21) and two are new:

$$\varphi_{y3\,3,4}=\pm\arccos\left(0.25\cdot\left(-\frac{H_0}{r_0\nabla H}-\sqrt{\left(\frac{H_0}{r_0\nabla H}\right)^2+8}\right)\right).$$

When $H_0/(r_0\nabla H)\to 0$ we are changing over to case 2, i.e. to the purely quadrupole case (fig. 2 e).

In this way, we have studied the manner in which the nature of the winding changes during a steady transition from the dipole case to the quadrupole case through a constant gradient field with a horizontal plane of symmetry. As the position of the

nodal points does not depend on the "thickness" of the winding the qualitative picture of the change in the nature of the winding is similar for windings having any "thickness".

In the expansion for the external field (2) for multipoles, there are multipoles of all orders, and all $\psi_n = 0$.

4. $H_0 \neq 0;\ \nabla H \neq 0;\ \psi_n = -\pi/2$: - is the superposition of a dipole and quadrupole field with a vertical plane of symmetry. As was pointed out in /12,13/, an accelerator can be constructed using these fields.

It follows from (15) that such a field in the "thin" case is produced by the winding

$$-\frac{j(\varphi)}{j}\cdot\frac{\Delta(\varphi)}{z_0} = \frac{1}{\frac{2\pi}{c} j z_0}\cdot\left(H_0 \cos\varphi + z_0 \nabla H \sin 2\varphi\right).$$

Let us study the manner in which the winding varies with a gradual reduction in the $H_0/(z_0 \nabla H)$ ratio.

When $H_0/(2 z_0 \nabla H) \gg 1$ we have case 1 (fig. 2 a).

When $H_0/(2 z_0 \nabla H) > 1$ is finite the nodal points are the same as in case 1, i.e. $\varphi_{yz\,1,2} = \pm \pi/2$ (2B).

When $H_0/(2 z_0 \nabla H) = 1$, the slope of the external boundary of the conductor towards the inner circumference tends to zero at the point $\varphi_{yz\,2} = -\pi/2$, i. e the internal and external

boundaries of the conductor touch each other (fig. 2C).

When $H_0/(2r_0\nabla H) < 1$, two new nodal points are added to the points $\varphi_{y3\,1,2} = \pm \pi/2$ (fig. 2D.):

$$\varphi_{y3\,3,4} = -\frac{\pi}{2} \pm \left(\arcsin\left(H_0/(2r_0\nabla H)\right) - \pi/2\right).$$

When $H_0/(r_0\nabla H) \to 0$, we are changing over to the case of a quadrupole which is rotated through $\pi/4$ (fig. 2E).

We have thus studied the manner in which the nature of the winding changes during a continuous transition from the dipole case to that of the quadrupole through a constant gradient field with a vertical plane of symmetry. The qualitative nature of this picture does not depend on the "thickness" of the winding.

In the expansion for the field outside the shaping winding (2) all orders of multipoles exist in which

$\psi_n = 0$ when $= 1,3,5\ldots;$

$\psi_n = \pi/2$ when $= 2,4,6\ldots.$

§ 6. "Centres" of the windings and maximum possible fields that can be obtained for a given current density.

An examination of the picture of the lines of force of the magnetic field in the forming winding of any iron-free magnet (e.g. fig. 14) shows that the lines of force have a "centre" which lies

outside the winding; we shall call this the "centre" of the winding. The true "thickness" of the winding can be determined only by a numerical calculation, and the position of the "centre" of the winding is determined by an elementary method, in which it to some extent characterizes also the "half-thickness" of the entire winding. In the case of the "thin" winding the "centre" is precisely in the half of the maximum thickness of the winding. In the case of a winding having an arbitrary "thickness", the azimuthal and radial position of the "centre" is determined by the fact that, at the "centre" point, the components of the magnetic field (6) tend to zero, but in the most interesting cases the azimuthal position of the "centre" is obvious from symmetry considerations. Thus, for example, having used (6) and (14) we find that the "centre" of a dipole winding is at the point

$$z_y = z_0\left(a/2 + \sqrt{1+(a/2)^2}\right), \quad \text{where} \quad a = H_0 \Big/ \left(\tfrac{2\pi}{c} j z_0\right).$$

In other words, a dipole winding with a centre at z_y produces in the circle a field:

$$a = \left[(z_y/z_0)^2 - 1\right] \Big/ (z_y/z_0).$$

Consequently, for a given current density which increases the "thickness" of the winding any number of strong dipole fields may be produced in the circle; in this case when $z_y/z_0 \gg 1$:

$$H_0 \doteq \tfrac{2\pi}{c} j \cdot z_y$$

In a similar way, we find that the "centre" of a quadrupole

winding is at the point

$$r_y = r_0/\sqrt{1-b}, \quad \text{where} \quad b = \nabla H/\left(\frac{2\pi}{c} j\right).$$

In other words a quadripole winding with a "centre" of r_y produces a field with

$$b = 1 - (r_0/r_y)^2.$$

Consequently, for a given current density, if we increase the "thickness" of the quadrupole winding we obtain in the limits of $r_y / r_0 \gg 1$:

$$b = 1, \quad \text{i.e.} \quad \nabla H_{max} = \frac{2\pi}{c} j. \tag{16}$$

§ 7. Numerical method for solving "thick" winding equations.

In paragraph 3 we obtained a system of boundary equations (7) for an unshielded iron-free magnet, and in paragraph 4 a system of equations (11) for an iron-free magnet with current screening, and a system (13) for the case in which iron shielding was used. In paragraph 5 nodal points were found, as well as the step functions of $j(\varphi)/j$ for fields of type (14). In this section we shall describe schematically an interaction method which can be used for a numerical solution of systems (7), (11) and (13).

Let us assume that the field produced has a symmetry of the

order of P (for a dipole and a field having a constant gradient, P = 2, for a quadrupole P = 4; see paragraph 5). The numerical solution can then be carried out only on one of the intervals of symmetry $\varphi_c = 2\pi/P$. We retain on the right hand-side of the equations for the system which is being solved, a finite number of terms N + 1; this denotes that we approximate the magnetic field outside the forming system by the sum of a finite number of multipoles. From paragraph 5 it follows that the number of the highest multipole remaining on the right hand side n_{max} is equal in the case of the production of a dipole field to $n_{max}=2.N+1$, and in the case of a quadrupole field $n_{max}=2+4.N$, whilst in the case of constant gradient fields $n_{max}=N+1$. Let us divide the interval φ_c into $n_{max}.K$ equal intervals by a sequence of points $\varphi_m = \varphi_c \cdot m/(n_{max} \cdot K)$, where $m = 1,\ldots,Kn_{max}$, and K is the number of nodal points on one half period of the highest multipole.

Let us suppose, for example, that as a result of an ℓ-th iteration when resolving the system of (11) we obtained the value $z_\ell(\varphi_m)$ and $z_{3\ell}(\varphi_m)$ for all $m\,(1 \leq m \leq n_{max} \cdot K)$. The $(\ell + 1)$-th iteration cycle will then consist of the following. We determine the system of co-efficients $(\alpha_n)_{\ell+1}$ and $(C_n)_{\ell+1}$, which best satisfy with regard to the mean square the equations (11.1) and (11.3) on the sequence of points φ_m, whilst considering that

$$z(\varphi_m) = (z(\varphi_m))_\ell \,, \quad z_3(\varphi_m) = (z_3(\varphi_m))_\ell .$$

It is usually convenient to transfer part of the terms from the left hand side of equations (11.2) and (11.4) to the right hand side. Having substituted $(r(\varphi_m))_\ell$, $(r_3(\varphi_m))_\ell$ and $(d_n)_{\ell+1}$, $(C_n)_{\ell+1}$ in the right hand side of equations (11.2) and (11.4) we find, from the left hand parts $(r(\varphi_m))_{\ell+1}$ and $(r_3(\varphi_m))_{\ell+1}$. Thus, if the problem is solved for fields of type (14), then provided the right hand sides are known equations (11.2) and (11.4) determine directly $(r^2(\varphi_m))_{\ell+1}$ and $(r_3^2(\varphi_m))_{\ell+1}$.

Let us carry out a Lanczos averaging of the shapes obtained for $r(\varphi)$ and $r_3(\varphi)$. With this, the $(\ell+1)$- th iteration cycle is completed.

The zero approximation chosen was that of a "thin" winding. The iterations stopped when the relationship of the difference in the areas of the windings, obtained during two successive iterations, to one of these areas fell below a given value, i.e. when the given relative accuracy was achieved.

Having obtained in this manner the shape of the windings, we can now find the field (see Chapter II), which they produce in a circle and at the same time estimate whether the number of multipoles N+1 remaining on the right hand sides of the equations and the number of K nodal points on the half period of the highest multipole are sufficient. It is clear that the "thicker" the

winding, the greater the N+1 must be, but within the limits of the "thin" winding N+1 = 1. (In the case of a pure multipole).

In Chapter II we give equation systems for each concrete case in the most convenient form for using the iteration process described. The programme was written in the language of the "Alfa" system /26/, and calculations were made on the M-220 and BESM-6 machines at the computer centre of the Siberian Division of the Academy of Sciences.

II. RESULTS OF A NUMERICAL CALCULATION FOR A CIRCULAR DOMAIN

For convenience, we give at the beginning of each section the expressions for the fields and magnetic potentials, as well as the system of corresponding boundary equations in the form in which the iteration process described in paragraph 7 was applied to it. We separated these factors C_n or d_n from the co-efficients H_0 and $r_0 \nabla H$.

In each of the drawings which give a general view of the systems, the windings in which the current flows in opposite directions are shaded with lines which run perpendicular to each other. On each of the graphs showing the area of the windings the unit of area is r_0^2, whilst on the energy graphs, the unit of energy is the energy of the field produced in the circle, i.e. the energy of the "useful" field.

§ 1. Iron-free unshielded magnets

1.1. Dipole field.

An overall view of the system is shown in the figure 2 a.

Let us denote $x = r/r_0, \quad \alpha = H_0 / \left(\frac{2\pi}{c} j r_0\right).$

The field produced is:

$$\begin{aligned} H_{0r}/H_0 &= \sin\varphi, \\ H_{0\varphi}/H_0 &= \cos\varphi, \\ A_0/(r_0 H_0) &= -x\cdot\cos\varphi. \end{aligned} \tag{17}$$

The field in the winding is:

$$\begin{aligned} H_{мет\,r}/H_0 &= \sin\varphi, \\ H_{мет\,\varphi}/H_0 &= \cos\varphi - \frac{1}{\alpha}\left(x - \frac{1}{x}\right), \\ A_{мет}/(r_0 H_0) &= -\left(x\cos\varphi - \frac{1}{2\alpha}\left(x^2 - 1 - 2\ln x\right)\right). \end{aligned} \tag{18}$$

The field outside the winding is:

$$\begin{aligned} H_{нар\,r}/H_0 &= \sum_{n=0}^{N} d_n \left(\frac{1}{x}\right)^{2n+2}\cdot\sin(2n+1)\varphi, \\ H_{нар\,\varphi}/H_0 &= \sum_{n=0}^{N} d_n \left(\frac{1}{x}\right)^{2n+2}\cos(2n+1)\varphi, \\ A_{нар}/(H_0 r_0) &= -\sum_{n=0}^{N} \frac{d_n}{2n+1}\cdot\left(\frac{1}{x}\right)^{2n+1}\cos(2n+1)\varphi. \end{aligned}$$

The system of equations is:

$$x(\varphi)\cdot\sin\varphi = \sum_{n=0}^{N} d_n \cdot \left(\frac{1}{x(\varphi)}\right)^{2n+1}\cdot\sin(2n+1)\varphi.$$

$$x^2(\varphi) = 1 + \alpha\cdot\left[x(\varphi)\cdot\cos\varphi + \sum_{n=0}^{N} d_n \left(\frac{1}{x(\varphi)}\right)^{2n+1}\cos(2n+1)\varphi\right],$$

where $x(\varphi) = r(\varphi)/r_0$, $r(\varphi)$ is the external boundary of the forming winding.

By using symmetry it is easy to show that the dipole winding of the shape $r(\varphi)$ produces, in the circle, a field which at point r_1 on the horizontal diameter is determined by the formula:

$$H_\varphi(r_1, 0)/H_0 = -\frac{2}{a\pi}\int_0^{\pi/2}\int_1^{x(\varphi)}\left\{\frac{x_1 - x\cos\varphi}{x_1^2 + x^2 - 2x_1 x\cos\varphi} - \right. \tag{19}$$

$$\left. - \frac{x_1 + x\cos\varphi}{x_1^2 + x^2 + 2x_1 x\cos\varphi}\right\} x\,dx\,d\varphi,$$

$$H_z(r_1, 0)/H_0 = 0,$$

where $x_1 = r_1/r_0$.

These formulas are used for checking the winding shapes obtained.

Figure 5 shows the winding shapeswhich correspond to various values of the parameter a ; these were obtained from a numerical solution of the system.

Figure 6 shows the area of one "lobe" of the winding in units of r_0^2 , the field energy in the metal of the conductor $W_{мет}$, the field energy outside the system $W_{маг}$, and the total energy of the magnetic field $W_{полн}$ ($W_{полн} = W_0 + W_{мет} + W_{маг}$)

as a function of the parameter a , the energy unit chosen being the field energy in the circle $W_0 = H_0^2 r_0^2/8$ (the line where $\delta = 0$).

1.2. Quadrupole field

An overall view of the system is shown in figure 2 e.

Let us denote $x = r/r_0$: $\beta = \nabla H / \left(\frac{2\pi}{c} j\right)$.

The field produced is

$$H_{0r}/(r_0 \nabla H) = x \cdot \sin(2\varphi),$$
$$H_{0\varphi}/(r_0 \nabla H) = x \cdot \cos 2\varphi, \qquad (20)$$
$$A/(r_0^2 \nabla H) = -\frac{x^2}{2} \cos 2\varphi.$$

The field in the winding is

$$H_{мет\,r}/(r_0 \nabla H) = x \sin 2\varphi,$$
$$H_{мет\,\varphi}/(r_0 \nabla H) = x \cos 2\varphi - \frac{1}{6}\left(x - \frac{1}{x}\right), \qquad (21)$$
$$A_{мет}/(r_0^2 \nabla H) = -0.5 \cdot \left(x^2 \cos 2\varphi - \frac{1}{6}(x^2 - 1 - 2\ln x)\right).$$

The field outside the winding is

$$H_{нар\,r}/(r_0 \nabla H) = \sum_{n=0}^{N} d_n \cdot \left(\frac{1}{x}\right)^{3+4n} \sin(2+4n)\varphi,$$
$$H_{нар\,\varphi}/(r_0 \nabla H) = -\sum_{n=0}^{N} d_n \cdot \left(\frac{1}{x}\right)^{3+4n} \cos(2+4n)\varphi,$$
$$A_{нар}/(r_0^2 \nabla H) = -\sum_{n=0}^{N} \frac{d_n}{2+4N} \cdot \left(\frac{1}{x}\right)^{2+4n} \cos(2+4n)\varphi.$$

The system of equations is:

$$x^2(\varphi) \sin 2\varphi = \sum_{n=0}^{N} d_k \cdot \left(\frac{1}{x(\varphi)}\right)^{2+4n} \sin(2+4n)\varphi,$$
$$x^2(\varphi) = 1 + \beta\left(x^2(\varphi) \cos 2\varphi + \sum_{n=0}^{N} d_n \left(\frac{1}{x(\varphi)}\right)^{2+4n} \cos(2+4n)\varphi\right),$$

where $x(\varphi) = r(\varphi)/r_0$; $r(\varphi)$ - is the external boundary of the forming winding.

By using symmetry it is easy to show that a quadrupole winding having a shape $r(\varphi)$ produces, in the circle, a field which at a point r_1 on the horizontal diameter is determined by the formula

$$H_\varphi(r_1, 0)/(r_0 \nabla H) = -\frac{4}{\pi\alpha} \cdot x_1 \int_0^{\pi/4} \int_1^{x(\varphi)} \left\{ \frac{x_1^2 - x^2 \cos 2\varphi}{x_1^4 + x^4 - 2x^2 x_1^2 \cos 2\varphi} - \frac{x_1^2 + x^2 \cos 2\varphi}{x_1^4 + x^4 + 2x^2 x_1^2 \cos 2\varphi} \right\} x\, dx\, d\varphi, \qquad (22)$$

$$H_r(r_1, 0)/(r_0 \nabla H) = 0.$$

where $x_1 = r_1/r_0$.

Figure 7 shows the winding shapes which correspond to various values of the parameter b, obtained as a result of a numerical solution of the system.

Figure 8 shows the area of one "lobe" of the winding in r_0^2 units, the field energy in the metal of the conductor $W_{мет}$, the field energy outside the system $W_{нар}$ and the total energy of the magnetic field $W_{магн}$ ($W_{магн} = W_0 + W_{мет} + W_{нар}$) as a function of the parameter b, the unit of energy chosen being the field energy in the circle $W_0 = (r_0 \nabla H)^2 r_0^2/16$. If the winding is made with a normal conductor, then for a given value of the field produced b and a given radius of the forming domain r_0 the ohmic losses in the winding are proportional

to the value S/b^2 . From the graph of $S/2_0^2$ in figure 8 it is easy to deduce that the value of S/b^2 has a fairly flat minimum in the b = 0.45 - 0.7 range and grows rapidly outside of this range. The latter is optimum from the view point of ohmic losses, i.e. for lenses operating in quasi-constant conditions. In the case of lenses which operate in pulsed conditions with a high repetition frequency, it is necessary to aim also for a reduction in the value of W_{nark} / W_0 . The optimum b can easily be determined in each concrete case by minimizing the sum of the total energy of the magnetic field and energy of the ohmic losses. It is clear that the optimum b shifts towards the lower values, away from the ohmic-optimum from the above-mentioned range.

Similar arguments can be used also for the dipole field, but here the function of S/a^2 falls steadily, and the windings which are advantageous ohmically are those which have the max-imum thickness.

1.3. Constant gradient field with a horizontal plane of symmetry.

An overall view of the system is shown in figure 2 b.

Let us denote

$$x = z/z_0, \quad \alpha = H_0/(\tfrac{2\pi}{5} j z_0), \quad \delta = (z_0 \nabla H)/H_0.$$

The field produced is:

$$\begin{aligned} H_{0z}/H_0 &= \sin\varphi + \delta \cdot x \cdot \sin 2\varphi, \\ H_{0\varphi}/H_0 &= \cos\varphi + \delta \cdot x \cdot \cos 2\varphi, \\ A/(z_0 H_0) &= -(x\cos\varphi + 0.5 x^2 \delta \cos 2\varphi). \end{aligned} \tag{23}$$

The field in the winding is:

$$H_{мет\,r}/H_0 = \sin\varphi + x\cdot\delta\cdot\sin 2\varphi,$$
$$H_{мет\,\varphi}/H_0 = \cos\varphi + x\cdot\delta\cdot\cos 2\varphi - \frac{1}{a}\left(x - \frac{1}{x}\right), \qquad (24)$$
$$A_{мет}/(H_0 r) = -\left(x\cos\varphi + 0.5\,x^2\delta\cos 2\varphi - \right.$$
$$\left. - \frac{1}{2a}\left(x^2 - 1 - 2\ln x\right)\right).$$

The field outside the winding is:

$$H_{нар\,r}/H_0 = \sum_{n=1}^{N+1} d_n\,(1/x)^{n+1}\sin n\varphi,$$
$$H_{нар\,\varphi}/H_0 = -\sum_{n=1}^{N+1} d_n\,(1/x)^{n+1}\cos n\varphi,$$
$$A_{нар}/(r_0 H_0) = -\sum_{n=1}^{N+1} d_n\,(1/x)^{n}\,\frac{1}{n}\cdot\cos n\varphi.$$

The system of equations is:

$$x(\varphi)\cdot\sin\varphi + \delta\cdot x^2(\varphi)\cdot\sin 2\varphi = \sum_{n=1}^{N+1} d_n\cdot\left(1/x(\varphi)\right)^n\sin n\varphi,$$
$$x^2(\varphi) = 1 + a\cdot\left(x(\varphi)\cdot\cos\varphi + \delta\cdot x^2(\varphi)\cos 2\varphi + \right.$$
$$\left. + \sum_{n=1}^{N} d_n\,\left(1/x(\varphi)\right)^n\cos n\varphi\right),$$

where $x(\varphi) = r(\varphi)/r_0$, $r(\varphi)$ is the external boundary of the winding.

Figure 9 shows the shapes of the windings which correspond to various values of the parameter a , when δ =0.1 and when δ =0.2, obtained as a result of a numerical solution of the system. For each winding the areas of the "blunt" and"sharp"

"lobes", are, of course, identical, since their shape was determined taking into account the equality of direct and reverse currents (Chapter I, paragraph 1).

Figure 6 shows, for windings with δ =0.2, the area of one "lobe" of the winding in r_0^2 units, the field energy in the metal of the conductor W_{mem}, the field energy outside the system W_{Hap} and the total energy of the magnetic field W_{nanH} ($W_{nanH} = W_0 + W_{mem} + W_{Hap}$), as a function of the parameter a, the energy unit chosen being the field energy in the circle $W_0 = \frac{H_0^2 r_0^2}{8} \cdot (1 + \frac{\delta^2}{2})$ (the lines with δ =0.2). Similar dependences for the case δ =0.1 coincide in practice with the case δ =0.

1.4. Constant gradient field with a vertical plane of symmetry.

An overall view of the system is shown in figure 2 B.

Let us denote $x = r/r_0$; $a = H_0/(\frac{2\pi}{c} j r_0)$; $\delta = r_0 \nabla H / H_0$.

The field produced is:

$$H_{0r}/H_0 = \sin\varphi + x \cdot \delta \cdot \cos 2\varphi,$$
$$H_{0\varphi}/H_0 = \cos\varphi - x \cdot \delta \cdot \sin 2\varphi,$$
$$A_0/(r_0 H_0) = -(x\cos\varphi - 0.5 x^2 \cdot \delta \cdot \sin 2\varphi).$$

The field in the winding is:

$$H_{мет r}/H_0 = \sin\varphi + x \cdot \delta \cdot \cos 2\varphi,$$
$$H_{мет \varphi}/H_0 = \cos\varphi - x \cdot \delta \sin 2\varphi - \frac{1}{a}(x - \frac{1}{x}),$$
$$A_{мет}/(r_0 H_0) = -(x\cos\varphi - \frac{x^2}{2}\delta \sin 2\varphi - \frac{x^2 - 1 - 2\ln x}{2a}).$$

The field outside the winding (let N be an even number):

$$H_{нар\,r}/H_0 = \sum_{n=0}^{N/2} d_{2n+1}\cdot\left(\frac{1}{x}\right)^{2n+2}\sin(2n+1)\varphi +$$

$$+\sum_{n=1}^{N/2} d_{2n}\cdot\left(\frac{1}{x}\right)^{2n+1}\cos 2n\varphi,$$

$$H_{нар\,\varphi}/H_0 = -\sum_{n=0}^{N/2} d_{2n+1}\left(\frac{1}{x}\right)^{2n+2}\cos(2n+1)\varphi +$$

$$+\sum_{n=1}^{N/2} d_{2n}\left(\frac{1}{x}\right)^{2n+1}\sin 2n\varphi,$$

$$A/(r_0H_0) = -\sum_{n=0}^{N/2}\frac{d_{2n+1}}{2n+1}\cdot\left(\frac{1}{x}\right)^{2n+1}\cos(2n+1)\varphi +$$

$$+\sum_{n=1}^{N/2}\frac{d_{2n}}{2n}\cdot\left(\frac{1}{x}\right)^{2n}\sin 2n\varphi.$$

The system of equations is:

$$x(\varphi)\cdot\sin\varphi + \delta\cdot x^2\cos 2\varphi = \sum_{n=0}^{N/2} d_{2n+1}\left(\frac{1}{x}\right)^{2n+2}\sin(2n+1)\varphi +$$

$$+\sum_{n=1}^{N/2} d_{2n}\left(\frac{1}{x}\right)^{2n+1}\cos 2n\varphi,$$

$$x^2(\varphi) = 1 + a\left(x(\varphi)\cos\varphi - x^2(\varphi)\cdot\delta\cdot\sin 2\varphi\right) +$$

$$+\sum_{n=0}^{N/2} d_{2n+1}\left(\frac{1}{x}\right)^{2n+1}\cos(2n+1)\varphi -$$

$$-\sum_{n=0}^{N/2} d_{2n}\left(\frac{1}{x}\right)^{2n}\sin 2n\varphi.$$

Figure 10 shows winding shapes which correspond to various values of the parameter a when δ =0.1 and when δ =0.2, obtained as a result of a numerical solution of the system.

Figure 6 shows for a winding with δ =0.2 the area of one "lobe" of the winding in r_0^2 units, the field energy in the metal of the conductor $W_{мет}$, the field energy outside the system $W_{нар}$ and the total energy of the magnetic field $W_{полн}$ ($W_{полн} = W_0 + W_{мет} + W_{нар}$), as a function of the parameter a, the energy unit chosen being the field energy in the circle $W_0 = \frac{H_0^2 r_0^2}{8} \cdot \left(1 + \frac{\delta^2}{2}\right)$ (the lines where δ =0.2). The similar lines for the case δ =0.1 practically coincide with case δ =0.

Let us point out that with the calculation accuracy, all the dependences given in figure 6 are identical for the case of systems having horizontal and vertical planes of symmetry.

§ 2. Iron-free magnets with a co-axial iron cylinder as shielding.

2.1. Dipole field

An overall view of the system is shown in figure 4 D.

Let us denote $x = r/r_0$, $y_э = r_э/r_0$, $\alpha = H_0/\left(\frac{2\pi}{c} j r_0\right)$.

The field produced is given by equations (17).

The field in the winding is given by equations (18).

The field in the gap between the winding and the iron shielding is

$$H_{пр\,r}/H_0 = \sum_{n=0}^{N} d_n\left[\left(\frac{1}{x}\right)^{2n+2} + \left(\frac{1}{y_э}\right)^{2n+2}\left(\frac{x}{y_э}\right)^{2n}\right]\sin(2n+1)\varphi,$$

$$H_{пр\,\varphi}/H_0 = \sum_{n=0}^{N} d_n\left[-\left(\frac{1}{x}\right)^{2n+2} + \left(\frac{1}{y_э}\right)^{2n+2}\left(\frac{x}{y_э}\right)^{2n}\right]\cos(2n+1)\varphi,$$

$$A_{пр}/(H_0 r_0) = -\sum_{n=0}^{N} d_n\left[\left(\frac{1}{x}\right)^{2n+2} + \left(\frac{1}{y_э}\right)^{2n+2}\left(\frac{x}{y_э}\right)^{2n}\right]\frac{x\cdot\cos(2n+1)\varphi}{2n+1}.$$

The system of equations is:

$$x(\varphi)\cdot\sin\varphi = \sum_{n=0}^{N} d_n\left[\left(\frac{1}{x}\right)^{2n+1} + \left(\frac{1}{y_э}\right)^{2n+1}\left(\frac{x}{y_э}\right)^{2n+1}\right]\sin(2n+1)\varphi,$$

$$x^2(\varphi) = \underline{1} + \alpha\left\{x(\varphi)\cdot\cos\varphi + \sum_{n=0}^{N} d_n\left[\left(\frac{1}{x}\right)^{2n+1} - \left(\frac{1}{y_э}\right)^{2n+1}\left(\frac{x}{y_э}\right)^{2n+1}\right]\cdot\cos(2n+1)\varphi\right\},$$

where $x(\varphi) = r(\varphi)/r_0$, $r(\varphi)$ is the external boundary of the winding.

Having made use of equations (24) it can easily be shown that if there is co-axial iron shielding, a dipole winding having the shape $r(\varphi)$ forms in the circle a field which at the point r_1 on the horizontal diameter is determined by the formula

$$H_\varphi(r_1, 0)/H_0 = -\frac{2}{\alpha\pi}\cdot\int_0^{\pi/2}\int_1^{x(\varphi)}\left\{\frac{x_1 - x\cos\varphi}{x_1^2 + x^2 - 2x x_1\cos\varphi} - \right.$$

$$- \frac{x_1 + x\cos\varphi}{x_1^2 + x^2 + 2x_1 x\cos\varphi} + \frac{x_1 - x_i\cos\varphi}{x_1^2 + x_i^2 - 2xx_i\cos^2\varphi} -$$

$$- \frac{x_1 + x_i\cos\varphi}{x_1^2 + x_i^2 + 2x_1 x_i\cos\varphi} \Big\} x\,dx\,d\varphi,$$

$$H_2(r_1, 0)/H_0 = 0,$$

where

$$x_1 = r_1/r_0, \quad x_i = y_э^2/x, \quad y_э = r_э/r_0.$$

Figure 11 shows the winding shapes with a =0.6 and a = 1 for several radii of the shielding $r_э/r_0$, obtained as a result of a numerical solution of the system.

Figure 12 is a diagram of the force lines of the magnetic field for a winding with a =1.8 and a radius of the shielding $r_э/r_0 = 3$. The "centre" of the winding is marked by the letter $ц$.

Let us denote as the maximum relative thickness of the winding the value $\Delta_{max}/r_0 = (r_{max}(\varphi) - r_0)/r_0$. Figure 13 A shows the maximum relative thicknesses Δ_{max}/r_0 of windings with various values of the parameter a as a function of the shielding radius $r_э/r_0$.

In figure 13 B the relative areas S/r_0^2 of one "lobe" of the windings with various values of the parameter a are shown as a function of the shielding radius $r_э/r_0$.

Let us denote by W_0 ($W_0 = H_0^2 r_0^2/8$) the energy of the magnetic field produced in the circle.

In figure 14, the relative field energy in the metal of the winding $W_{мет}/W_0$, the field energy in the gap between the winding and the shielding $W_{пр}/W_0$ and the total field energy $W_{нагн}/W_0$ ($W_{нагн} = W_0 + W_{мет} + W_{пр}$) are shown as functions of the shielding radius $r_э/r_0$ for windings having various values of the parameter a .

On the surface of the iron-shielding, the field reaches a maximum value of H_{max} at points $\varphi = \pm \pi/2$ (figure 4 D). In Figure 13 C the maximum relative value of the field on the surface of the iron-shielding H_{max}/H_0 (H_0 is the value of the field produced in the circle) is shown as a function of the shielding radius $r_э/r_0$ for windings with a =0.2; 0.4; 0.6; 0.8; 1 and 1.2.

As a result of the magnetic forces present, a complex stressed state is brought about in the winding; this is determined by the concrete construction of the winding and its mode of attachment. We shall therefore confine our present study

to the total forces acting on the winding. Table 1 shows the total force f_ξ acting on the "lobe" ABCD of the winding (figure 4) along the axes ξ and the total force f_η with which parts ABC and ACD are pressed against each other for the case of a winding with α =1 for various radii of iron-shielding r_3/r_0 . The same table gives the first co-efficients for expanding the shape of the winding into a Fourier series:

$$r(\varphi)/r_0 = 1 + \sum_{n=0}^{N} \phi_{2n+1} \cdot \cos(2n+1)\varphi.$$

We should point out that for an unshielded dipole ($r_3/r_0 \gg 1$) within the limits of a thin winding ($\alpha \ll 1$)

$$f_\xi/(2F_0) = f_\eta/F_0 = 4/3,$$

$$\phi_1 = \alpha, \quad \phi_3 = \phi_5 = \cdots = 0.$$

Table 1

Total forces and Fourier co-efficients of the shape of the "lobe" of the dipole winding with iron shielding, case of $\alpha = 1$

r_3/r_0	15	5	4	3	2.5	1.96
$f_\xi/(2F_0)$	1.72	1.8	1.83	1.86	1.87	1.85
f_η/F_0	1.45	1.25	1.15	0.98	0.86	0.7
ϕ_1	0.986	0.92	0.88	0.82	0.77	0.69
ϕ_3	0.116	0.1	0.095	0.08	0.06	0.04
ϕ_5	-0.02	-0.018	-0.017	-0.0164	-0.017	-0.0185
ϕ_7	0.006	0.0055	0.0053	0.0049	0.0045	0.0043

where $F_0 = \frac{H_0^2 r_0}{8\pi}$.

It will be seen from the table that even when a =1, and the "thickness" of the winding is of the order of the radius of the circle r_0, a decisive contribution to the shape of the winding is made by the first harmonic, this contribution increasing comparatively as the shielding becomes closer.

2.2. Quadrupole field

An overall view of the system is shown in figure 4 K.

Let us denote $x = r/r_0$, $y_э = r_э/r_0$, $b = pH/\left(\frac{2\pi}{c} j\right)$.

The field produced is given by expression (20).

The field in the winding is given by the expressions of (21).

The field in the gap between the winding and the iron shielding is:

$$H_{пр\,r}/H_0 = \sum_{n=0}^{N} d_n \left[\left(\frac{1}{x}\right)^{3+4n} + \left(\frac{1}{y_э}\right)^{3+4n} \cdot \left(\frac{x}{y_э}\right)^{1+4n}\right] \cdot \sin(2+4n)\varphi,$$

$$H_{пр\,\varphi}/H_0 = \sum_{n=0}^{N} d_n \left[-\left(\frac{1}{x}\right)^{3+4n} + \left(\frac{1}{y_э}\right)^{3+4n} \cdot \left(\frac{x}{y_э}\right)^{1+4n}\right] \cos(2+4n)\varphi,$$

$$A_{пр}/H_0 = \sum_{n=0}^{N} d_n \left[\left(\frac{1}{x}\right)^{3+4n} + \left(\frac{1}{y_э}\right)^{3+4n} \cdot \left(\frac{x}{y_э}\right)^{1+4n}\right] \cdot$$

$$\frac{x}{2+4n} \cdot \cos(2+4n)\varphi.$$

The system of equations is:

$$x^2(\varphi)\sin 2\varphi = \sum_{n=0}^{N} d_n \left[\left(\frac{1}{x(\varphi)}\right)^{2+4n} + \left(\frac{1}{y_э}\right)^{2+4n} \cdot \left(\frac{x(\varphi)}{y_э}\right)^{2+4n}\right] \cdot \sin(2+4n)\varphi,$$

$$x^2(\varphi) = 1 + b\left(x^2(\varphi)\cos 2\varphi + \sum_{n=0}^{N} d_n \left[\left(\frac{1}{x(\varphi)}\right)^{2+4n} - \left(\frac{1}{y_э}\right)^{2+4n} \cdot \left(\frac{x(\varphi)}{y_э}\right)^{2+4n}\right] \cdot \cos(2+4n)\varphi.\right.$$

where $x(\varphi) = r(\varphi)/r_0$, $r(\varphi)$ - is the external boundary of the winding.

By making use of the expressions of (27), it is easy to show that in the presence of the co-axial iron shielding a quadrupole winding having the shape $r(\varphi)$ produces in the ring a field which at the point r_1 on the horizontal diameter is determined by the formula

$$H_\varphi(r_1, 0)/H_0 = -\frac{4}{\pi b} \cdot x_1 \cdot \int_0^{\pi/4} \cdot \int_1^{x(\varphi)} \left\{ \frac{x_1^2 - x^2\cos 2\varphi}{x_1^4 + x^4 - 2x^2x_1^2\cos 2\varphi} - \frac{x_1^2 + x^2\cos 2\varphi}{x_1^4 + x^4 + 2x^2x_1^2\cos 2\varphi} + \frac{x_1^2 - x_i^2\cos 2\varphi}{x_1^4 + x_i^4 - 2x_i^2x^2\cos 2\varphi} + \frac{x_1^2 + x_i^2\cos 2\varphi}{x_1^4 + x_i^4 + 2x_1^2x_i^2\cos 2\varphi} \right\} x\,dx\,d\varphi, \quad H_z(r_1, 0) = 0,$$

where $x_1 = r_1/r_0$, $x_i = y_3^2/x$, $y_э = r_э/r_0$.

Figure 15 shows the winding shapes with b =0.4 for several shielding radii $r_э/r_0$ obtained by a numerical solution of the system (49).

Let us designate as the maximum relative thickness of the winding the value

In figure 16 A the maximum relative thicknesses of the windings with various values of the parameter β are shown as functions of the shielding radius r_3/r_0 .

In figure 16 B the relative areas S/r_0^2 of one "lobe" of windings with various values for the parameter β are shown as functions of the shielding radius r_3/r_0 .

Let us designate the energy of the magnetic field produced in the ring by W_0 ($W_0 = (r_0 \nabla H)^2 r_0^2/16$.

In figure 17, the relative field energy in the metal of the winding W_{mem}/W_0 , the field energy in the gap between the winding and the shielding W_{np}/W_0 and the total field energy W_{nanH}/W_0 ($W_{nanH} = W_0 + W_{mem} + W_{np}$) are shown as functions of the shielding radius r_3/r_0 for windings with various values of the parameter β .

On the surface of the iron shielding the field value reaches a maximum at the points $\varphi = \pm \frac{\pi}{4}, \pm \frac{3\pi}{4}$ (figure 8 a). In figure 16 C the maximum relative field value on the surface of the iron shielding H_{max}/H_0 ($H_0 = r_0 \cdot \nabla H$ is the field value on the boundary of the shaping field) is shown as a function of the shielding radius r_3/r_0 for windings with

b =0.1; 0.2; 0.3; 0.4; 0.5 and 0.6.

Table 2 gives the total force f_ξ acting on the "lobe" ABCD of the winding (fig. 4K) along the axis ξ and the total force f_η with which the parts ABC and ACD are pressed against each other for the case of a winding with b =0.4 for various radii of iron shielding r_3/r_0. This same table gives the first co-efficients of the expansion of the shape of the winding into a Fourier series:

$$r(\varphi)/r_0 = 1 + \sum_{n=0}^{N}{}' \phi_{2+4n} \cos(2+4n)\varphi.$$

Table 2

The total forces and Fourier co-efficients of the "lobe" form of a quadrupole winding with iron shielding, the case $b = \nabla H/\left(\frac{2\pi}{c} j\right) = 0.4$.

r_3/r_0	100	5	3	2	1.741
$f_\xi/(2F_0)$	1.69	1.72	1.84	2.18	2.33
f_η/F_0	3.63	3.61	3.45	2.93	2.62
ϕ_2	0.483	0.481	0.467	0.416	0.382
ϕ_6	0.089	0.088	0.083	0.066	0.054
ϕ_{10}	-0.0023	-0.0023	-0.0022	-0.0024	-0.0032
ϕ_{14}	-0.0075	-0.0073	-0.0063	-0.0028	0,0011

where $F_0 = \frac{(r_0 \nabla H)^2 r_0}{24\pi}$.

We should point out that for an unshielded quadrupole ($r_э/r_0 \gg 1$), within the limits of the thin winding ($b \ll 1$):

$$f_\xi/(2F_0) = 0.8\cdot\sqrt{2} \approx 1.13,$$
$$f_\eta/F_0 = 1.6\cdot(1+\sqrt{2}/2) \approx 2.73,$$
$$\phi_2 = b,\ \phi_6 = \phi_{10} = \cdots = 0.$$

§ 3. Iron-free magnets with co-axial current shielding.

Here we shall examine the case in which the current density in the shielding winding is equal in value to the current density in the forming winding. On each azimuth, the current in the shielding winding is opposed to the current in the forming winding.

3.1. Dipole field

An overall view of the system is shown in figure 3 D.

Let us denote $x = r/r_0$, $y_э = r_э/r_0$, $a = H_0/\left(\frac{2\pi}{c} j r_0\right)$.

The field produced is given by the expressions of (17).

The field in the forming winding is given by the expressions of (18).

The field in the gap between the forming and shielding winding is:

$$H_{пр2}/H_0 = \sum_{n=0}^{N}\left[d_n\cdot\left(\frac{1}{x}\right)^{2n+2} + C_n\left(\frac{x}{y_э}\right)^{2n}\right]\sin(2n+1)\varphi,$$

$$H_{пр\varphi}/H_0 = \sum_{n=0}^{N}\left[-d_n\left(\frac{1}{x}\right)^{2n+2} + C_n\left(\frac{x}{y_э}\right)^{2n}\right]\cos(2n+1)\varphi,$$

$$A_{пр}/(H_0 r_0) = -\sum_{n=0}^{N}\left[d_n\left(\frac{1}{x}\right)^{2n+2} + C_n\left(\frac{x}{y_э}\right)^{2n}\right]\cdot\frac{x\cdot\cos(2n+1)\varphi}{2k+1}.$$

The field in the shielding winding is:

$$H_{r0}/H_0 = H_{rпр}/H_0,$$

$$H_{\varphi э}/H_0 = H_{\varphi пр}/H_0 + \frac{1}{\alpha}\left(x - y_э^2/x\right),$$

$$A_э/(H_0 r_0) = A_{пр}/(H_0 r_0) - \frac{1}{2\alpha}\left(x^2 - y_э^2 - 2y_э^2\ln(x/y_э)\right).$$

The system of equations is:

$$x(\varphi)\cdot\sin\varphi = \sum_{n=0}^{N}\left[d_n\cdot\left(\frac{1}{x(\varphi)}\right)^{2n+1} + C_n y_э\left(\frac{x(\varphi)}{y_э}\right)^{2n+1}\right]\sin(2n+1)\varphi,$$

$$0 = \sum_{n=0}^{N}\left[d_n\cdot\left(\frac{1}{y(\varphi)}\right)^{2n+1} + C_n y_э\left(\frac{y(\varphi)}{y_э}\right)^{2n+1}\right]\sin(2n+1)\varphi,$$

$$x^2(\varphi) = 1 + \alpha\left[x(\varphi)\cdot\cos\varphi + \sum_{n=0}^{N}\left[d_n\left(\frac{1}{x(\varphi)}\right)^{2n+1} - C_n y_э\left(\frac{x(\varphi)}{y_э}\right)^{2n+1}\right]\cos(2n+1)\varphi,\right.$$

$$y^2(\varphi) = y_э^2 + \alpha\cdot\sum_{n=0}^{N}\left[d_n\left(\frac{1}{y(\varphi)}\right)^{2n+1} - C_n y_э\cdot\left(\frac{y(\varphi)}{y_э}\right)^{2n+1}\right]\cos(2n+1)\varphi,$$

where $x(\varphi) = r(\varphi)/r_0$, $y(\varphi) = r_э(\varphi)/r_0$,

$r(\varphi)$ - is the external boundary of the forming winding

$r_э(\varphi)$ - is the external boundary of the shielding winding.

By using formula (19) we can find the field produced by the forming and shielding windings on the horizontal diameter of the domain of formation.

Figure 18 shows the shapes of the windings with a =0.6 and a =1 for several shielding radii $r_э/r_0$, obtained as a result of a numerical solution of the system; to save space, all the dimensions shown in these figures which relate to shielding windings have been reduced $r_э/r_0$ times.

Let us designate $\Delta_{max}/r_0 = (r(\varphi)_{max} - r_0)/r_0$ and

$\Delta_{эmax}(r_0) = (r_э(\varphi)_{max} - r_0)/r_0$ - as the maximum relative thicknesses corresponding to the forming and shielding windings. Figure 19 A gives the values of Δ_{max}/r_0 and $\Delta_{эmax}/r_0$ for windings with various values of the parameter as functions of the internal radius of the current shielding $r_э/r_0$.

In figure 19 B (19 C) the relative areas S/r_0^2 ($S_э/r_0^2$)

of one "lobe" of the forming (shielding) windings with various values of the parameter are shown as functions of the shielding radius $r_э/r_0$.

We shall designate the energy of the magnetic field produced in the circle by W_0 ($W_0 = H_0^2 r_0^2/8$) . In figure 20 the relative field energies in the metal of the shielding winding $W_{экр}/W_0$, in the metal of the forming winding $W_{мет}/W_0$, in the gap between the forming and shielding windings $W_{пр}/W_0$ and the total field energy $W_{магн}/W_0$ ($W_{магн} = W_0 + W_{мет} + W_{пр} + W_{экр}$) are shown as functions of the internal shielding radius r_0/r_0 for windings with various values of the parameter a .

The corresponding value of the parameter is shown near each curve on each of the graphs.

Table 3 shows the total force $f_ξ$ acting on the "lobe" ABCD (and shielding)winding (figure 3 D) along the axis $ξ$ and the total force $f_η$, with which the path ABC and ACD are pressed against one another for the case of a winding with a =1 for current shielding of various internal radii.

This table also gives the first co-efficients for the expansion of the shape of the forming and shielding winding into a Fourier series:

$$r(\varphi)/r_0 = 1 + \sum_{n=0}^{N} \phi_{1+2n} \cos(1+2n)\varphi.$$

Table 3

Total forces and Fourier co-efficients for the shape of the "lobe" of a quadrupole winding with co-axial current shielding, case $a = 1$.

Forming Winding

z_3/z_0	15	5	4	3
$\ell_3/(2F_0)$	1.686	1.49	1.27	0.166
ℓ_2/F_0	1.514	1.83	2.1	3.087
ϕ_1	1	1.1	1.17	1.4
ϕ_3	0.12	0.14	0.157	0.224
ϕ_5	-0.0203	-0.023	-0.024	-0.024
ϕ_7	0.006	0.0065	0.0068	0.0076

Shielding Winding

z_3/z_0	15	5	4	3
$\ell_{03}/(2F_0)$		0.284	0.685	2.875
ℓ_{37}/F_0		-0.135	0.32	-1.31
ϕ_{31}	$0.66 \cdot 10^{-3}$	0.02	0.044	0.134
ϕ_{33}	$0.294 \cdot 10^{-5}$	$0.73 \cdot 10^{-3}$	$0.26 \cdot 10^{-2}$	0.0015
ϕ_{35}	$0.36 \cdot 10^{-6}$	$0.5 \cdot 10^{-4}$	$0.2 \cdot 10^{-3}$	0.0017
ϕ_{37}	$0.3 \cdot 10^{-6}$	$0.66 \cdot 10^{-5}$	$0.1 \cdot 10^{-4}$	$0.1 \cdot 10^{-4}$

3.2 Quadrupole Field

An overall view of the system is shown in figure 3K.

Let us denote $x = z/z_0$, $y_э = z_э/z_0$, $b = \nabla H/\left(\frac{2\pi}{c} j\right)$.

The field produced is given by the expressions of (20).

The field in the forming winding is given by the expressions of (21).

We shall write the field in the gap between the forming and shielding windings in the form obtained from the corresponding expressions for the field in the intermediate domain in the case of iron shielding (section 2.2) by means of the following substitution in the second terms under the sum sign: $d_n (1/y_э)^{3+4n} \to c_n$.

The field in the shielding winding is:

$$H_{эz}/(z_0 \nabla H) = H_{прz}/(z_0 \nabla H),$$

$$H_{э\varphi}/(z_0 \nabla H) = H_{пр\varphi}/(z_0 \nabla H) + \frac{1}{b}\cdot(x - y_э^2/x),$$

$$A_э/(z_0^2 \nabla H) = A_{пр}/(z_0^2 \nabla H) - \frac{1}{2b}(x^2 - y_э^2 - 2y_э^2 \ln(x/y_э)).$$

The system of equations is:

$$x^2(\varphi)\sin 2\varphi = \sum_{n=0}^{N}\left[d_n\cdot\left(\frac{1}{x(\varphi)}\right)^{2+4n} + c_n y_э\left(\frac{x(\varphi)}{y_э}\right)^{2+4n}\right]\sin(2+4n)\varphi,$$

$$0 = \sum_{n=0}^{N}\left[d_n\left(\frac{1}{y(\varphi)}\right)^{2+4n} + c_n y_э\left(\frac{y(\varphi)}{y_э}\right)^{2+4n}\right]\cdot\sin(2+4n)\varphi,$$

$$x^2(\varphi) = 1 + b\Big(x^2(\varphi)\cdot\cos 2\varphi + \sum_{n=0}^{N}\left[d_n\cdot\left(\frac{1}{x(\varphi)}\right)^{2+4n} - c_n y_э\left(\frac{x(\varphi)}{y_э}\right)^{2+4n}\right]\cos(2+4n)\varphi\Big),$$

$$y^2(\varphi) = y_э^2 + b\sum_{n=0}^{N}\left[d_n\cdot\left(\frac{1}{y(\varphi)}\right)^{2+4n} - c_n y_э\cdot\left(\frac{y(\varphi)}{y_э}\right)^{2+4n}\right]\cos(2+4n)\varphi.$$

where $x(\varphi) = r(\varphi)/r_0$, $y(\varphi) = r_э(\varphi)/r_0$,

$r(\varphi)$ - is the boundary of the forming winding

$r_э(\varphi)$ - is the boundary of the shielding winding.

By using the expressions of (22) we can find the field which is produced by the forming and shielding windings on the horizontal diameter of the domain of formation.

Figure 21 shows the windings shapes with b =0.4 for several screening radii $r_э/r_0$, obtained as a result of a numerical solution of the system; to save space on the drawing, all the dimensions which relate to shielding windings have been reduced $r_э/r_0$ times.

In figure 22 A the maximum relative thicknesses $\Delta_{max}/r_0 = (r(\varphi)_{max} - r_0)/r_0$ of the forming windings with equal values of the parameter b are shown as functions of the internal radius of the current shielding $r_э/r_0$. The dotted curve in the lower part of the figure shows the maximum relative thickness $\Delta_{эmax}/r_0 = (r_э(\varphi)_{max} - r_0)/r_0$ of the shielding winding with the parameter b = 0.6.

In figure 22 B (22 C) the relative areas S_ϕ/r_0^2 (S_D^2/r_0^2) of one lobe of the forming (shielding) windings with various values of the parameter are shown as functions of the internal radius of the current shielding $r_э/r_0$.

We shall designate by W_0 ($W_0 = (r_0 \nabla H)^2 r_0^2/16$) the energy of the magnetic field produced in the circle.

In figure 23 the relative field energies in the metal of the shielding winding $W_{0\,кр}/W_0$, in the metal of the forming winding $W_{мет}/W_0$, in the gap between the forming and shielding windings $W_{нр}/W_0$, and the total field energy

$$W_{полн}/W_0 \quad (W_{полн} = W_0 + W_{мет} + W_{нр} + W_{экр})$$

are shown as functions of the internal radius of the current shielding $r_э/r_0$ for windings with various values of the parameter b.

The corresponding value of the parameter b is shown near each curve on all of the graphs.

Table 4 shows the total force f_ξ acting on the "lobe" ABCD of the forming (and shielding) winding (fig.3 K) along the axis ξ and the total force f_n with which the parts ABC and ACD are pressed against one another for the case of a winding with b =0.4 for various internal radii of the current shielding $r_э/r_0$. The same table gives the first expansion co-efficients for the shape of the forming and (shielding) winding into a Fourier series:

$$r(\varphi)/r_0 = 1 + \sum_{n=0}^{N-1} \phi_{2+4n} \cdot \cos(2+4n)\varphi.$$

Table 4

Total forces and Fourier co-efficients for the shape of the "lobe" of a quadrupole winding with co-axial current shielding, the case $b = \nabla H/(\frac{2\pi}{c} j) = 0.4$

Forming winding

$r_э/r_0$	5	4	3	2	1.857
$f_3/(2F_0)$	1.676	1.645	1.52	0.243	-0.734
f_4/F_0	3.65	3.69	3.83	5.01	5.79
ϕ_2	0.485	0.489	0.501	0.596	0.65
ϕ_6	0.09	0.091	0.095	0.13	0.15
ϕ_{10}	-0.0024	-0.0024	-0.0025	-0.0053	-0.0097
ϕ_{14}	-0.0077	-0.008	-0.0092	-0.0192	-0.0249

Shielding Winding

$r_э/r_0$	5	4	3	2	1.857
$f_{э3}/(2F_0)$	0.0159	0.0494	0.222	2.57	4.49
$f_{э4}/F_0$	0.0038	0.019	0.054	0.728	1.42
$\phi_{э2}$	0.0015	0.0037	0.012	0.0743	0.1092
$\phi_{э6}$	$0.23\cdot10^{-5}$	$0.1\cdot10^{-4}$	$0.93\cdot10^{-4}$	0.002	0.0025
$\phi_{э10}$	$0.11\cdot10^{-5}$	$0.355\cdot10^{-5}$	$0.2\cdot10^{-4}$	$0.44\cdot10^{-4}$	$0.567\cdot10^{-3}$
$\phi_{э14}$	$0.75\cdot10^{-6}$	$0.10\cdot10^{-5}$	$0.21\cdot10^{-5}$	$0.125\cdot10^{-3}$	$0.36\cdot10^{-3}$

where $F_0 = \frac{(r_0 \nabla H)^2 r_0}{24\pi}$.

§ 4. Points of the winding where the maximum field value is achieved.

When designing magnets of the type examined, having superconductor windings, it is important to know the maximum field value in the domain of the winding. The field in the winding is determined in the general case by the formulas of (6) and in the various individual cases by the formulas (18, 21, 24). At the "centre" of the winding the field tends to zero and the maximum field value is attained on the surface of the winding.

In the case of unshielded magnets within the limits of infinitely-"thin" windings the field values on the internal and external surfaces of the winding on each given azimuth are identical; as the thickness of the winding increases, provided that the value of the field produced in the circle is fixed, the field values on the external boundary of the winding on each given azimuth falls.

If we surround such a winding with iron shielding and reduce its radius,whilst the values of the field produced in the circle and current density in the winding remain fixed, the "thickness" of the winding is reduced (for example figure 11, 15), and this means that, in accordance with (6) (and also (18, 21, 24) the field on the external boundary of the winding is also reduced. It follows from this, for example, that in the case of dipole and quadrupole magnets which are shielded or not by iron shielding the maximum field value on the external boundaries of the domain

is achieved at the nodal points of the windings (for example points **B**, D of figure 4), i.e for these magnets the maximum value of the field is achieved on the boundary of the forming domain.

If, however, the winding is surrounded by current shielding, the reduction in its radius, provided the values of the field produced in the circle and the current density in the windings remain fixed, leads to an increase in the "thickness" of the forming winding (for example figures 18 and 21) and this means that, in accordance with (6)(and also (18, 21 24)), it also leads to an increase in the field value on the external surface of the winding. In the case of the dipole field (paragraph 3), it is easy to show by using (18) that the field value at the point C (figure 3 D) becomes equal to the value of the field produced in the circle at the moment when the radius r of point C attains the value

$$r_c = r_0 \cdot (\alpha + \sqrt{1+\alpha^2}), \quad \alpha = H_0 / (\tfrac{2\pi}{c} j r_0).$$

When the radius of the current shielding is further reduced, point C becomes the point of the maximum field value.

An identical situation applies to the case of a quadrupole with current shielding (paragraph 3); by using (21) we find that at the moment when the radius r_c of point C (figure 3 K) reaches the point $r_c = r_0(1-\beta)$ with an increase in the radius of the current shielding, the field value at the point C attains a value of $r_0 \nabla H$, i.e. the field value at points B and D of figure 3 K. If the radius of the shielding is further

reduced, point C becomes that of the maximum field value. The field value at C for the cases of the dipole or quadrupole fields can easily be determined concretely by using as appropriate expressions (18) or (21) and the relative "thicknesses" of the windings in figures 13 or 16 - in the case of iron shielding, and in figures 19 or 22 - in the case of current shielding. The fields on the shielding winding is always smaller than on the forming winding.

III. FORMING TWO-DIMENSIONAL MAGNETIC FIELDS BY THE IRON-FREE METHOD IN THE ELLIPTICAL DOMAIN

The contents of this chapter are, in essence, a generalization of the results obtained for a circular domain in chapter I applied to the case of the elliptical domain; we shall therefore expound the problem in a similar manner to that used for chapter I, whilst attempting to avoid, in so far as is possible, any repetition in the arguments. We did not carry out any numerical calculations for the elliptical domains, but it is clear that if the method described in chapter I, paragraph 7 is used, it is possible to solve also the equations for "thick" windings which are obtained in this chapter for unshielded and shielded systems. The examination is best carried out in the elliptical system of co-ordinates (ξ , η), in which the boundary of the forming domain is one of the co-ordinate lines (see Appendix).

§ 1. Formulation of the problem and breakdown of the fields.

In an elliptical domain with semi-axes (a, b) (figure 24), it is necessary to produce a two-dimensional field $\vec{H}_0(r, \varphi)$ with the aid of currents which flow along conductors of infinite length perpendicular to the plane of the ellipse (a,b) and closely surrounding it. The field produced $\vec{H}_0(r, \varphi)$ is usually set in the form of an expansion into series in polar multipoles:

$$H_{0z}(z, \varphi) = \sum_{n=1}^{\infty} b_n z^{n-1} \sin(n\varphi + \psi_n),$$
$$H_{0\varphi}(z, \varphi) = \sum_{n=1}^{\infty} b_n z^{n-1} \cos(n\varphi + \psi_n). \qquad (25)$$

We should point out that the co-efficients b_n in these expansions (and throughout this chapter) are equal to the similar co-efficients in the expansions of (1) (and throughout chapter I) multiplied by the factor $1/r_0^{n-1}$. Let us change, in the expansion of the corresponding vector potential $A_0(r, \varphi)$, to the intermediate Cartesian system of co-ordinates (x,y):

$$A_0(z, \varphi) = -\sum_{n=1}^{\infty} \frac{b_n}{n} z^n \cos(n\varphi + \psi_n) =$$
$$= -\sum_{n=1}^{\infty} \frac{b_n}{n} \operatorname{Re}\{(ze^{i\varphi})^n e^{i\psi_n}\} = -\sum \frac{b_n}{n} \operatorname{Re}\{e^{i\psi_n}(x+iy)^n\}.$$

By using the formulas of the Appendix we shall now change to the elliptical system of co-ordinates:

$$A_0(\xi,\eta) = -\sum_{n=1}^{\infty} \frac{b_n}{n} \cdot \frac{d^n}{2^n} \cdot Re\left\{ e^{i\psi_n} \left(e^{(\xi-\beta)+i\eta} + e^{-(\xi-\beta)-i\eta} \right)^n \right\} =$$

$$= -\sum \frac{b_n}{n} \cdot \frac{d^n}{2^n} \cdot \left\{ \left[\left(e^{n(\xi-\beta)} + e^{-n(\xi-\beta)} \right) \cos n\eta \cdot \cos\psi_n - \right.\right.$$

$$\left. - \left(e^{n(\xi-\beta)} - e^{-n(\xi-\beta)} \right) \cdot \sin n\eta \cdot \sin\psi_n \right] +$$

$$\binom{n}{1} \cdot \left[\left(e^{(n-2)\cdot(\xi-\beta)} + e^{-(n-2)(\xi-\beta)} \right) \cos(n-2)\eta \cdot \cos\psi_n - \right. \quad (26)$$

$$\left. - \left(e^{(n-2)(\xi-\beta)} - e^{-(n-2)\cdot(\xi-\beta)} \right) \sin(n-2)\eta \cdot \sin\psi_n \right] + \cdots$$

$$\left. + \cdots \right\}. \qquad d = \sqrt{a^2 - b^2}. \quad \beta = \ln(d/2).$$

Here and in the subsequent text we shall use the designation

$$\binom{n}{k} = \frac{n \cdot (n-1) \cdots (n-k+1)}{k!}$$

Having grouped the terms of this series with the identical $\cos n\eta$ and $\sin n\eta$, we will obtain the expansion of the field formed into a series in elliptical multipoles. We shall begin with an examination of unshielded magnets, which is the simplest case.

As in the circular domain, the fastest drop in the field outside of the system occurs when the direct and reverse currents in the cross-section of the winding are equal, i.e. when the total flow in the cross-section is zero. In this case, the expansions of the vector magnetic potential and field in the external domain in elliptical multipoles have the form:

$$\mathcal{A}_{нар}(\xi,\eta)=\sum_{n=1}^{\infty} e^{-n(\xi-\beta)}\cdot(A_n\cos n\eta+B_n\cdot\sin n\eta),$$

$$H_{нар\,\xi}(\xi,\eta)=-\frac{1}{d\sqrt{\sin^2\eta+\operatorname{sh}^2(\xi-\beta)}}\cdot$$

$$\cdot\sum_{n=1}^{\infty} e^{-n(\xi-\beta)}\cdot n\cdot(-A_n\sin n\eta+B_n\cos n\eta),$$

$$H_{нар\,\eta}(\xi,\eta)=\frac{1}{d\sqrt{\sin^2\eta+\operatorname{sh}^2(\xi-\beta)}}\cdot \tag{27}$$

$$\cdot\sum_{n=1}^{\infty} e^{-n(\xi-\beta)}\cdot n(A_n\cos n\eta+B_n\sin n\eta).$$

$$d=\sqrt{a^2-b^2}.$$

§ 2. The "thin" winding of unshielded magnets

The "thin" winding can be considered as a current layer, and the boundary conditions on the boundary of the forming domain - the ellipse (a, b) have the form:

$$H_{нар\,\xi}(\xi_0,\eta)=H_{0\xi}(\xi_0,\eta),$$

$$H_{нар\,\eta}(\xi_0,\eta)-H_{0\eta}(\xi_0,\eta)=\frac{4\pi}{c}j(\eta)\sqrt{a^2\sin^2\eta+b^2\cos^2\eta}\cdot\Delta(\eta) \tag{28}$$

where $\Delta(\eta)=\xi(\eta)-\xi_0$ - is the thickness function of the winding,

$\xi(\eta)$ is the external boundary of the winding,

ξ_0 is the boundary of the forming domain, i.e. the ellipse (a, b).

Within the limits of $a=b=r_0$, by using the formulas of the Appendix, we find :

$$\Delta(\eta)=\ln r-\ln r_0=\ln\left(1+\frac{\Delta(\varphi)}{r_0}\right)\approx\Delta(\varphi)/r_0,$$

i.e. the thickness function $\Delta(\eta)$ becomes a relative thickness function of the circular domain $\Delta(\varphi)/r_0$, and the expressions of (28) become (3).

Let us assume that among the co-efficients of expansion (28) only one co-efficient b_n is non-vanishing, i.e. in the ellipse (a, b) a polar multipole of the order of n is formed. By using the first equation of (28) and the expansion in elliptical multipoles of the field of the polar multipole produced in the ellipse in accordance with (26), where only $b_n \neq 0$, we obtain the following expressions for the non-zero co-efficients of the expansion (27) of the field outside the system into a series in elliptical multipoles:

$$A_{n-2\kappa} = \binom{n}{\kappa} \frac{b_n}{n \cdot 2^n} \cdot (a^2 - b^2)^{n/2} \cdot \left(\left(\frac{a+b}{a-b}\right)^{n-2\kappa} + 1\right) \cos\psi_n, \tag{29}$$

$$B_{n-2\kappa} = \binom{n}{\kappa} \frac{b_n}{n \cdot 2^n} \cdot (a^2 - b^2)^{n/2} \cdot \left(\left(\frac{a+b}{a-b}\right)^{n-2\kappa} - 1\right) \cdot \sin\psi_n,$$

where the total κ varies within the limits of $0 \leqslant \kappa \leqslant n/2$.

If we substitute these co-efficients in (27), we obtain $\vec{H}_{\text{нар}}(\xi, \eta)$, - the field outside the system. If we use the $H_{\text{нар}}(\xi, \eta)$ obtained and the expansion corresponding to (26) for $H_{on}(\xi, \eta)$, we obtain from the second boundary condition (28) the equation for a "thin" winding of an iron-free unshielded magnet, producing in the ellipse (a, b) a field of a pure polar multipole of the order of n. Owing to the linearity

of the equations of (28) for the fields inside and outside the ellipse (a, b) and for the thickness function of the winding $\Delta(\eta)$, all of these values are subject to the principle of superposition. Consequently, to the formation of a random superposition (25) of polar multipoles in the ellipse (a, b) corresponds the following equation for a thin winding:

$$-\frac{j(\eta)}{j}\cdot\Delta(\eta)=\sum_{n=1}^{\infty}\frac{b_n}{\frac{2\pi j}{\alpha}\,\frac{a+b}{2}}\cdot\frac{\frac{a+b}{2}}{a^2\sin^2\eta+b^2\cos^2\eta}\cdot\frac{1}{2^n\cdot n}\cdot S_n, \qquad (30)$$

where $$S_n=\sum_{k=0}^{k\le n/2}\binom{n}{k}\cdot(n-2k)\cdot(a+b)^{n-2k}\cdot(a^2-b^2)\cdot\cos\left((n-2k)\eta+\tfrac{\pi}{n}\right).$$

This equation, in accordance with the known combination of coefficients b_n for the expansion of the field produced in the ellipse (a, b) into a series in polar multipoles determines the function $j(\eta)/j$ (which is stepped and alternating), and for a given j it also determines the thickness function of the winding $\Delta(\eta)$, i.e. the shape of the winding. The function $j(\eta)/j$ changes its sign at those points η, where the right hand side of equation (30) tends to zero and changes sign; at these points $\Delta(\eta) = 0$. As in the case of the circle we shall call these points "nodal".

All the subsequent reasoning is identical to that of the case of the circular domain (chapter I, paragraph 2) with the exception that η should be read instead of φ.

§ 3. The "thick" winding of unshielded magnets

As in the case of the circular domain of chapter I, paragraph 3, we may draw the following conclusions:

1. The external boundaries of the windings which produce in an elliptical domain (a, b) a two-dimensional field of a given configuration form a single-parametric family of lines

$$\xi(\alpha, \eta) = \xi_0 + \Delta(\alpha, \eta),$$

having nodal points η_{yz}, lying on the boundary of the domain of formation, i.e. on the ellipse (a, b) - the lines $\xi = \xi_0$;

2. The parameter of the family is the thickness parameter of the windings $\alpha = b_A \Big/ \left(\frac{2\pi}{C} j \cdot \frac{a+b}{2}\right)$, b_A is the co-efficient of the amplitude multipole of the field produced;

3. The position of the nodal points η_{yz} on the boundary ellipse (a, b) is determined exclusively by the configuration of the field produced;

4. The thickness function $\Delta(\alpha, \eta)$ is proportional to the parameter α .

These conclusions were shown to be true in paragraph 2 only for the case of the "thin" winding (i.e. when $\Delta(\alpha, \eta) \ll \xi_0$ or otherwise $\alpha \ll 1$).

As was done in chapter I, paragraph 3, we can show that conclusions 1, 2 and 3 are correct for a winding of any thickness, i.e. for any values of the parameter α (conclusion 4 is correct only for a thin winding). In accordance with this affirmation the position of the nodal points does not depend on the thickness of the winding and can be determined from the equation for the thin winding (30).

The nodal points break down the winding into a series of separate elementary parts, each of which have only one common nodal point with its neighbour. The current density is constant in value over the entire cross-section of the winding ($|j(\eta)| = j = \text{const}$) but changes in sign when it passes through each nodal point. In other words, in each two neighbouring elementary parts of the winding, currents which are identical in density j flow in opposite directions. Consequently, the vector potential of the magnetic field in the metal of each elementary part of the winding is described by the equation (the sign $j(\eta)$ is not of any consequence, and we can therefore simply write j)

$$\Delta A_{мет}(\xi, \eta) = -\frac{4\pi}{c} j.$$

Or, in accordance with the Appendix, in the elliptical system of co-ordinates:

$$\frac{1}{d^2[sh^2(\xi-\beta)+\sin^2\eta]} \cdot \left(\frac{\partial^2}{\partial \xi^2} + \frac{\partial^2}{\partial \eta^2}\right) \cdot A_{мет}(\xi, \eta) = \frac{4\pi}{c} j. \quad (31)$$

It is easy to check that the potential

$$A_{мет}(\xi, \eta) = A_0(\xi, \eta) - \frac{2\pi}{c} j \cdot \frac{d^2}{4} \cdot \{ch\, 2(\xi-\beta) - ch\, 2(\xi_0-\beta) +$$
$$+ \cos 2\eta\,(1 - ch\, 2(\xi-\xi_0)) - 2sh\, 2(\xi_0-\beta)\cdot(\xi-\xi_0)\}, \quad (32)$$

where $A_0(\xi,\eta)$ - the potential of the field produced inside the ellipse (a, b) (25 and 26), satisfies the equation (31). To the vector potential $A_{mem}(\xi,\eta)$ corresponds a magnetic field $\vec{H}_{mem}(\xi,\eta)$:

$$H_{mem\,\xi}(\xi,\eta) = H_{0\xi}(\xi,\eta) + \frac{\frac{\pi}{c} j d}{\sqrt{sh^2(\xi-\beta)\cdot sin^2\eta}} \cdot \sin 2\eta \cdot (1 - ch\,2(\xi-\xi_0)),$$

$$H_{mem\,\eta}(\xi,\eta) = H_{0\eta}(\xi,\eta) + \frac{\frac{\pi}{c} j d}{\sqrt{sh^2(\xi-\beta)+sin^2\eta}} \cdot \{sh\,2(\xi-\beta) - \cos 2\eta \cdot sh\,2(\xi-\xi_0) - sh\,2(\xi_0-\beta)\}. \quad (33)$$

It is obvious that $\vec{H}_{mem}(\xi_0,\eta) = \vec{H}_0(\xi_0,\eta)$ i.e. the boundary conditions on the boundary of the forming domain and the metal of the elementary part of the winding considered (the corresponding section of the ellipse (a, b)) are satisfied. Consequently $A_{mem}(\xi,\eta)$ and $\vec{H}_{mem}(\xi,\eta)$ are the desired vector potential and magnetic field in the metal of the conductor. As the elementary part of the winding which we have examined is not separated by anything and during the transition from one such part to another the only change is in the sign of $f(\eta)$ (i.e. the sign in front of j) and in the domain of the change in the variables (ξ,η) we know the potential and field throughout the winding.

It follows from the expressions of (33) that the configuration of the field in the metal of the conductor (for a

given elliptical domain (a, b)) is completely determined by the configuration of the field produced $\vec{H}_0(\xi, \eta)$.

If in equations (32) and (33) we make a boundary transition of $\beta \to -\infty$ which corresponds to the transition to the polar system of co-ordinates (see Appendix) we obtain respectively expressions (5) and (6) for the case of the circular domain, as must be the case.

By using (27) and (33) we can write the boundary conditions on the external boundary of the winding $\xi(\eta)$:

$$H_{0\xi}(\xi(\eta), \eta) \cdot \sqrt{sh^2(\xi(\eta)-\beta)+\sin^2\eta} + \frac{\pi}{c} j(\eta) \cdot \sin 2\eta \cdot (1 - ch\, 2(\xi(\eta)-\xi_0)) = \frac{1}{d} \sum_{n=1}^{\infty} e^{-n(\xi(\eta)-\beta)} \cdot n \cdot (-A_n \sin n\eta + B_n \cos n\eta),$$

$$H_{0\eta}(\xi(\eta), \eta) \cdot \sqrt{sh^2(\xi(\eta)-\beta)+\sin^2\eta} + \tag{34}$$

$$+ \frac{\pi}{c} j(\eta) \cdot d \cdot \{ sh\, 2(\xi(\eta)-\beta) - \cos 2\eta \cdot sh\, 2(\xi(\eta)-\xi_0) -$$

$$- sh\, 2(\xi_0-\beta) = \frac{1}{d} \cdot \sum_{n=1}^{\infty} e^{-n(\xi(\eta)-\beta)} n \cdot (A_n \cos n\eta + B_n \sin n\eta).$$

These are the equations for "thick" windings; they determine the field outside the system and the external boundary of the conductor $\xi(\eta)$ for unshielded magnets which in the ellipse (a, b) produced a field of $\vec{H}_0(\xi, \eta)$.

§ 4. Shielding

A system which produces a field in the elliptical domain can be shielded by surrounding it either with iron shielding or with a special current screening system - current shielding, as was proposed in /5,6 and 7/ for the case of "thin" windings. We shall confine ourselves here only to the case when the internal boundary of the shielding (iron or system of shielding currents) is an ellipse with semi-axes A and B, the ellipse being confocal with the boundary of the forming domain, i.e. the ellipse (a, b). Confocality denotes, in particular, that $A^2 - B^2 = a^2 - b^2$.

On the basis of considerations of the field decay rate in the intermediate domain between the forming and shielding windings, we shall confine ourselves only to those systems whose integral of the current density for the total cross-section of the forming winding is zero. In the case of current shieldings the requirement for the field decay rate outside the system results in the fact that the integral of the current density for the total cross-section of the shielding winding is also zero. The expansion of the vector potential and magnetic field of this system in the gap between the forming and shielding windings is of the form:

$$A_{np}(\xi, \eta) = \sum_{n=1}^{\infty} \left\{ e^{-n(\xi-\beta)} \cdot (A_n \cos n\eta + B_n \sin n\eta) + \right.$$
$$\left. + e^{n(\xi-\beta)} \cdot (C_n \cos n\eta + D_n \sin n\eta) \right\},$$

$$H_{np\xi}(\xi,\eta)=\frac{1}{d\sqrt{sh^2(\xi-\beta)+\sin^2\eta}}\cdot\sum_{n=1}^{\infty}n\Big\{e^{-n(\xi-\beta)}\cdot(-A_n\cos n\eta+$$
$$+B_n\cos n\eta+e^{n(\xi-\beta)}\cdot(-C_n\sin n\eta+D_n\cos n\eta)\Big\},\qquad(35)$$
$$H_{np\eta}(\xi,\eta)=\frac{1}{d\sqrt{sh^2(\xi-\beta)+\sin^2\eta}}\cdot\sum_{n=1}^{\infty}n\Big\{e^{-n(\xi-\beta)}\cdot(A_n\cos n\eta+$$
$$+B_n\sin n\eta-e^{n(\xi-\beta)}\cdot(C_n\cos n\eta+D_n\sin n\eta)\Big\}.$$

In order to write out the equations for the "thick" winding for a shielded system we must, as in the unshielded system, find the elementary parts of the winding. We shall therefore commence our examination by finding the equations for a "thin" winding and determining the position of the nodal points.

4.1. Current shielding

We shall examine only the case which is of greatest interest for practical purposes: when there is no field outside the shielding winding, i.e. the case of total shielding.

Having examined the "thin" forming and shielding windings as current layers we shall write the boundary conditions on them:

$$H_{np\xi}(\xi_0,\eta)=H_{0\xi}(\xi_0,\eta),$$
$$H_{np\eta}(\xi_0,\eta)-H_{0\eta}(\xi_0,\eta)=\frac{4\pi}{c}j(\eta)\cdot\Delta(\eta,\eta),\qquad(36)$$
$$H_{np\xi}(\xi_2,\eta)=0,$$
$$H_{np\eta}(\xi_2,\eta)=\frac{4\pi}{c}j_2(\eta)\cdot\Delta_2(\eta,\varphi),$$

where $\Delta(\alpha,\eta)=\xi(\alpha,\eta)-\xi_0$, $\Delta_э(\alpha_э,\eta)=\xi_э(\alpha_э,\eta)-\xi_{э0}$,

ξ_0 is the boundary of the forming domain

$\xi(\alpha,\eta)$ is the external boundary of the forming winding

$\xi_э$ is the internal boundary of the shielding winding

$\xi_э(\alpha_э,\eta)$ is the external boundary of the shielding winding

The thinness condition of the windings:

Let us suppose that among the co-efficients of expansion (25), there is only one co-efficient b_n which is non-vanishing, i.e. in the ellipse (a,b) a polar multipole of the order of n is produced.

From the third equation of system (36) we obtain

$$C_p=-A_p\cdot e^{-2p(\xi_э-\beta)}=-A_p\cdot\left(\frac{A-B}{A+B}\right)^p,$$

$$D_p=-B_p\cdot e^{-2p(\xi_э-\beta)}=-B_p\cdot\left(\frac{A-B}{A+B}\right)^p.$$

The components of the field in the intermediate domain (35) can now be written as follows:

$$H_{np\xi}(\xi,\eta)=\frac{1}{d\sqrt{\sin^2\eta+\mathrm{sh}^2(\xi-\beta)}}\cdot\sum_{n=1}^{\infty}n\left(e^{-n(\xi-\beta)}-e^{n(\xi-\beta)-2n(\xi_э-\beta)}\right)\cdot\left(-A_n\sin n\eta+B_n\cos n\eta\right),$$

$$H_{np\eta}(\xi,\eta)=\frac{1}{d\sqrt{\sin^2\eta+\mathrm{sh}^2(\xi-\beta)}}\cdot\sum_{n=1}^{\infty}n\left(e^{-n(\xi-\beta)}+e^{n(\xi-\beta)-2n(\xi_э-\beta)}\right)\cdot\left(A_n\cos n\eta+B_n\sin n\eta\right).\qquad(37)$$

By using the component $H_{np\xi}$ and the expansion in elliptical multipoles of the field of the polar multipole produced in the ellipse in accordance with (26), where only $b_n = 0$, we obtain from the first equation of system (36) the following equations for the non-zero co-efficients of expansion (35) of the field in the intermediate domain into a series in elliptical multipoles:

$$A_{n-2k} = -\frac{b_n}{n}\cdot\frac{d^k}{2^n}\cdot\cos\varphi_n\cdot\binom{n}{k}\cdot\frac{\left(\frac{a+b}{a-b}\right)^{n-2k}+1}{1\mp\left(\frac{a+b}{A+B}\right)^{2(n-2k)}},$$

$$B_{n-2k} = \frac{b_n}{n}\cdot\frac{d^n}{2^n}\cdot\sin\varphi_n\cdot\binom{n}{k}\cdot\frac{\left(\frac{a+b}{a-b}\right)^{n-2k}-1}{1\mp\left(\frac{a+b}{A+B}\right)^{2(n-2k)}}, \qquad (38)$$

where the integer k varies within the limits of $0 \le k \le n/2$. The sign at the top refers to the case of current shielding, whilst the sign at the bottom refers to the case of iron shielding (section 4.2). After substituting these co-efficients in (35) we obtain $\vec{H}_{np}(\xi, \eta)$, - the field in the gap between the forming and shielding winding. By using the $H_{np\xi}(\xi, \eta)$ obtained and the expansion in elliptical multipoles of the field of the n - th of the polar multipole produced in the ellipse (a, b) in accordance with (29) where only $b_n \neq 0$ we obtain from the second and fourth boundary conditions (36) equations for the "thin" forming and shielding windings of the n - th polar multipole. In view of the linearity of the equations of (36) for the fields $\vec{H}_0(\xi, \eta)$ and $\vec{H}_{np}(\xi, \eta)$ and for the thickness functions $\Delta(\eta)$ and $\Delta_3(\eta)$, all of these values are subject to the

principle of superposition. Consequently, to the formation in the ellipse (a, b) of the random superposition (25 and 26) of polar multipoles, correspond the equations for "thin" windings, obtained by summing the corresponding equations found above for n - th polar multipoles.

The equation for a "thin" forming winding is:

$$-\frac{j(\eta)}{j}\cdot\Delta(\eta)=\frac{1}{\frac{2\pi}{c}j\,\frac{a+b}{2}}\cdot\frac{\frac{a+b}{2}}{a^2\sin^2\eta+b^2\cos^2\eta}\cdot\sum_{n=1}^{\infty}{}'\frac{b_n}{n\cdot 2^n}\cdot S_{\phi n},$$

where $$S_{\phi n}=\sum_{k=0}^{k\le n/2}{}'\binom{n}{k}(a+b)^{n-2k}\cdot(a^2-b^2)^k\cdot(n-2k)\cdot$$

$$\cdot\left\{\frac{1\pm\left(\frac{A-B}{A+B}\right)^{n-2k}}{1\mp\left(\frac{a+b}{A+B}\right)^{2(n-2k)}}\cdot\cos\psi_n\cdot\cos(n-2k)\eta-\right. \qquad (39)$$

$$\left.-\frac{1\mp\left(\frac{A-B}{A+B}\right)^{n-2k}}{1\mp\left(\frac{a+b}{A+B}\right)^{2(n-2k)}}\cdot\sin\psi_n\cdot\sin(n-2k)\eta\right\}.$$

The upper sign refers to the case of current shielding, and the lower sign to the case of iron shielding (section 4.2).

The equation for a "thin" shielding winding is:

$$\frac{j_э(\eta)}{j_э}\cdot\Delta(\eta)=\frac{1}{\frac{2\pi}{c}j_э\,\frac{a+b}{2}}\cdot\frac{\frac{a+b}{2}}{A^2\sin^2\eta+B^2\cos^2\eta}\cdot\sum_{n=1}^{\infty}{}'\frac{b_n}{n\cdot 2^n}\cdot S_{эn},$$

where $$S_{эn}=\sum_{k=0}^{k\le n/2}{}'\binom{n}{k}(a+b)^{n-2k}\cdot(a^2-b^2)^k\cdot(n-2k)\cdot$$

$$\cdot\left\{\frac{\left(\frac{a+b}{A+B}\right)^{n-2k}+\left(\frac{a-b}{A+B}\right)^{n-2k}}{1-\left(\frac{a+b}{A+B}\right)^{2(n-2k)}}\cdot\cos\psi_n\cdot\cos(n-2k)\eta-\right. \qquad (39.э)$$

$$\left.-\frac{\left(\frac{a+b}{A+B}\right)^{n-2k}-\left(\frac{a-b}{A+B}\right)^{n-2k}}{1-\left(\frac{a-b}{A+B}\right)^{2(n-2k)}}\cdot\sin\psi_n\cdot\sin(n-2k)\eta\right\}.$$

These equations for a known combination of the co-efficients b_n determine the alternating step functions $j(\eta)/j$ and $j_3(\eta)/j$, and for given j and j_3 determine also the thickness functions of the forming $\Delta(\alpha, \eta)$ and shielding $\Delta_3(\alpha_3, \eta)$ windings, i.e. also their shapes ("thin" windings).

Having reduced the right hand sides of these equations to zero we determine the position of the nodal points. Consequently, we now know how the forming and shielding windings of a random thickness are broken down into their elementary parts. We can now proceed to an examination of the "thick" windings.

The magnetic field in the metal of a random elementary part of the forming winding is determined as before by the expressions of (33) whilst the field in the metal of the elementary parts of the shielding winding is similarly determined by the following expressions:

$$H_{эмет\,\xi}(\xi,\eta) = H_{пр\,\xi}(\xi,\eta) + \frac{\frac{\pi}{c} j(\eta)\, d \cdot \sin 2\eta \cdot (1 - ch\,2(\xi - \xi_0))}{\sqrt{sh^2(\xi-\beta) + \sin^2\eta}},$$

$$H_{эмет\,\eta}(\xi,\eta) = H_{пр\,\eta}(\xi,\eta) + \frac{\frac{\pi}{c} j(\eta)\, d}{\sqrt{sh^2(\xi-\beta) + \sin^2\eta}} \cdot \tag{40}$$

$$\cdot \left\{ sh\,2(\xi-\beta) - \cos 2\eta \cdot sh\,2(\xi-\xi_0) - sh\,2(\xi_0-\beta) \right\}.$$

The boundary conditions on the external boundaries of the forming $\xi(\eta)$ and shielding $\xi_3(\eta)$ winding are of the form:

$$\vec{H}_{мет}(\xi(\eta),\eta) = \vec{H}_{пр}(\xi(\eta),\eta),$$

$$\vec{H}_{э\,мет}(\xi_э(\eta),\eta) = 0.$$

By using the expressions (24), (33), (35) and (40) we can re-write these equations in the following form:

$$H_{0\xi}(\xi(\eta),\eta)\cdot\sqrt{sh^2(\xi(\eta)-\beta)+\sin^2\eta} + \frac{\pi}{c} j(\eta) d \cdot \sin 2\eta \cdot \left(1 - ch\,2(\xi(\eta)-\xi_0)\right) =$$

$$= \frac{1}{d}\sum_{n=1}^{\infty} n\left\{ e^{-n(\xi(\eta)-\beta)}\cdot\left(-A_n \sin n\eta + B_n \cos n\eta\right) + e^{n(\xi(\eta)-\beta)}\cdot\left(-C_n \sin n\eta + D_n \cos n\eta\right)\right\},$$

$$H_{0\eta}(\xi(\eta),\eta)\cdot\sqrt{sh^2(\xi(\eta)-\beta)+\sin^2\eta} + \frac{\pi}{c} j(\eta) d \cdot \left\{ sh\,2(\xi(\eta)-\beta) - \cos 2\eta \cdot sh\,2(\xi(\eta)-\xi_0) - sh\,2(\xi_0-\beta)\right\}$$

$$= \frac{1}{d}\cdot\sum_{n=1}^{\infty} n\left\{ e^{-n(\xi(\eta)-\beta)}\cdot\left(A_n \cos n\eta + B_n \sin n\eta\right) - e^{n(\xi(\eta)-\beta)}\cdot\left(C_n \cos n\eta + D_n \sin n\eta\right)\right\}, \quad (41)$$

$$\frac{1}{d}\sum_{n=1}^{\infty} n\left\{ e^{-n(\xi(\eta)-\beta)}\cdot\left(-A_n \sin n\eta + B_n \cos n\eta\right) + e^{n(\xi(\eta)-\beta)}\cdot\left(-C_n \sin n\eta + D_n \cos n\eta\right)\right\} + \frac{\pi}{c} j_э(\eta) d \sin 2\eta \cdot \left(1 - ch\,2(\xi(\eta)-\xi_0)\right) = 0,$$

$$\frac{1}{d}\sum_{n=1}^{\infty} n\left\{ e^{-n(\xi(\eta)-\beta)}\cdot(A_n\cos n\eta + B_n\sin n\eta) - \right.$$
$$- e^{+n(\xi(\eta)-\beta)}\cdot(C_n\cos n\eta + D_n\sin n\eta) +$$
$$+ \frac{\pi}{c} j_3(\eta)\, d\cdot\left\{ sh\,2(\xi(\eta)-\beta) - \cos 2\eta\cdot sh\,2(\xi(\eta)-\xi_0)\right.$$
$$\left.\left. - sh\,2(\xi_0-\beta)\right\} = 0.$$

These are the equations for "thick" windings of iron-free magnets with current shielding; they determine the field in the gap between the forming and shielding windings (the combination of A_n, B_n, C_n, and D_n) and the external boundaries of the forming $\xi(\eta)$ and screening $\xi_3(\eta)$ windings. Within the limits of $\xi(\eta) - \xi_0 \ll 1$ and $\xi_3(\eta) - \xi_3 \ll 1$, these equations for thick windings become equations for "thin" windings (39).

4.2. Iron shielding

We consider the magnetic permeability of the iron shielding to be infinite ($\mu = \infty$). We shall write the boundary conditions on a "thin" forming winding and on iron shielding:

$$H_{np\xi}(\xi_0,\eta) = H_{o\xi}(\xi_0,\eta),$$
$$H_{np\eta}(\xi_0,\eta) - H_{o\eta}(\xi_0,\eta) = \frac{4\pi}{c} j(\eta)\cdot\Delta(\xi_0,\eta), \qquad (42)$$
$$H_{np\eta}(\xi_3,\eta) = 0.$$

where $\Delta(\alpha,\eta) = \xi(\alpha,\eta) - \xi_0$, $\xi(\alpha,\eta)$ is the outer boundary of the forming winding. The thinness condition of the winding is: $\Delta(\alpha,\eta) \ll 1$. Let a polar multipole of the order of n be formed in the ellipse (a, b). From the third equation of system (42) we obtain

$$C_p = A_p \cdot e^{-2p(\xi_3-\beta)} = A_p \cdot \left(\frac{A-B}{A+B}\right)^p,$$
$$D_p = B_p \cdot e^{-2p(\xi_3-\beta)} = B_p \cdot \left(\frac{A-B}{A+B}\right)^p. \qquad (43)$$

The field components in the intermediate domain (35) can now be written as follows:

$$H_{np\xi}^{(\xi,\eta)} = \frac{1}{\sqrt{a^2\sin^2\eta + b^2\cos^2\eta}} \cdot \sum_{n=1}^{\infty} n \cdot \left(e^{-n(\xi-\beta)} + e^{n(\xi-\beta)-2n(\xi_3-\beta)}\right) \cdot \left(-A_n \sin n\eta + B_n \cos n\eta\right), \qquad (44)$$

$$H_{np\eta}^{(\xi,\eta)} = \frac{1}{\sqrt{a^2\sin^2\eta + b^2\cos^2\eta}} \cdot \sum_{n=1}^{\infty} n \left(e^{n(\xi-\beta)} - e^{n(\xi-\beta)-2n(\xi_3-\beta)}\right) \cdot \left(A_n \cos n\eta + B_n \sin n\eta\right).$$

Using from now on the component $H_{np\xi}$ and the expansion in elliptical multipoles of the field of the polar multipole formed in the ellipse in accordance with (26) where only $b_n \neq 0$ we obtain from the first equation of the system (42) again the equations (38) for non-zero co-efficients of the expansion (35) of the field in the intermediate domain into a series in elliptical multipoles. Let us recall that in (38) the lower sign corresponds to the case of iron shielding.

Having substituted these co-efficients in (44) we obtain $\vec{H}_{np}(\xi,\eta)$ - the field in the gap between the forming

winding and the iron shielding. By now using the second equation of (42), we obtain the equation for a "thin" winding of the n-th polar multipole. By virtue of the principle of superposition of "thin" windings, there is, corresponding to the formation of a random superposition (25) of polar multipoles in the ellipse (a,b) an equation for the "thin" winding, obtained by summing the corresponding equations of the n-th polar multipoles. As a result, we obtain the equation (39) where in the equation for $S_{\varphi n}$ the lower sign should be taken. Having reduced the right hand side of this equation to zero, we determine the position of the nodal points. Consequently we now have the forming winding of a random thickness is broken down into its elementary parts. We can now proceed to an examination of the "thick" winding.

The magnetic field $\vec{H}_{мет}(\xi, \eta)$ in the metal of a random elementary part of the forming winding is determined as before by the equations of (33), whilst the field in the gap between the winding and the iron screen is determined by the equations of (35).

The boundary conditions on the external boundary of the forming winding $\xi(\eta)$ and on the boundary of the iron shielding $\xi_э(\eta)$ are of the form:

$$\vec{H}_{мет}(\xi(\eta), \eta) = \vec{H}_{пр}(\xi(\eta), \eta),$$
$$H_{пр\eta}(\xi_э, \eta) = 0. \qquad (45)$$

By using (33) and (35), we find that the first equation of (45) leads to the first two equations of system (41) and the last

equation, as in the case of the "thin" winding leads to the relationships (43) between the co-efficients.

§ 5. Equations for "thin" windings and nodal points for the superposition of dipole and quadrupole fields.

We shall write out here the basic formulas for iron-free magnets with "thin" windings, which produce in an elliptical domain with the semi-axes a and b a field of the form (25 and 26) (the system of co-ordinates used in figure 1).

$$H_{oz}(z,\varphi) = H_o \sin\varphi + z\nabla H \sin(2\varphi+\psi), \quad (46)$$

$$H_{o\varphi}(z,\varphi) = H_o \cos\varphi + z\nabla H \cos(2\varphi+\psi).$$

and with the potential

$$A_o(z,\varphi) = -H_o z\cos\varphi - 0.5 z^2 \nabla H \cos(2\varphi+\psi).$$

Having used the formulas of the Appendix we change over in this expression to the elliptical co-ordinates:

$$A_o(\xi,\eta) = -H_o d\, ch(\xi-\beta)\cdot\cos\eta -$$

$$-\frac{\nabla H\cdot d^2}{4}\cdot\{(ch\,2(\xi-\beta)\cdot\cos 2\eta+1)\cos\psi - sh\,2(\xi-\beta)\cdot\sin 2\eta\sin\psi\}.$$

Consequently, the field produced, which is described in polar co-ordinates by the components of (46) has, in the elliptical system, the form:

$$H_{0\xi}^{(\xi,\eta)} = \frac{1}{\sqrt{sh^2(\xi-\beta)+\sin^2\eta}} \cdot \left\{ H_0\, ch(\xi-\beta)\sin\eta + \right.$$

$$\left. + \frac{\nabla H \cdot d}{2} \cdot \left(ch\,2(\xi-\beta)\sin 2\eta\cos\psi + sh\,2(\xi-\beta)\cos 2\eta\sin\psi \right) \right\}, \qquad (47)$$

$$H_{0\eta}(\xi,\eta) = \frac{1}{\sqrt{sh^2(\xi-\beta)+\sin^2\eta}} \cdot \left\{ H_0\, sh(\xi-\beta)\cos\eta + \right.$$

$$\left. + \frac{\nabla H \cdot d}{2} \cdot \left(sh\,2(\xi-\beta)\cos 2\eta\cos\psi - ch\,2(\xi-\beta)\sin 2\eta\cdot\sin\psi \right) \right\}.$$

1. The case of the unshielded magnet.

We find from (29) the non-zero co-efficients in the expansion (25) of the field outside the system into a series in elliptical multipoles:

$$A_1 = -H_0 a \sqrt{\frac{a+b}{a-b}}\,; \quad A_2 = -\frac{\nabla H}{8}(a^2-b^2)\cdot\left(\left(\frac{a+b}{a-b}\right)^2+1\right)\cos\psi;$$

$$B_1 = 0\,; \quad B_2 = -\frac{\nabla H}{8}(a^2-b^2)\cdot\left(1-\left(\frac{a+b}{a-b}\right)^2\right)\cdot\sin\psi.$$

The equation for the "thin" winding (30) is of the form:

$$-\frac{j(\eta)}{j}\cdot\Delta(\eta) = \frac{1}{a^2\sin^2\eta + b^2\cos^2\eta}\cdot$$

$$\cdot\left\{\frac{H_0}{\frac{2\pi}{c}j}\cdot\frac{a+b}{2}\cdot\cos\eta + \frac{\nabla H}{\frac{2\pi}{c}j}\cdot\left(\frac{a+b}{2}\right)^2\cdot\cos(2\eta+\psi)\right\}. \qquad (48)$$

2. The case of magnets with current or iron shielding. Let us recall that the internal boundary of the shielding is an ellipse with semi-axes A and B, which is confocal with the ellipse of the forming domain (a, b). In the formulas given

below the upper sign refers to the case of current shielding and the lower one to the case of iron shielding.

We obtain from (38) and (44) the non-zero co-efficients in expansions (37) and (44) of the field in the gap between the forming winding and the shielding into a series in elliptical multipoles.

$$A_1 = -H_0 \cdot \frac{\alpha\sqrt{\frac{\alpha+\beta}{\alpha-\beta}}}{1 \pm \left(\frac{\alpha+\beta}{A+B}\right)^2},$$

$$A_2 = -\frac{\nabla H}{8}\cdot(\alpha^2-\beta^2)\cdot\frac{1+\left(\frac{\alpha+\beta}{\alpha-\beta}\right)^2}{1 \mp \left(\frac{\alpha+\beta}{A+B}\right)^4}\cdot\cos\psi, \qquad (49)$$

$$B_2 = -\frac{\nabla H}{8}\cdot(\alpha^2-\beta^2)\cdot\frac{1-\left(\frac{\alpha+\beta}{\alpha-\beta}\right)^2}{1 \mp \left(\frac{\alpha+\beta}{A+B}\right)^4}\cdot\sin\psi.$$

The equations for a "thin" forming winding (39 ф) are of the form:

$$-\frac{j(\eta)}{j}\cdot\Delta(\eta) = \frac{1}{\alpha^2\sin^2\eta+\beta^2\cos^2\eta}\cdot\left\{\frac{H_0}{\frac{2\pi}{c}j}\cdot\frac{\alpha+\beta}{2}\cdot\frac{1 \pm \frac{A-B}{A+B}}{1 \mp \left(\frac{\alpha+\beta}{A+B}\right)^2}\cos\eta\right.$$

$$+\frac{\nabla H}{\frac{2\pi}{c}j}\cdot\left(\frac{\alpha+\beta}{2}\right)^2\cdot\left[\frac{1 \pm \left(\frac{A-B}{A+B}\right)^2}{1 \mp \left(\frac{\alpha+\beta}{A+B}\right)^4}\cdot\cos\psi\cdot\cos 2\eta -\right.$$

$$\left.\left. -\frac{1 \mp \left(\frac{A-B}{A+B}\right)^2}{1 \mp \left(\frac{\alpha+\beta}{A+B}\right)^4}\sin\psi\cdot\sin 2\eta\right]\right\}. \qquad (50)$$

The equation for a "thin" shielding winding (39.э) is of the form:

$$-\frac{j_э(\eta)}{j_э}\cdot\Delta_э(\eta)=\frac{1}{A^2\sin^2\eta+B^2\cos^2\eta}\cdot$$

$$\cdot\left\{\frac{H_0}{\frac{2\pi}{c}j}\cdot\frac{a+b}{2}\cdot\frac{\frac{a+b}{A+B}+\frac{a-b}{A+B}}{1-\left(\frac{a+b}{A+B}\right)^2}\cos\eta+\right.$$

$$+\frac{\nabla H}{\frac{2\pi}{c}j_э}\cdot\left(\frac{a+b}{2}\right)^2\cdot\left[\frac{\left(\frac{a+b}{A+B}\right)^2+\left(\frac{a-b}{A+B}\right)^2}{1-\left(\frac{a-b}{A+B}\right)^4}\cdot\cos\psi\cdot\cos2\eta-\right.$$

$$\left.\left.-\frac{\left(\frac{a+b}{A+B}\right)^2-\left(\frac{a-b}{A+B}\right)^2}{1-\left(\frac{a+b}{A+B}\right)^4}\cdot\sin\psi\cdot\sin2\eta\right]\right\}. \qquad (51)$$

We do not make any trivial reductions in these formulas in order to maintain the structure of the expressions. Having equated to zero the right hand parts of the equations for a "thin" winding for the magnet under consideration we determine the position of its nodal points. We may make the following statements about the windings of unshielded magnets, windings of magnets with iron shielding and about the forming and shielding windings of magnets having current shielding.

1. Dipole field: $H_0 \neq 0,\ \nabla H = 0$

In all there are two nodal points: $\eta_{y3} = \pm \pi/2$, which corresponds in polar co-ordinates to the angles $\psi_{y3} = \pm \pi/2$ (the elliptical equivalent of figure 2a);

2. Quadrupole field with axes which coincide with the axes of the elliptical forming domain

$$H_0 = 0,\ \nabla H \neq 0,\ \psi = \pm \pi/2,$$

in all four nodal points: $\eta_{y3} = 0, \pm \frac{\pi}{2}, \pi$, which corresponds in polar co-ordinates to the angles $0, \pm \frac{\pi}{2}, \pi$;

3. Quadrupole field with axes rotated through 45° in relation to the axis of the elliptical forming domain

$$H_0 = 0, \quad \nabla H \neq 0, \quad \psi = 0$$

As follows from the equations (50 and 51) the position of the nodal points is determined by the equation $\cos 2\eta = 0$, consequently $\eta_{y3} = \pm \pi/4, \pm 3\pi/4$. The connection with the polar angle is given by the expression $tg\, \varphi = \frac{b}{a} \cdot tg\, \eta$, consequently during transition from the case of the circular domain (figure 2) to the case of the elliptical domain, the nodal points are shifted in the direction of the ends of the major semi-axis;

4. In the case of the superposition of the fields ($H_0 \neq 0, \nabla H \neq 0$), as was done in paragraph 5 of chapter I for the case of the circular forming domain, we can make a qualitative examination of the transition from the magnet which produces a dipole field through the magnet for a constant gradient field to the quadrupole field magnet (the elliptical analogy of the sequence of images shown in figures 2 a to 2 e and figures 2A to 2E). After comparing the equations for the nodal points obtained from (50 and 51) with the equation obtained from (15) when $\psi = 0$ and $\psi = \pm \pi/2$, we see that they are of the same type and, apart from the substitution $\psi \rightarrow \eta$ differ only in the co-efficients. Consequently, all the results concerning the position of the nodal points during superposition

of the dipole and quadripole fields for the case of an elliptical domain are obtained from the corresponding results for the circular case of paragraph 5 chapter I by making the following substitutions:

1. Unshielded magnets:

$$H_0 \to H_0\,, \quad r_0 \nabla H \to \frac{a+b}{2} \nabla H.$$

2. Shielded magnets (the upper sign relates to current shielding and the lowersign to iron shielding)

Case $\psi = 0$.

$$H_0 \to H_0 \frac{1 \pm \frac{A-B}{A+B}}{1 \mp \left(\frac{a+b}{A+B}\right)^2},$$

$$r_0 \nabla H \to \frac{a+b}{2} \nabla H \cdot \frac{1 \pm \left(\frac{A-B}{A+B}\right)^2}{1 \mp \left(\frac{a+b}{A+B}\right)^4}.$$

Case $\psi = -\pi/2$.

$$H_0 \to H_0 \cdot \frac{1 \pm \frac{A-B}{A+B}}{1 \mp \left(\frac{a+b}{A+B}\right)^2},$$

$$r_0 \nabla H \to \frac{a+b}{2} \nabla H \frac{1 \mp \left(\frac{A-B}{A+B}\right)^2}{1 \mp \left(\frac{a+b}{A+B}\right)^4}.$$

§ 6. The position of the centre of the windings and maximum achievable fields for a given current density

As in the case of the circular domain, the diagram of the force lines of the magnetic field have "centres" which lie inside the metal of the forming winding. We shall call these the "centres" of the winding. The position of the "centre" characterizes qualitatively the "thickness" of the winding. In the "centre", the magnetic field is zero and consequently if we make use of the expressions of (33) for the field components in the metal of the winding and of (26) for the components of the field produced in the ellipse, we find the position of the "centres" of the winding. We shall confine ourselves to examining the position of the centres of windings which produce in the ellipse the dipole and quadrupole fields determined by the expressions of (46) (the system of co-ordinates used in figure 1).

1. Dipole field: $H_0 \neq 0$, $\nabla H = 0$; (the elliptical equivalent of figure 2 a).

It is clear from considerations of symmetry that the "centres" lie on the x axis. We easily find, for the "centre" of the right-hand"lobe" of the winding

where $\alpha = H_0 / (\frac{2\pi}{c} j a)$, x_y is the Cartesian co-ordinate of the "centre".

In the case of a "thin" winding, i.e. when $\alpha \ll 1$ we have: $x_4 = a(1 + \alpha/2)$.

From the equation for the "thin" winding for an unshielded dipole magnet, it follows that the outer boundary of the winding intersects the x axis at the point

$$x_2 = a \cdot \left(1 + \frac{\alpha}{2} \cdot \left(1 + a/b\right)\right).$$

By comparing x_y and x_2 we see that the "centre" of the "thin" winding when $a > b$ lies closer to the inner boundary of the winding, when $a = b$ it lies in the middle of the winding, and when $a < b$ it lies closer to the outer boundary.

In the case when $\left(\frac{\alpha}{2} \cdot \frac{a}{b}\right)^2 = \left(\frac{H_0}{\frac{4\pi}{c} j b}\right)^2 \gg 1$, i.e. in the case of an extremely "thick" winding we have:

$$\frac{x_y}{a} = \frac{\alpha}{2}\left(1 + \frac{a}{b}\right) = \frac{H_0}{\frac{2\pi}{c} j} \cdot \frac{a+b}{2b}, \qquad (52)$$

$$\text{i.e.} \quad H_0 = \frac{2\pi}{c} j \cdot \frac{2b}{a+b} \cdot x_y.$$

Consequently, during the production of the dipole field in the elliptical domain with a given current density we can obtain any field strength by increasing the thickness of the winding.

2. Quadrupole field

1. The case $\psi = 0$, i.e. the axes of the quadrupole field produced are rotated through 45° in relation to the axes of the elliptical forming domain (the elliptical equivalent of figure 2e).

From considerations of symmetry it is clear that the "centres" lie on the x and y axes. We easily find that the

"centres" of the right hand and upper "lobes" of the winding lie respectively at points

$$\frac{x_y}{a} = \frac{1}{\sqrt{1-\delta-(\delta/2)^2\cdot\left(\left(\frac{a}{b}\right)^2-1\right)}}; \quad \frac{y_y}{b} = \frac{1}{\sqrt{1-\delta-(\delta/2)^2\left(\left(\frac{b}{a}\right)^2-1\right)}},$$

where $\delta = \nabla H/\left(\frac{2\pi}{c} j\right)$, $(x_y, 0)$ and $(0, y_y)$ are the Cartesian co-ordinates of the "centres".

In the case of a "thin" winding, i.e. when $\delta \ll 1$, we have $x_y = a(1+\delta/2)$, $y_y = b(1+\delta/2)$.

It follows from the equation for a "thin" winding for an unshielded quadrupole magnet, that the outer boundary of the winding intersects the x and y axes at the points

$$x_2 = a + \frac{\delta}{b}\left(\frac{a-b}{2}\right)^2 = a + \frac{a\delta}{2}\cdot\left(1+\frac{a^2+b^2}{2ab}\right),$$

$$y_2 = b + \frac{\delta}{a}\left(\frac{a+b}{2}\right)^2 = b + \frac{b\delta}{2}\cdot\left(1+\frac{a^2+b^2}{2ab}\right).$$

By comparing x_y with x_2 and y_y with y_2, we see that the centres of the "lobes" of a "thin" quadrupole ($\psi = 0$) winding when $a \neq b$ lie always closer to the inner boundary of the winding, but when $a = b$, i.e. in the case of the circular forming domains they lie in the middle of the "thickness" of the winding.

It follows from the reality of the radicands in x_y/a and y_y/b that it is necessary that

$$\delta \leq \frac{2}{1+a/b} \quad \text{and} \quad \delta \leq \frac{2}{1+b/a},$$

Therefore, if $a > b$, then δ is limited on the upper side by the first relation; if, however, $b > a$, then it is limited by the second relation. Thus, if a is the major semi-axis of the forming ellipse, then

$$\nabla H \leq \frac{2\pi}{c} j \cdot \frac{2}{1 + a/b},$$

The sign of the equality corresponding to the limit of an infinitely "thick" winding.

Consequently when a quadrupole field (ψ =0) is produced in the elliptical domain, for a given current density we can, by increasing the thickness of the winding, obtain only the following limit value of the gradient:

$$\nabla H_{max} = \frac{2\pi}{c} j \frac{2}{1 + a/b}. \qquad (53)$$

We see that this limit value in the case of the elliptical domain ($a > b$) is always less than in the circular case ($a = b$).

2. The case $\psi = \pi/2$, i.e. the axes of the quadrupole field produced are directed along the axes of the elliptical forming domain (the elliptical equivalent of figure 2E).

Let us examine the right hand upper "lobe" of the winding.

By using (36) and (50) we obtain the following system for determining the elliptical co-ordinates η_y and ξ_y of the "centre" of the"lobe".

$$\sin 2\eta_y \cdot (1 - ch\,2(\xi_y - \xi_0)) = \delta \cdot sh\,2(\xi_y - \beta)\cdot \cos 2\eta_y,$$
$$sh\,2(\xi_y - \beta) - \cos 2\eta_y \cdot sh\,2(\xi_y - \xi_0) - sh\,2(\xi_0 - \beta) = \qquad (54)$$
$$= -\,2ch\,2(\xi_y - \beta)\cdot \sin 2\eta_y,$$

where $\delta = \nabla H / \left(\frac{2\pi}{c} j\right)$.

The first equation determines the dependence of η_y on ξ_y, which can be used to reduce the second equation to a quadratic equation in respect of δ^2; the solution of this determines $\delta(\xi_y)$ or, on the other hand, $\xi(\delta)$. The resulting expressions are, however, unwieldy and we will not give them here. An examination, however, of the limit cases of a "thin" ($\delta \ll 1$, $\xi_y - \xi_0 \ll 1$) and infinitely "thick" ($\xi_y - \xi_0 \gg 1$) winding is useful when a transition is made directly to the limits in the equations of (54).

If the winding is "thin" we obtain:

$$\eta_y = \pi/4, \quad \xi_y = \xi_0 + \delta/2,$$

or, in polar co-ordinates:

$$\varphi_y = arc\,tg\,(b/a), \quad r_y = \sqrt{\frac{a^2+b^2}{2}}\cdot(1+\delta/2).$$

From the equation for a "thin" winding (48) for an unshielded quadrupole magnet with $\varphi = \pi/2$ it follows that the external boundary of the winding on the azimuth $\eta = \pi/4$ is situated at the point

$$\xi_{2p} = \xi_0 + \delta \cdot \frac{2(a+b)^2}{a^2+b^2}.$$

or, in polar co-ordinates:

$$r_{2p} = \sqrt{\frac{a^2+b^2}{2}}\cdot\left(1+\frac{\delta}{2}\left(1+\frac{2ab}{a^2+b^2}\right)\right).$$

If we compare η_y and η_2 we see that the "centre" of the "lobe" of a "thin" winding lies closer to the external boundary, but when $a = b$ i.e. in the case of a circular shaping domain, the "centre" lies in the middle of the "thickness" of the winding.

For a winding having a random thickness we find that the following relation should always be satisfied

$$\delta \leq \sqrt{1-\left(\frac{a-b}{a+b}\right)^2} \quad \text{i.e.} \quad H \leq \frac{2\pi}{c} j \cdot \sqrt{1-\left(\frac{a-b}{a+b}\right)^2},$$

the sign of the equality being achieved for a winding of infinite thickness.

Consequently when a quadrupole field is produced ($\psi = \pi/2$) in an elliptical domain for a given current density, we can, by increasing the thickness of the winding obtain only the following limit value of the gradient

$$\nabla H_{max} = \frac{2\pi}{c} j \cdot \sqrt{1-\left(\frac{a-b}{a+b}\right)^2} \qquad (55)$$

The "centre" of the "lobe" of an infinitely "thick" winding has an azimuthal elliptical co-ordinate determined by the relation

$$\cos 2\eta_4 = \frac{a-b}{a+b},$$

To η_y in polar co-ordinates corresponds the angle

$$\varphi_4 = \operatorname{arc\,tg}\left(\frac{b}{a} \cdot \operatorname{tg} \eta_4\right).$$

IV. THE RECTANGULAR DOMAIN

We did not make a numerical calculation for this domain, and figure 25 is purely of a qualitative nature. The fact that the boundary of a rectangular domain is not set analytically as in the case of a circle or an ellipse leads to the fact that in the general case the equations for "thin" windings cannot be written in an elementary manner and the nodal points must be found by numerical means. It is clear from considerations of symmetry that for a dipole field parallel to one of the sides of a rectangle, the nodal points must be in the middle of adjacent sides (see figure 25 D). For a quadrupole field with axes parallel to the sides of the rectangle, we may state, on the basis of an examination of the Hand-Panofsky lattice (see chapter IV) that the nodal points co-incide with the vertices of the rectangle (see figure 25 K). In more complex fields we may, in order to obtain a numerical determination of the position of the nodal points, use a method similar to that described in /14/, in which an examination was made of the production of a dipole field in a rectangular domain by a system having a lens geometry of the Hand-Panofsky type (figure 35) with the iron moved away, and the winding being composed of one layer of rectangular conductors all having the same cross-section. The linear dimensions of the conductor cross-section must, generally speaking, be small in comparison with the linear dimensions of the forming domain (the "thin" winding). Having considered the field produced by the system, we can minimize its deviation from the dipole field, seen

from the mean square aspect, by selecting the appropriate current value in each conductor.

The results of /14/ are given in figure 27 D, in which the curves show the linearity of the current density for a winding of a constant thickness. However, it is possible also to produce a field which has a constant current density but in which the thickness of the "thin" winding varies, and in this case the curves of figure 25 D can be considered as the outside boundaries of such a winding (in figure 25 D the thickness of the "thin" winding is proportionally increased).

Let us assume that the position of the nodal points for a given field produced in the rectangle $\vec{H}_0(x,y)$ has been found. This means that we know the individual elementary parts of the winding in which flow currents that are constant and have the same density, but in each two adjacent elementary parts the directions of the currents are opposed. Consequently, the vector potential of the field inside each elementary part of the winding is described by the following equation (the sign of $j(\varphi)$ is of no consequence and consequently we may simply write j):

$$\Delta A(x,y) = -\frac{4\pi}{c} j. \qquad (56)$$

Below, the index 1 (2) denotesvalues which relate to those parts of the winding whose boundary with the forming domain is parallel to the x (y) axis.

It is easy to see that the vector potentials

$$A_{мем1}(x,y) = -\frac{2\pi}{c} j (y-b)^2 + A_0(x,y),$$
$$A_{мем2}(x,y) = -\frac{2\pi}{c} j (x-a)^2 + A_0(x,y), \qquad (57)$$

and

where $A_0(x,y)$ - the potential of the field produced in the rectangle $\vec{H}_0(x,y)$, - satisfy the equation (56). The following fields correspond to these potentials

$$H_{мем1x}(x,y) = \frac{4\pi}{c} j (y-b) + H_{ox}(x,y), \qquad (58)$$
$$H_{мем1y}(x,y) = H_{oy}(x,y),$$
$$H_{мем2x}(x,y) = H_{ox}(x,y), \qquad (59)$$
$$H_{мем2y}(x,y) = \frac{4\pi}{c} j (x-a) + H_{oy}(x,y).$$

It is obvious that $\vec{H}_{мем2}(x,b) = \vec{H}_0(x,b)$ and $\vec{H}_{мем2}(a,y) = \vec{H}_0(a,y)$, i.e. the boundary conditions on the boundary of the forming domain and metal of the elementary part of the winding under consideration are satisfied. Consequently $A_{мем2}(x,y)$ and $H_{мем2}(x,y)$, $A_{мем2}(x,y)$ and $H_{мем2}(x,y)$ are the desired vector potential and magnetic field in the metal of the elementary parts of the winding with the horizontal and vertical sections of the boundary respectively. As the elementary parts under consideration are not separated and during a transition from one of these to the next there is only a change in the sign of $j(x,y)$ i.e. the sign in front of j, we know the potential and field throughout the winding. In an examination of unshielded systems, it is convenient to re-write (58) and (59) in

polar co-ordinates, whilst the field outside of the system should be chosen in the form of (2); it is then easy to write out the system of boundary equations equivalent to (7), and by solving this with the method given in paragraph 7 of chapter I it is possible to find the shape of the "thick" winding and the field outside it.

We shall write the potentials and fields in the metal of the windings for a dipole and quadrupole field. The dipole field (figure 25 D):

$$A_0 = -H_0 x, \quad \vec{H_0} = H_0 \cdot \vec{e_y}.$$

$$A_1 = -\frac{2\pi}{c} j (y-\beta)^2 - H_0 x, \quad A_2 = \frac{2\pi}{c} j (x-\alpha)^2 - H_0 x,$$

$$H_{1x} = \frac{4\pi}{c} j (y-\beta), \qquad H_{2x} = 0, \qquad (60)$$

$$H_{1y} = H_0. \qquad H_{2y} = -\frac{4\pi}{c} j (x-\alpha) + H_0.$$

We should point out that the lines of force in the conductor two are parallel to the field produced, and therefore in the case of pulsed field conductor two can be assembled from flat sheets.

The quadrupole field (figure 25 K) is

$$A_0 = \frac{\nabla H}{2} (y^2 - x^2), \quad H_{0y} = \nabla H \cdot x, \quad H_{0x} = \nabla H \cdot y.$$

$$A_1 = -\frac{2\pi}{c} j (y-\beta)^2 + \frac{\nabla H}{2} (y^2 - x^2), \qquad (61)$$

$$H_{1x} = -\frac{4\pi}{c} j (y-\beta) + \nabla H \cdot y,$$

$$H_{1y} = \nabla H \cdot x.$$

$$A_2 = \frac{2\pi}{c} j (x-a)^2 + \frac{\nabla H}{2} \cdot (y^2 - x^2),$$
$$H_{2x} = \nabla H \cdot y.$$
$$H_{2y} = -\frac{4\pi}{c} j (x-a) + \nabla H \cdot x. \qquad (62)$$

If we take the Hand-Panofsky lens (figure 35), remove the iron and shorten slightly the conductors in a symmetrical manner whilst retaining, of course, the equality of the areas of all four conductors, the field in the forming domain will not be a purely quadrupole one. An analytical expression for this field was obtained in /15/ by the conformal mapping method. It was found that for certain relations between the dimensions of the forming domain, the thickness of the conductors and the degree of conductor shortening, the field in the forming domain is very close to quadrupole. The calculation method used in /15/, is not, however, valid if the system is shielded.

V. IRON-CONDUCTOR MAGNETS

In this type of magnet a specified field is produced in a given domain determined by the shape of the common boundary between the conductor and the iron which surrounds the forming domain. Consequently, the design of such magnets is, as a rule, more complex than that of the iron type of magnet in which only the iron has a specific shape. The great merit of this type of magnet is, however, its compactness, economic utilization of the energy in the magnetic field and particularly the fact that the maximum field value on the boundary of the iron does not exceed the maximum field value on the boundary of the field forming domain, in other words, the maximum field in magnets of this type always lies on the boundary of the useful domain. Thus, for example, in the case of a circular domain having a radius r_0 when a dipole field $\vec{H}_0$ or a quadrupole field ∇H is produced, the maximum field values on the boundary of the iron are H_0 and $r_0 \nabla H$ respectively and are achieved at the points where the boundary of the iron makes contact with that of the circle where the field is produced (see figures 26 and 28). When a constant gradient field is produced in the circle with a horizontal plane of symmetry (23), i.e. the field of a normal strong focusing accelerator, the maximum value of the field on the boundary of the iron, e.g. for the case when $r_0 \nabla H/H_0 = 0.2$, does not exceed 1.11 x H_0 whilst the maximum field value on the boundary of the forming circle is 1.2 x H_0. Let us recall that when such a field is produced by the "iron" method in normal cyclic accelerators, the field at the point closest to the forming

hyperbolic poles exceeds the maximum field on the edge of the useful aperture by several tens of per cent.

In this chapter we shall examine the iron-conductor magnets for forming in a circular domain two dimensional fields, of the most important types used in accelerator technology, and we shall give the results of a numerical calculation and show the way in which the analog problem can be solved for the elliptical domain and, in conclusion, examine in detail combined magnets (lenses) for producing a quadrupole field in a rectangular domain.

§ 1. Iron-conductor magnets for producing fields in a circular domain.

By using the expressions for the magnetic potentials of the field produced (1), the corresponding field in the conductor (5) and the field outside the forming winding, it is easy to construct a complete picture of the lines of force for any type of magnet examined in chapters I and II. If a closed non-hollow line is drawn (i.e. which contains within it any desired conductors), being perpendicular at each point to the lines of force of the magnetic field, and if all of the space outside this area is filled with iron, then the field inside this area will not change. If a perpendicular line is chosen which lies completely in the domain of formation and of the conductors, the system obtained will be in fact an iron-conductor magnet, which produces in the forming domain (or its enclosed part) the same field as produced by the

initial magnet (for the same current density in the parts of the conductor contained in this area). We shall confine ourselves to a study of only those cases when the selected perpendicular line lies outside the forming circle and passes through all of the nodal points (chapter I, paragraph 5). It appears that this line lies completely in the domain occupied previously by the conductor and passes, of course, through their "centres" (chapter I, paragraph 6).

As was pointed out in chapter I paragraph 3, the field in the conductor is determined completely by the field produced in the circle, and consequently the perpendicular lines chosen also are determined completely by this field and do not depend on the type of iron-free magnet (unshielded or shielded by a current or iron) chosen as the initial one.

If a field is produced in the circle with components $H_{0z}(r, \varphi)$ and $H_{0\varphi}(r, \varphi)$, the field components, $H_{\text{мет}z}(r, \varphi)$ and $H_{\text{мет}\varphi}(r, \varphi)$ in the metal of the winding conductors are determined by the expressions of (9) and the equation for the perpendicular line is of the form

$$\frac{1}{r}\frac{dr}{d\varphi} = \frac{H_{\text{мет}\varphi}(r, \varphi)}{H_{\text{мет}z}(r, \varphi)} = \frac{H_{0\varphi}(r, \varphi) + \frac{2\pi}{c} j\left(r - \frac{r_0^2}{r}\right)}{H_{0z}(r, \varphi)} \quad . (63)$$

This equation can be solved numerically, by choosing the nodal point as the initial one. The point of the desired perpendicular line which is most distant from the centre of the circle of formation

co-incides with the "centre" of the initial iron-free winding, the position of which is known (chapter I, paragraph 6).

1.1. Dipole Field

An overall view and the direction of the currents are shown in figure 26.

The field produced is determined by the expressions of (17), and the field in the metal of the conductor is determined by the expressions of (18).

The equation (63) assumes the form

$$\frac{dx}{d\varphi} = \frac{x\cdot\cos\varphi - \frac{1}{\alpha}(x^2-1)}{\sin\varphi},$$

where $x = r(\varphi)/r_0$, $\alpha = H_0/(\frac{2\pi}{c} j r_0)$.

$r(\varphi)$ is the desired perpendicular line.

This equation was solved numerically, for various values of the parameter a. The shapes for the perpendicular lines obtained are given in figure 26 (the symmetric half of one "lobe" of the winding is shown).

Having considered the field circulation along the line of force which passes along the vertical diameter AB of the circle, and having used the definition of parameter a we obtain the expression for the area of one "lobe" of the winding $S = r_0^2 \cdot a$

The energy of the field formed in the circle is:

$$W_0 = H_0^2 r_0^2 / 8.$$

The field energy in the metal of the winding is:

$$W(\alpha) = \frac{H_0^2}{8\pi} \cdot r_0^2 \cdot 4 \cdot \int_0^{\pi/2} \left\{ \frac{x^2-1}{2} - \frac{2}{\alpha}\left(\frac{x^3-1}{3} - (x-1)\right)\cos\varphi \right.$$

$$\left. + \frac{1}{\alpha^2}\left(\frac{x^4-1}{4} - (x^2-1) + \ln x\right)\right\} d\varphi,$$

where $x = r(\varphi)/r_0$

The function $W(\alpha)/W_0$ is shown in figure 27 (line $\delta = 0$).

1.2. Quadrupole Field

An overall view and the direction of the currents are shown in figure 28.

The field produced is determined by the expressions of (20) whilst the field in the metal of the conductor is determined by the expressions of (21).

The equation (63) assumes the form

$$\frac{dx}{d\varphi} = \frac{x^2 \cos(2\varphi) - \frac{1}{6}(x^2-1)}{x \sin(2\varphi)},$$

where $x(\varphi) = r(\varphi)/r_0, \quad \delta = \nabla H / \left(\frac{2\pi}{c} j\right).$

$r(\varphi)$ is the desired perpendicular line.

This equation was obtained and used in /23/. After solving

it numerically for various values of the parameter b we obtain the summary of the desired perpendicular lines shown in figure 28 (the symmetrical half of one "lobe" of the winding is shown). Having examined the field circulation along a line passing through two adjacent nodal points and using the definition of the parameter b, we will obtain the expression for the area of one "lobe" of the winding

$$S = b r_0^2/2$$

The energy of the field produced in the circle is:

$$W_0 = \frac{(r_0 \nabla H)^2}{16} r_0^2$$

The energy in the metal of the winding is

$$W_{мет}(b) = \frac{(r_0 \nabla H)^2}{8\pi} r_0^2 \cdot 8 \cdot$$

$$\cdot \int_0^{\pi/4} \left\{ \frac{x^4-1}{4} - \frac{2}{b} \cdot \left(\frac{x^4-1}{4} - \frac{x^2-1}{2} \right) \cos 2\varphi + \frac{1}{b^2} \left(\frac{x^4-1}{4} - (x^2-1) + \ln x \right) \right\} d\varphi,$$

where $x = r(\varphi)/r_0$.

The function $W_{мет}(b)/W_0$ is shown in figure 29.

1.3. Constant gradient field with a horizontal plane of symmetry.

An overall view of the system and current directions are shown in figure 30.

The field produced is determined by the equations (23), and the field in the metal of the winding by the expressions of (24).

The equation (63) assumes the form

$$\frac{dx}{d\varphi} = \frac{x\cos\varphi + \delta x^2 \cos 2\varphi - \frac{1}{a}(x^2-1)}{\sin\varphi + \delta x \sin 2\varphi},$$

where $x = r(\varphi)/r_0$, $a = H_0/\left(\frac{2\pi}{c} j r_0\right)$, $\delta = r_0 \nabla H / H_0$,

$r(\varphi)$ is the desired perpendicular line.

The perpendicular lines pass through nodal points, the position of which, for the system under consideration, is defined in chapter I, paragraph 5. By solving the equation numerically, and having taken the nodal points as the initial ones, we obtain the desired perpendicular lines.

Figure 30 shows the shapes of these lines for magnets with various values of a, for $\delta = 0.1$ and $\delta = 0.2$, respectively.

As in the case of an iron-free winding, the areas of both "lobes" are, of course, identical. Having considered the field circulation along any desired line passing through the nodal points of the system and using the determinations of a and δ we will obtain the following expression for the area of one "lobe" of the winding:

$$S = r_0^2 a \cdot f(\delta)$$

$$\oint(\delta) = \sqrt{1-x_1^2}\cdot(1+\delta x_1),$$

where $$x_1 = \left(\sqrt{1+8\delta^2}-1\right)/(4\delta).$$

When $\delta \ll 1$ $\quad \oint(\delta) \approx 1+\delta^2/2.$

The energy of the field produced in the circle is

$$W_0 = \frac{H_0^2 r_0^2}{8}\cdot(1+\delta^2/2).$$

The field energy in the metal of the conductor is:

$$W_{мет\,k}(\alpha,\delta) = \frac{H_0^2 r_0^2}{8\pi}\cdot 2\cdot\int_\alpha^\beta\left\{\frac{x^2-1}{2}+2\delta\frac{x^3-1}{3}\cos\varphi+\right.$$

$$\delta^2\cdot\frac{x^4-1}{4}+\frac{1}{\alpha^2}\cdot\left(\frac{x^4-1}{4}-(x^2-1)+\ln x\right)-$$

$$\left.-\frac{2}{\alpha}\cos\varphi\cdot\left(\frac{x^3-1}{3}-(x-1)\right)+2\frac{\delta}{\alpha}\left(\frac{x^4-1}{4}-\frac{x^2-1}{2}\right)\cos 2\varphi\right\}d\varphi,$$

where $x = r(\varphi)/r_0$, k = 1.2 is the number of the conductor studied (lobe).

To calculate the energy in the metal of conductor 1, it is necessary to pose $\alpha = 0$, $\beta = \varphi_{yz}$; and pose that for conductor 2 $\alpha = \varphi_{yz}$, $\beta = \pi$. The position of the nodal point φ_{yz} is determined in accordance with chapter I, paragraph 5 by the equation

$$\varphi_{yz} = \arccos\left(\left(-1/(2\delta)+\sqrt{2+(1/(2\delta))^2}\right)/2\right).$$

Figure 27 shows the functions $W_{мет\,1}(\alpha,\delta)/W_0$, $W_{мет\,2}(\alpha,\delta)/W_0$ and $W_{полн}/W_0$ for various values of the parameter δ ($W_{мет\,1} + W_{мет\,2} = W_{полн}$ - the total field energy in the winding). The corresponding value of δ is shown near each curve.

§ 2. Iron-conductor magnets for producing fields in an elliptical domain

Magnets for producing fields in an elliptical domain may be considered in exactly the same way as for the case of the circular domain. The field produced is usually set in the form of an expansion in polar multipoles; by changing to elliptical coordinates we obtain the vector potential $A_0(\xi, \eta)$ in the form of (26) and the corresponding components $H_{0\xi}(\xi, \eta)$ and $H_{0\eta}(\xi, \eta)$ of the field produced. The components $H_{\text{меди}\,\xi}(\xi, \eta)$ and $H_{\text{меди}}(\xi, \eta)$ of the field in the metal of the winding are determined by the expressions of (33).

The equation for the line perpendicular to the lines of force of the magnetic field and lying completely in the metal of the winding is of the form:

$$\frac{d\xi}{d\eta} = \frac{H_{\text{меди}\,\eta}(\xi, \eta)}{H_{\text{меди}\,\xi}(\xi, \eta)} =$$

$$\frac{H_{0\eta}(\xi,\eta)\cdot\sqrt{\operatorname{sh}^2(\xi-\beta)+\sin^2\eta} + \frac{\pi}{c} j d\left\{\operatorname{sh} 2(\xi-\beta) - \cos 2\eta \operatorname{sh} 2(\xi-\xi_0) - \operatorname{sh} 2(\xi_0-\beta)\right\}}{H_{0\xi}(\xi,\eta)\cdot\sqrt{\operatorname{sh}^2(\xi-\beta)+\sin^2\eta} + \frac{\pi}{c} j d\left\{1 - \operatorname{ch} 2(\xi-\xi_0)\right\}\cdot \sin 2\eta}$$

where $d = \sqrt{a^2 + b^2}$ (see Appendix).

The desired perpendicular line must pass through the nodal points and "centres" of the winding [x]. In the case of a numerical solution of the equation, it is convenient to take the nodal points as the initial points, the position of these being easy to determine from the equations for the "thin" winding (33, 42, 48). The expressions for $H_{0\xi}(\xi, \eta)$ and $H_{0\eta}(\xi, \eta)$ for the superposition of dipole and quadrupole fields are given by the expressions set out in chapter III, paragraph 5, and indications concerning the nodal points are also given there.

Let us compare the areas of the windings and the maximum achievable gradients of the fields of lenses with an elliptical (indexed "e") and circular (indexed "k")forming domains.

1. The elliptical lens with $\psi = 0$ (see (46)), i.e. the axes of the quadrupole field produced are turned through 45° in relation to the axes of the forming domain.

Having considered the field circulation along a line passing through two adjacent nodal points, we obtain:

$$\frac{\nabla H_э \cdot S_{\phi э}}{\nabla H_к \cdot S_{\phi к}} = \frac{j_э S_э}{j_к S_к},$$

---

x) It is, of course, possible to choose any other perpendicular line, but then it passes outside of the domain occupied by the conductor in the initial magnet.

where $S_э$ and $S_к$ are the areas of the "lobes" of the windings,

$S_{фэ}$ and $S_{фк}$ are the areas of the forming domains,

$j_э$ and $j_к$ are the current densities in the windings.

Consequently, for the production of a quadrupole field ($\psi = 0$) in the elliptical domain it is necessary to have as many ampere-windings as when producing the same field in a circular domain of the same area.

In accordance with (53) and (16) the maximum achievable gradients are: $\nabla H_{max} = \frac{2\pi}{c} j$,

$\nabla H_{э\,max} = \frac{2\pi}{c} j_э \cdot \frac{2}{1+a/b}$, where a and b are semi-axes of the ellipse ($a > b$),

2. The elliptical lens with $\psi = \pi/2$ (see 49) i.e. the axes of the quadrupole field produced are directed along the axes of the forming domain.

As before we obtain (the designations are the same):

$$\frac{\nabla H_э \cdot S_{фэ}}{\nabla H_к \cdot S_{фк}} \cdot \frac{a^2+b^2}{2ab} = \frac{j_э S_э}{j_к S_к} .$$

Consequently for producing a quadrupole field ($\psi = \pi/2$)

in an elliptical domain it is necessary to have $(a^2+b^2)/(2ab)$ times more ampere-terms than for the production of the same field in a circular domain of the same area.

In accordance with (55) the maximum achievable gradient in the elliptical domain is:

$$\nabla H_{max} = \frac{2\pi}{c} j \cdot \sqrt{1-\left(\frac{\alpha-\beta}{\alpha+\beta}\right)^2}.$$

§ 3. Iron-conductor magnets for producing a quadrupole field in a rectangular domain.

In the monographs /16, 17, 18/ mention is made of several types of such magnets (lenses), and references are given to original works in the form of preprints /19, 2o, 21, 22/ but unfortunately we were unable to obtain these and acquaint ourselves with them. Since no formulas of any sort are given in /16,17, 18/ which enable us to compare concretely, select and design magnets of this type, we will give here a short theory, particularly as all the results are obtained in this case by analytical methods without numerical calculations.

3.1. The Hand-Panofsky lattice

From an infinite number of long conductors of two types oriented in parallel and rectangular in cross-section, with an identical cross-sectional area, we shall establish a system, any section of which has the appearance of figure 31 in its cross-section. Along all the conductors flows a current the density

of which is constant over their cross-section and equal in value, but the direction of the currents in each of the two conductors which touch at angles are opposed and consequently in figure 31 these conductors (their cross-sections) have been shaded in with lines which are perpendicular to each other. This system is called the Hand-Panofsky lattice /24/. Let us combine the beginning of the system of co-ordinates with the centre D of one of the empty rectangles of the lattice. When $a \neq e$ there are two types of conductors (the cross-section 2a x 2e and 2a x 2d) and two types of empty rectangles (the cross-sections 2a x 2b and 2e x 2d). It follows from the condition of equality of the areas of the cross-sections of the conductors $a \cdot d = b \cdot e$ that:

1. the empty rectangles are similar

2. the empty rectangles having a cross-section 2a x 2b are surrounded by the conductors in such a way that the relation of the linear dimensions of the conductors to the linear dimensions of the empty rectangles along the x and y axes is identical and equal to e/a. Let us call this relation the thickness parameter of an empty rectangle having a cross-section 2a x 2b. The thickness parameter for an empty rectangle having a cross-section 2ex2d is equal to a/e.

An elementary box of symmetry is, for example, the rectangle BDEF. If we carry out the reflection in the planes BD and BF without changing the direction of the currents and without any translation in the x and y directions we obtain the entire lattice.

If $a = e$ there is only one type of conductor in the lattice and one type of empty rectangle (their cross-sections being identical), and therefore the box BDEF becomes symmetrical in relation to the turns around the axis P through an angle π by the change in the direction of the currents flowing back.

We shall call the empty rectangles and conductors, the quarters of which compose the box BDEF, by the letter which designates their centre. Let us consider the field which is produced in the box BDEF. Let us assume that in an empty rectangle B a quadrupole field of the type (61) is produced. Then the field in the conductors B and F should be of the form determined by (61 and 62). In view of the equal validity of B and E the field in E is also quadrupole. Let us write the potential of this field in the form

$$A_E = \frac{\nabla H_E}{2}\left((y-b-d)^2-(x-a-c)^2\right) + A_{OE}.$$

If we pose

$$\nabla H = \frac{4\pi}{c} j \frac{e/a}{1+e/a},$$
$$\nabla H_E = -\frac{a}{c}\nabla H$$
$$A_{OE} = \frac{\nabla H}{2}(b^2-a^2)(1+e/a),$$

where $j = -j_z$ is the current density along the conductor,

all of the boundary conditions on the boundaries between the empty rectangles B, E and the conductors D and F will be satisfied. By virtue of the symmetry, the solution obtained may be extended to the entire lattice.

Let us write for convenience the expressions obtained for the fields. The link between ∇H and j is given by the relation

$$\nabla H = \frac{4\pi}{c} j \frac{e/a}{1+e/a}, \qquad (64)$$

i.e. ∇H increases monotonously with a growth in the thickness parameter e/a of the rectangle where the field is produced, and reaches an upper limit of $\nabla H_{max} = \frac{4\pi}{c} j$ when $e/a \to \infty$.

The empty rectangle B (forming domain) is :

$$A_B = \frac{\nabla H}{2}(y^2 - x^2), \quad H_{Bx} = \nabla H \cdot y, \quad H_{By} = \nabla H \cdot x. \qquad (65)$$

The empty rectangle E is:

$$\begin{aligned} A_E &= -\frac{\nabla H}{2} \cdot \frac{a}{e} \cdot \left((y-b-d)^2 - (x-a-c)^2\right) + \frac{\nabla H}{2}(b^2-a^2)\left(1+\frac{e}{a}\right), \\ H_{Ex} &= -\nabla H \cdot \frac{a}{e}(y-b-d), \\ H_{Ey} &= -\nabla H \cdot \frac{a}{e}(x-a-e). \end{aligned} \qquad (66)$$

The conductor D is:

$$A_D = -\frac{2\pi}{c} j (y-b)^2 + \frac{\nabla H}{2}(y^2-x^2) =$$
$$= -\frac{\nabla H}{2}\left\{ x^2 + \frac{b}{d}(y-b-d)^2 - b^2 - bd \right\}, \qquad (67)$$
$$H_{Dx} = -\nabla H \frac{b}{d}(y-b-d), \quad H_{Dy} = \nabla H \cdot x.$$

The conductor F is:

$$A_F = \frac{2\pi}{c} j (x-a)^2 + \frac{\nabla H}{2}(y^2-x^2) = \frac{\nabla H}{2}\left\{\frac{a}{e}(x-a-e)^2 + y^2 - a^2 - ae\right\}, \qquad (68)$$
$$H_{Fx} = y \cdot \nabla H,$$
$$H_{Fy} = -\frac{y\pi}{c} j \cdot (x-a) + x\nabla H = -\frac{a}{e}\nabla H \cdot \{ x-a-e \}.$$

By using the expressions given above for magnetic potentials we can write the equations for the lines of force in the field:

The empty rectangle B: $y^2 - x^2 = C.$ (69)

The conductor D:

$$x^2 + \frac{b}{d}(y-b-d)^2 - bd = C. \qquad (70)$$

The empty rectangle E:

$$-\frac{a}{e}\left((y-b-d)^2 - (x-a-e)^2\right) + (b^2-a^2)\left(1+\frac{e}{a}\right) = C, \qquad (71)$$

The conductor F:

$$\frac{a}{e}(x-a-e)^2 + y^2 - a^2 - ae = C. \qquad (72)$$

where C is a constant.

It will be seen that the lines of force in the conductors D and F are confocal ellipses with centres at the points $D(x=0, y=\beta+d)$ and $F(x=a+c, y=0)$ respectively, the shape of the ellipses depending only on the thickness parameter (let us recall that $d/\beta = e/a$). When $e/a = 1$ the ellipses are converted into circumferences, this factor simplifies the production of the windings of such lenses by combinations, in order that the field is produced in the system in much less time than the duration of the actual pulse of the current in the windings. The diagrams of the lines of force (dotted lines) in the box of symmetry for the cases e/a = 0.4 and e/a = 1 are shown in figure 32.

3.2. The iron-conductor surface and three types of lenses

Let us draw any closed non-empty (i.e. enclosing within it any conductors) line which is perpendicular at every point to the lines of force of the magnetic field; if, now, the space outside the area is replaced by iron , the field inside will be as in the initial system. We shall be interested in the surfaces which in general contain one empty rectangle of the lattice, for example the rectangle B.

The equation for a line perpendicular to the lines of force of the field is:

$$dy/dx = -H_x/H_y.$$

By using expressions (65-68) for the components of the magnetic field, when solving this equation, we find that the perpendicular line which intersects the boundary of the conductor F and domain B at a point $y = y_0 < b$ (figure 32), is determined by the expressions:

In the domain of the conductor F: $y = y_0 \left(\frac{a+e-x}{e}\right)^{e/a}$,

In the forming domain B : $xy = a y_0 = x_0 b$,

In the conductor domain D : $x = x_0 \left(\frac{b+d-y}{d}\right)^{d/b}$.

It follows from these expressions that for given dimensions of the forming domain, i.e. for given a, b and y_0, the character of the line is determined by the thickness parameter e/a ($d/b = e/a$); this is natural since this is the parameter which determines the diagram of the force lines of the field (69-72). It can be seen that the perpendicular line, i.e. the iron-conductor boundary has the shape:

1. of a cupola, if $e/a < 1$,
2. of a triangle, if $e/a = 1$,
3. an acute angle, if $e/a > 1$.

Within the limits of $e/a \to \infty$ it has an exponentially decaying character in the conductors:

in the domain of the conductor F: $y = y_0 \cdot e^{-\left(\frac{x}{a} - 1\right)}$,

in the domain of the conductor D:

$$x = x_0 \cdot e^{-\left(\frac{y}{\delta} - 1\right)}.$$

Figure 32 shows a diagram of the lines of force (the dotted lines) and the lines perpendicular to them (the thin continuous line) in the box of symmetry BDEF (the boundaries of the conductors are the thick continuous lines, the boundaries of the box of symmetry are shown by the dashed line). For an empty rectangle B (top of fig. 32) is the thickness parameter $e/a = 0.4 < 1$, and consequently the perpendicular lines in the conductors surrounding this rectangle have a cupola shape (in respect to the domain B). For the empty rectangle E, the thickness parameter is $e/a = 2.5 > 1$ and consequently the perpendicular lines in the conductors surrounding this rectangle have the shape of an acute angle (in relation to the domain E). At the bottom of fig. 32 is a diagram of the lines of force and the lines perpendicular to these for the case $e/a = 1$. The figure is cut off at the line UV since the entire picture is symmetrical when rotated around the axis P through an angle π. The lines of force with an identical value of the constant C in expressions 69-72 are marked in fig. 32 with identical figures.

If the perpendicular line is chosen in the form of a rectangle, the middles of its sides coinciding with the centres of the conductors (the line DEF in figure 32, if B is a rectangle of formation) the quadrupole lens proposed by Hand and Panofsky will be obtained /24/.

If the perpendicular line passes through corners of the rectangle where the field is formed (the line DPE of fig. 32) a lens is obtained which, for convenience, we shall call the "Blewett" lens since in accordance with /17/ a rhomb-shaped quadrupole of this type ($e/a = 1$) was proposed and built by M.H. Blewett /22/.

If, however, the perpendicular line passes partly inside the initial rectangle of formation (for example the line DQTE, fig. 32, if B is the rectangle of formation, or DLMF if E is the rectangle of formation) then a quadrupole lens is obtained, which we shall call the Lublov - Morpurgo - Steffen lens, since in accordance with /17, 18/ a lens of this type was proposed in /19, 20 and 21*/.

In conclusion we shall quote the formulas which characterise these lenses.

3.3. The Lublov-Morpurgo-Steffen Lens

Figure 33 shows lenses of this type with a thickness parameter e/a equal respectively to 0.4; 1 and 2.5. The

---

* A similar sub-division into types is possible also in the case of iron-conductor magnets for circular and elliptical domains.

designations are set out only in the first drawing since they are the same for all the rest. We shall recall that ad = be.

The shape of the boundary of the conductor F :

$$y = y_0 \left(\frac{a+e-x}{e}\right)^{e/a},$$ in the limit of $e/a \to \infty$ $y = y_0 \cdot e^{-\left(\frac{x}{a}-1\right)}$

The shape of the boundary of the conductor D :

$$x = x_0 \left(\frac{b+d-y}{d}\right)^{d/b},$$ in the limit of $e/a \to \infty$ $x = x_0 \cdot e^{-\left(\frac{y}{b}-1\right)}$

The shape of the iron on the section between the conductors F and D :

$$xy = ay_0 = bx_0.$$

The gradient of the field formed is linked with the current density in the winding:

$$\nabla H = \frac{4\pi}{c} j \frac{e/a}{1+e/a}.$$

The surface of the domain where the field is formed is:

$$S_B = 4 y_0 a \cdot (1 - \ln(y_0/b)).$$

The area of one "lobe" of the winding is:

$$S_F = S_D = 2 y_0 a \frac{e/a}{1+e/a}.$$

It is interesting to note that this area, for a given value of the thickness parameter e/a depends only on the product of $y_0 a$.

The total current in one "lobe" of the winding is:

$$J_F = J_D = \frac{\nabla H}{(2\pi/c)} \cdot a y_0.$$

The ohmic losses per unit of time in one "lobe" of the winding are:

$$W_{OM} = \rho \cdot \left(\frac{\nabla H}{2\pi/c}\right)^2 \frac{a y_0}{2} \cdot \frac{1 + e/a}{e/a} .$$

It can be seen that the ohmic losses diminish with an increase in the thickness of the winding.

The energy of the magnetic field in the domain where the field is formed is:

$$W_B = 4 \cdot \frac{(\nabla H)^2}{8\pi} a y_0 b^2 \left\{\frac{1}{3}\left[1 + \left(\frac{y_0 a}{b}\right)^2\right] + \frac{1}{2}\left[1 - \left(\frac{y_0}{b}\right)^2\right]\left[\frac{1}{3} + \left(\frac{a}{b}\right)^2\right]\right\}.$$

The energy of the magnetic field in the "lobe" D is:

$$W_D = 2 \cdot \frac{(\nabla H)^2}{8\pi} \cdot a y_0 \left\{\frac{1}{3} y_0^2 \frac{e/a}{1 + 3e/a} + a^2 \frac{e/a}{3 + e/a}\right\}.$$

The energy of the magnetic field in the "lobe" F is:

$$W_F = 2 \frac{(\nabla H)^2}{8\pi} \cdot a y_0 \cdot \left\{\frac{1}{3}\left(\frac{y_0 a}{b}\right)^2 \cdot \frac{e/a}{1 + 3e/a} + b^2 \frac{e/a}{3 + e/a}\right\}.$$

The total field energy in all conductors of the lens is:

$$W = 2\left(W_D + W_F\right) = 4 \frac{(\nabla H)^2}{8\pi} a y_0 (a^2 + b^2) \left\{\frac{1}{3}\left(\frac{y_0}{b}\right)^2 \cdot \frac{e/a}{1 + 3e/a} + \frac{e/a}{e/a + 3}\right\}.$$

The magnet field components in the domain of formation B and in the conductors D and F are determined by expressions (65, 67 and 68).

The field value in the conductor D is:

$$H_D = \sqrt{H_x^2 + H_y^2} = \nabla H \cdot \sqrt{x^2 + \frac{b^2}{a^2}(y - b - a)^2},$$

in the conductor:

$$H_F = \nabla H \cdot \sqrt{\frac{a^2}{e^2}(x-a-c)^2 + y^2},$$

in the domain of formation of B

$$H_B = \nabla H \cdot \sqrt{x^2+y^2}.$$

By substituting H_D and H_F of the expression for the shape of the boundaries of the conductors D and F we determine the field on the boundary of the iron and conductor. It can, however, be seen immediately that the maximum field is always obtained at the point on the boundary of the domain of formation situated at the furthest distance from B; if r_{max} is the distance of this point from the centre, the maximum field value in the system generally and on the boundary of the iron is: $H_{max} = \nabla H \cdot r_{max}$. For example, in the geometry of Fig. 33, the point furthest removed from the centre is m, $r_{max} = \sqrt{a^2+y_0^2}$ and the maximum field is:

$$H_{max} = \nabla H \cdot \sqrt{a^2+y_0^2}.$$

3.4. The Blewett Lens

Figure 34 shows lenses of this type with a thickness parameter e/a of 0.4, 1 and 2.5 respectively. This type of lens can be considered as the frequency case of the Lublov-Morpurgo-Steffen lenses, and consequently all of the formulae of the previous sub-division are applicable here as well; in this case we must pose $y_0 = b$, and will only write the following:

The field energy in the domain where the field is formed:

$$W_B = 4 \cdot \frac{(\nabla H)^2}{8\pi} \cdot \frac{ab\,(a^2+b^2)}{3},$$

The total field energy in all conductors of the lens:

$$W = 4 \cdot \frac{(\nabla H)^2}{8\pi} \cdot \frac{ab\,(a^2+b^2)}{3} \left\{ \frac{e/a}{1+3e/a} + \frac{3e/a}{e/a+3} \right\}.$$

Consequently, when $e/a = 1$, $W/W_B = 1$ when $e/a \to \infty$ $W/W_B \to 10/3$

3.5. The Hand Panofsky lens

Figure 35 shows a lens of this type with a thickness parameter e/a = 0.4.

The gradient of the field formed is:

$$\nabla H = \frac{4\pi}{c} j \, \frac{e/a}{1+e/a} .$$

The current in one bar is:

$$J = \frac{\nabla H}{2\pi/c} \cdot ab\,(1+e/a).$$

The ohmic losses, per unit of time, in one bar are:

$$W_{OM} = \rho \left(\frac{\nabla H}{2\pi/c} \right)^2 \cdot \frac{ab}{2} \cdot (1+e/a)^2 \cdot a/e .$$

It can be seen that there is a minimum when e/a = 1,:

$$\nabla H = \frac{2\pi}{c} j, \quad W_{OM} = \rho \cdot \left(\frac{\nabla H}{2\pi/c} \right)^2 \cdot 2ab.$$

i.e. ∇H is equal to half of $\nabla H_{max} = 4\pi j/c$ which is obtained when $e/a \to \infty$.

The energy of the magnetic field in the region in which the field is formed is:

$$W_B = 4 \cdot \frac{(\nabla H)^2}{8\pi} \cdot \frac{ab}{3} \cdot (a^2 + b^2).$$

The field energy in the conductors F and D is :

$$W_F = W_D = \frac{(\nabla H)^2}{8\pi} \cdot \frac{2eb}{3} \cdot (a^2 + b^2).$$

The field energy in the four empty corners is:

$$W_{пуст} = 4 \frac{(\nabla H)^2}{8\pi} \cdot \frac{ed}{3} \cdot (a^2 + b^2).$$

The total magnetic field energy in the system is:

$$W_{полн} = W_B + 4W_F + W_{пуст} = 4 \frac{(\nabla H)^2}{8\pi} \cdot \frac{a^2+b^2}{3} \cdot ab(1+e/a)^2.$$

Let us write out also the following relations:

$$W_F/W_B = e/(2a), \quad W_{пуст}/W_B = (e/a)^2, \quad W_{полн}/W_B = (1+e/a)^2.$$

3.6. Comparison of iron-conductor lenses with rectangular and circular domains of formation

When a quadrupole field is formed in a circle with a radius r_0 (see Ch. I, §6 and Ch. V, §1), the area of one "lobe" of the winding on the gradient has the form:

$$S_к = \delta r_0^2/2, \quad \nabla H_к = \frac{2\pi}{c} j \cdot \delta$$

The thickness parameter (denoted by the letter b in Ch. I and II) is linked, in accordance with Ch. I, §6 with the position of the "centre" of the winding r_y by the relation:

$$\delta = \frac{r_y^2 - r_0^2}{r_0^2} = \frac{(1 + \Delta/r_0)^2 - 1}{(1 + \Delta/r_0)^2}, \quad r_y = r_0 + \Delta.$$

Δ characterises the "semi-thickness" of the winding.

When a quadrupole field is being formed in a rectangle, the field gradient is determined by the expression:

$$\nabla H_{np} = \frac{4\pi}{c} j_{np} \cdot \frac{e/a}{1+e/a},$$

the area of one "lobe" of the winding in the case of the Blewett lens is:

$$S_{np} = 2ab \cdot \frac{e/a}{1+e/a},$$

and in the case of the Hand-Panofsky lens is $S_{np} = 2eb$ (the designations of a, b and e are given in figs. 34 and 35).

These formulas give the following results:

1. The Blewett lens

$$\frac{S_{np} \cdot j_{np}}{S_k j_k} = \frac{\pi}{2} \cdot \frac{S_{\phi np}}{S_{\phi k}} \cdot \frac{\nabla H_{np}}{\nabla H_k}.$$

The Hand-Panofsky lens:

$$\frac{S_{np} \cdot j_{np}}{S_k j_k} = \frac{\pi}{2} \cdot (1+e/a) \cdot \frac{S_{\phi np}}{S_{\phi k}} \cdot \frac{\nabla H_{np}}{\nabla H_k},$$

where $S_{\phi np} = 4ab$ and $S_{\phi k} = \pi r_0^2$ are the areas of the rectangle and of the circle in which the field is formed.

Consequently, to form a quadrupole field in a rectangular domain using a Blewett lens $\pi/2$ times, and in the Hand-Panofsky case, $\pi/2\,(1 + e/a)$ times more ampere-turns than for forming the same field in a circular domain of the same area.

II. When $j_{пр} = j_к = j$ we have:

$$\frac{\nabla H_{пр}}{\nabla H_к} = 2\frac{e/a}{1+e/a}\cdot\frac{1}{\delta} = 2\cdot\frac{e/a}{1+e/a}\cdot\frac{(1+\Delta/r_0)^2}{(1+\Delta/r_0)^2-1}.$$

As only relative dimensions are introduced here (e/a and Δ/r_0) the conclusions drawn below do not depend on the absolute dimensions of the domains of formation.

Let $\Delta/r_0 \to \infty$, then $\nabla H_{пр} = \nabla H_{к\,max}$ when $e/a = 1$.

(In this instance $\delta = 1$; $\nabla H_{к\,max} = 2\pi j/c$; $S_{к\,max} = r_0^2/2$, $S_{пр} = ab$).

This means that for identical current densities in the windings in the lens with a rectangular domain of formation and a thickness parameter $e/a = 1$ a similar field is formed to that in a lens with a circular domain and with infinitely thick (radially) windings.

Let $\Delta/r_0 \to \infty$ and $e/a \to \infty$, then $\nabla H_{пр\,max} = 2\nabla H_{к\,max}$.

This means that for identical current densities in the windings the maximum achievable gradient in a lens with a rectangular domain of formation is twice as great as a lens with a circular domain.

(In this instance, $\delta = 1$, $\nabla H_{к\,max} = 2\pi j/c$, $S_{к\,max} = r_0^2/2$, $\nabla H_{пр\,max} = 4\pi j/c$, $S_{пр\,max} = 2ab$).

The last two conclusions are correct also for the case of the formation of quadrupole fields by the "iron-free" method, in view of the one to one correspondence between lenses of the iron-conductor and the initial "iron-free"type.

In conclusion, I wish to express my profound gratitude to G.I. Budker for his initiative in examining "thick" windings and the interest he has constantly shown in this work; to J.P. Blewett*) for discussing a number of questions and for the material which he gave me /1,5/; to F.A. Vodop'yanov**) and those who attended the seminar at the Institute of Nuclear Physics' laboratory for colliding beams for useful discussions of the results obtained.

---

*) Brookhaven National Laboratory, U.S.A.

**) Radiotechnical Institute of the USSR Academy of Science.

A P P E N D I X

When examining the formation of a field in an elliptical domain (figure 24) it is convenient to change over to an elliptical system of coordinates ξ, η, in which the boundary of the domain of field formation i.e. the ellipse with semi-axes a and b is one of the coordinate lines /25/:

$$x = d \cdot ch(\xi - \beta) \cdot \cos\eta,$$
$$y = d \cdot sh(\xi - \beta) \cdot \sin\eta,$$

where $d = \sqrt{a^2 - b^2}$, $\beta = \ln(d/2)$.

In these coordinates, the boundary ellipse (a,b) corresponds to the coordinate line

$$\xi_0 = \ln\left(\frac{a+b}{2}\right),$$

the domain $\beta < \xi < \xi_0$ is the inner domain of the ellipse, whilst $\xi_0 < \xi$ is the outer domain of the ellipse.

When $\beta \to -\infty$ the system of coordinates selected becomes polar $(a = b = r_0)$, in which case

$$r = \sqrt{x^2 + y^2} = e^{\xi}, \quad r_0 = e^{\xi_0}.$$

The square of the element of length:

$$dl^2 = d^2 \cdot (sh^2(\xi - \beta) + \sin^2\eta) \cdot (d\xi^2 + d\eta^2).$$

The element of area:

$$dS = d^2 \cdot (sh^2(\xi - \beta) + \sin^2\eta) \cdot d\xi\, d\eta.$$

Let us note that when $\xi = \xi_0$:

$$d^2 \cdot (sh^2(\xi - \beta) + \sin^2\eta) = a^2 \sin^2\eta + b^2 \cos^2\eta.$$

The Laplacian operator is of the form:

$$\Delta_{\xi,\eta} = \frac{1}{a^2(sh^2(\xi-\beta)+\sin^2\eta)} \cdot \left(\frac{\partial^2}{\partial\xi^2} + \frac{\partial^2}{\partial\eta^2}\right).$$

The curl of the vector directed along the z axis, perpendicular to the plane (ξ, η) has the components:

$$rot_\xi (A\cdot\vec{e}_z) = \frac{1}{a\sqrt{sh^2(\xi-\beta)+\sin^2\eta}} \cdot \frac{\partial A}{\partial \eta},$$

$$rot_\eta (A\cdot\vec{e}_z) = \frac{1}{a\sqrt{sh^2(\xi-\beta)+\sin^2\eta}} \cdot \frac{\partial A}{\partial \xi}.$$

References

1. Proceedings of the 1968 summer study on superconducting devices and accelerators. Brookhaven National Laboratory, 1968.

2. A.B. Nelidov, I.M. Samojlov, A.A. Sokolov. Zh.Tekh.Fiz. XXXVI, 1536, 1966.

3. G.B. Badalyan Zh. Tekh. Fiz. XXXIII, 345, 1963.

4. J.P. Blewett. Journ. Appl. Phys., 18, 968, 1947.

5. R.A. Beth. Brookhaven National Laboratory, Accelerator Dept. Report. AADD-102, 103, 110, 112 (1966). AADD-135 (1967).

6. R.A. Beth. IEEE Trans. Nucl. Sci. Ns-14, No. 3,386, 1967.

7. R.A. Beth. /1/ page 843.

8. J.P. Blewett. /I/.page 1042.

9. L.D. Landau, E.M. Livshits. Electrodynamics of continuous media. Fizmatgiz, 1959.

10. M.L. Oliphant. Proc. Roy. Soc. A., 234, 441, 1956.

11. A. Asner. /I/. page 866.

12. J.K. Yakobsen. The 25 GeV synchrophasotron. Control of scientific and technical data and displays. Moscow, 1956.

13. V.N. Melekhin, Letters to Zh. Eksper. Teor. Fiz., 9,552, 1969.

14. G. Parzen. /I/. page 860.

15. A.G. Septier. Nucl. Instrum. Meth., 7,217, 1960.

16. S.Ya. Yavor. Focusing charged particles with quadrupole lenses. "Atomizdat" Moscow, 1968.

17. A. Benford. Beam transportation of charged particles. Published by "Atomizdat", Moscow, 1969.

18. K.G. Steffen. Optics of high energy beams. Published by "Mir", Moscow, 1969.

19. D. Lublov. DESY-Notiz A2.78, Hamburg (1961).

20. M. Morpurgo, CERN. 64-34. 1964.

21. K.G. Steffen, DESY-Notiz A2.81, Hamburg (1961).

22. M.H. Blewett, BNL. Engineering Drawing.
D-12-187-6, Brookhaven. D-12-18-5, Brookhaven.

23. M.H. Blewett, G.T. Danby "Proceedings of the International Conference on Accelerators", Dubna, 1963, page 767, Atomizdat, Moscow, 1964.

24. L.N. Hand, W.K.H. Panofsky. Rev. Sci. Instr. 30, No. 10,927, 1959

25. F.M. Mors, G.F. Fensbakh. Methods of theoretical physics. Published by "Inostrannaya Literatura", 1958.

26. A.P. Ershov, G.I. Kozhukhin, I.V. Pottosin. Guide to the use of the Alfa system. Novosibirsk, "Nauka", Sib.Division, 1968.

F i g u r e s

Figure 1: (see text)

Figure 2: View (qualitative of windings which form in a circle a dipole (a) and quadrupole (e, E) field, a constant gradient field with horizontal (b,c and d) and vertical (B, C and D) planes of symmetry.

Figure 5: Unshielded dipole magnet. Shapes of the windings for various values of the parameter $a = H_0/(\frac{2\pi}{c} j r_0)$.

Figure 6: Unshielded dipole magnet and a magnet with a constant gradient field having a parameter $\delta = r_0 \nabla H/H_0$ with a value of 0.2. The relative area of the "lobe" of the winding S/r_0^2, the energy of the magnetic field in the metal of the winding $W_{мет}/W_0$, outside the winding $W_{нар}/W_0$ and a total energy $W_{полн}/W_0$ as a function of the parameter $a = H_0/(\frac{2\pi}{c} j r_0)$.

Figure 7: Unshielded quadrupole magnet. Shapes of the windings for various values of the parameter $\beta = \nabla H/(\frac{2\pi}{c} j)$.

Figure 8: Unshielded quadrupole magnet. The relative area of the "lobe" of the winding S/r_0^2, the energy of the magnetic field in the metal of the winding $W_{мет}/W_0$, outside the winding $W_{нар}/W_0$ and the total energy $W_{полн}/W_0$ as a function of the parameter $\beta = \nabla H/(\frac{2\pi}{c} j)$.

Figure 9: Unshielded magnet with a constant gradient field having a horizontal plane of symmetry; cases with the parameter $\delta = r_0 \nabla H/H_0$ having a value of 0.1 and 0.2. Shapes of the windings for various values of the parameter $a = H_0/(\frac{2\pi}{c} j r_0)$.

Figure 10: Unshielded magnet having a constant gradient field with a vertical plane of symmetry; cases with the parameter $\delta = r_0 \nabla H/H_0$ having a value of 0.1 and 0.2. Shapes of the windings for various values of the parameter $a = H_0/(\frac{2\pi}{c} j r_0)$.

Figure 11: Dipole Magnet with iron shielding; the case with the parameter $a = H_0/(\frac{2\pi}{c} j r_0)$ having a value of 0.6 and 1. Shapes of the windings for various positions of the shielding.

Figure 12: Dipole magnet with iron shielding. A picture of the lines of force of the magnetic field for the parameter $a = H_0/(\frac{2\pi}{c} j r_0)$ with a value of 1.8 and $r_э/r_0 = 3$.

Figure 13: Dipole magnet with iron shielding
A - maximum relative thicknesses of the windings Δ_{max}/r_0
B - relative areas of the "lobes" of the windings S/r_0^2
C - maximum fields on the surface of the iron shielding H_{max}/H_0 as a function of the position of the screen $r_э/r_0$ for various values of the parameter $a = H_0/(\frac{2\pi}{c} j r_0)$.

Figure 14: Dipole magnet with iron shielding. Relative field energies in the metal of the winding $W_{мет}/W_0$, outside the winding $W_{нр}/W_0$ and total field energy $W_{полн}/W_0$ as a function of the position of the shielding $r_э/r_0$ for various values of the parameter $a = H_0/(\frac{2\pi}{c} j r_0)$.

Figure 15: Quadrupole magnet with iron shielding; the case in which the parameter $b = \nabla H/(\frac{2\pi}{c} j)$ has a value of 0.4. Shapes of the windings for various positions of the shielding $r_э/r_0$.

Figure 16: Quadrupole magnet with iron shielding
A - maximum relative thicknesses of the windings Δ_{max}/r_0
B - relative areas of the "lobes" of the windings S/r_0^2,
C - maximum fields on the surface of the iron shielding H_{max}/H_0 as functions of the position of the shielding $r_э/r_0$ for various values of the parameter $b = \nabla H/(\frac{2\pi}{c} j)$.

Figure 17: Quadrupole magnet with iron shielding. Relative field energy in the metal of the winding $W_{мет}/W_0$, outside the winding $W_{нр}/W_0$, total field energy $W_{полн}/W_0$ as a function of the position of the shielding $r_э/r_0$ for various values of the parameter $b = \nabla H/(\frac{2\pi}{c} j)$.

Figure 18: Dipole magnet with current shielding; cases where the parameter $a = H_0/(\frac{2\pi}{c} j r_0)$ has a value of 0.6 and 1. Shapes of the windings for various positions of the shielding $r_э/r_0$.

Figure 19: Dipole magnet with current shielding

A - maximum relative thicknesses of the forming Δ_{max}/r_0 and shielding Δ_{3max}/r_0 windings.

B - relative areas of the "lobes" of the forming winding S/r_0^2

C - relative areas of the "lobes" of the shielding winding S_3/r_0^2 as functions of the position of the shielding r_3/r_0 for various values of the parameter $a = H_0/(\frac{2\pi}{c} j r_0)$.

Figure 20: Dipole magnet with current shielding. Relative fields in the metal of the winding W_{mem}/W_0 , between the windings W_{np}/W_0 , and total field energy W_{narH}/W_0 as functions of the position of the shielding r_3/r_0 for various values of the parameter $a = H_0/(\frac{2\pi}{c} j r_0)$.

Figure 21: Quadrupole magnet with current shielding; case where the parameter $b = \nabla H/(\frac{2\pi}{c} j)$ has a value of 0.4. Shapes of the windings for various positions of the shielding r_3/r_0 .

Figure 22: Quadrupole magnet with current shielding

A - maximum relative thicknesses of the forming Δ_{max}/r_0 winding

B - relative areas of the "lobes" of the forming winding S/r_0^2

C - relative areas of the "lobes" of the shielding winding S_3/r_0^2 as functions of the position of the shielding r_3/r_0 for various values of the parameter $b = \nabla H/(\frac{2\pi}{c} j)$.

Figure 23: Quadrupole magnet with current shielding. Relative energies of the field in the metal of the winding W_{mem}/W_0, between the windings W_{np}/W_0 and total field energy W_{narH}/W_0 as functions of the position of the shielding r_3/r_0 for various values of the parameter $b = \nabla H/(\frac{2\pi}{c} j)$.

Figure 25: View (qualitative) of dipole and quadrupole windings.

Figure 26: Iron-conductor dipole magnet. Overall view (qualitative) and shapes of the windings for various values of the parameter $a = H_0/(\frac{2\pi}{c} j r_0)$.

Figure 27: Iron-conductor magnet with a constant gradient field having a horizontal plane of symmetry. Relative energy of the magnetic field in sharp ($W_{mem\,OCTp}/W_0$) and blunt ($W_{mem\,Tyn}/W_0$) "lobes" of the winding and relative total field energy in the winding $(W_{mem\,aTp}+W_{mem\,Tyn})/W_0$ as functions of the parameter $a = H_0/\left(\frac{2\pi}{c} j r_0\right)$ for various values of $\delta = r_0 \nabla H/H_0$.

Figure 28: Iron-conductor quadrupole magnet. General view (qualitative) and shapes of the windings for various values of the parameter $b = \nabla H/\left(\frac{2\pi}{c} j\right)$.

Figure 29: Iron-conductor quadrupole magnet. Relative energy of the magnetic field in the winding W_{mem}/W_0 as a function of $b = \nabla H/\left(\frac{2\pi}{c} j\right)$.

Figure 30: Iron-conductor magnet with a constant gradient field having a horizontal plane of symmetry. Overall view (qualitative) and shapes of the windings for various $a = H_0/\left(\frac{2\pi}{c} j r_0\right)$ and for $\delta = (r_0 \nabla H)/H_0$ with a value of 0.1 and 0.2.

Figure 31: The Hand-Panofsky lattice.

Figure 32: Diagrams of the lines of force of the magnetic field and of the surfaces perpendicular to them in a box of symmetry in the Hand-Panofsky lattices, for the cases $e/a = 0.4$ and $e/a = 1$.

Figure 33: Lublov-Morpurgo-Steffen lenses.

Figure 34: Blewett lenses

Figure 35: Hand-Panofsky lens.

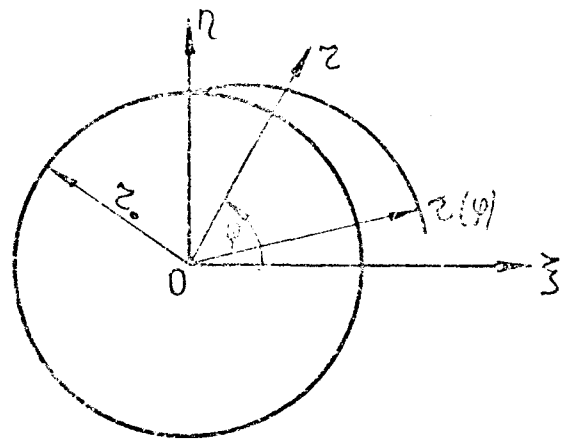

Fig. 1

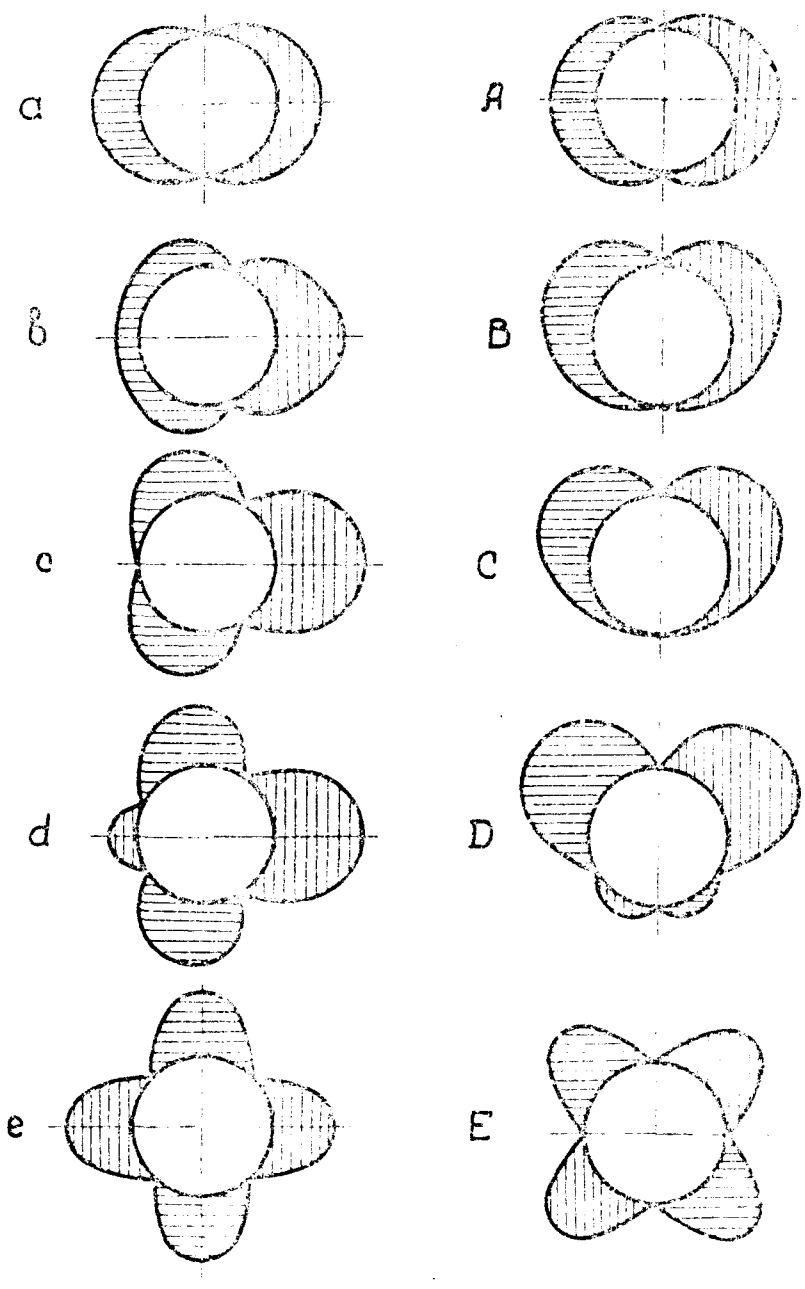

Fig. 2

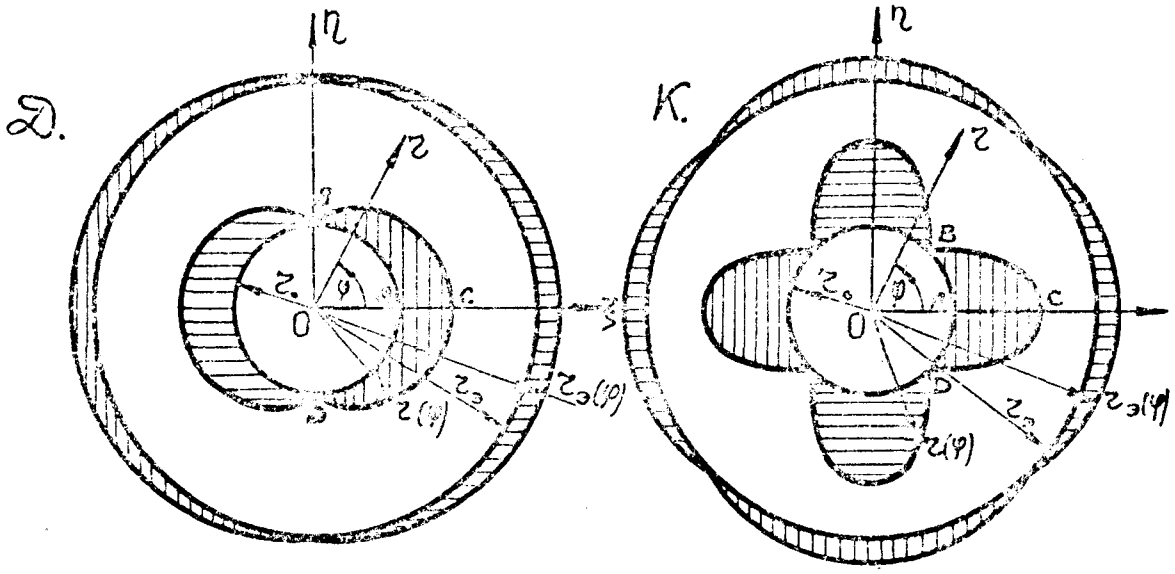

Fig. 3

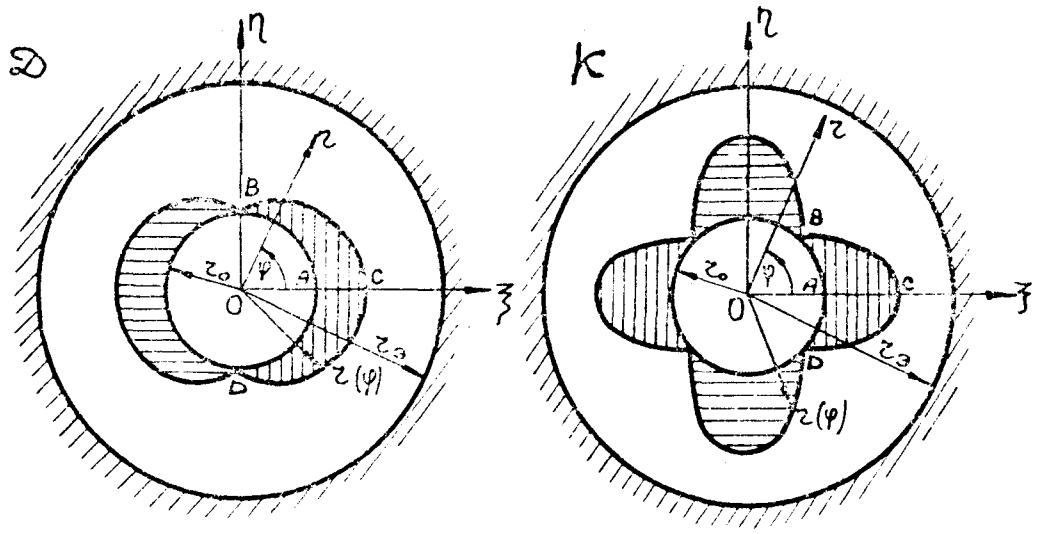

Fig. 4

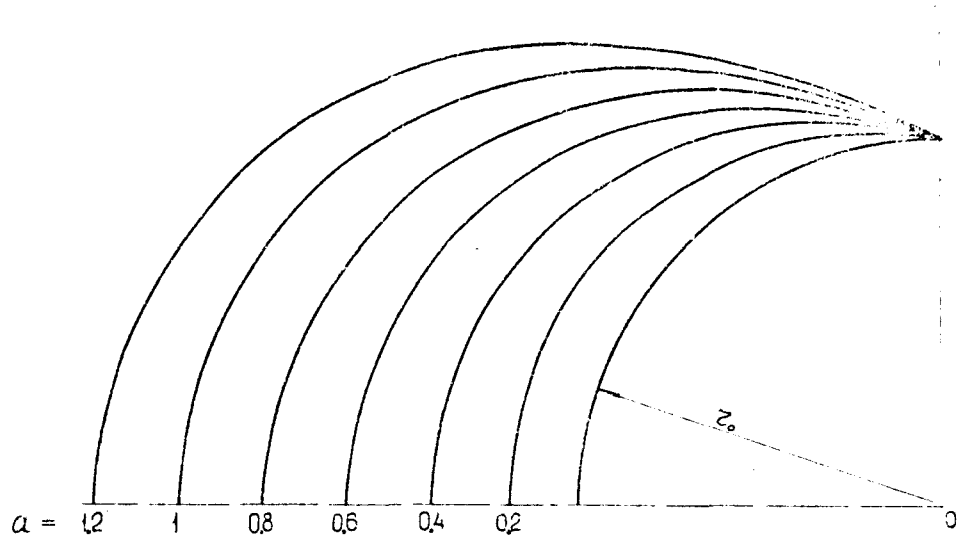
a =
1,2
1
0,8
0,6
0,4
0,2
0
z₀

Fig. 5

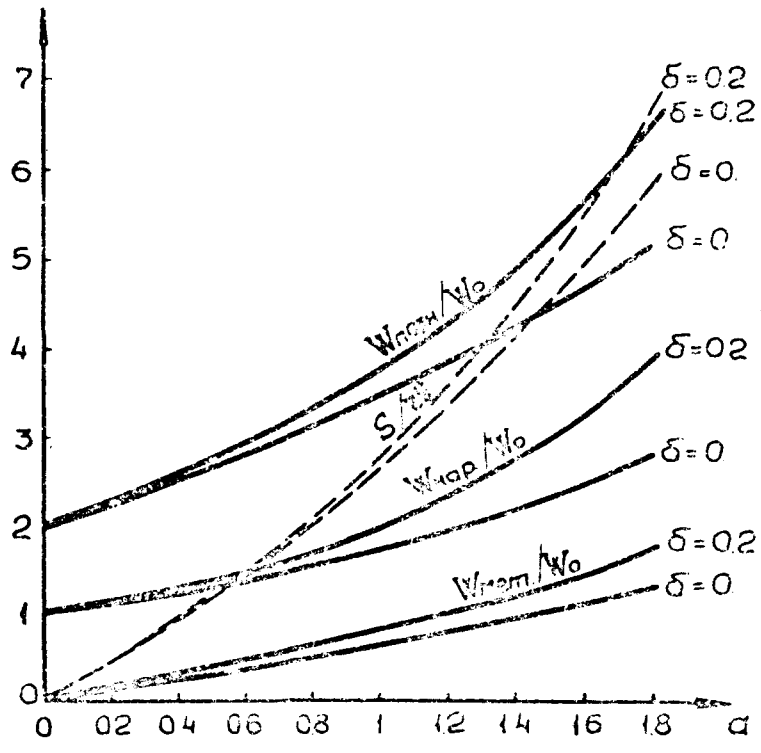
7
6
5
4
3
2
1
0
0
02
04
06
08
1
12
14
16
18
a
δ=02
δ=0.2
δ=0
δ=0
δ=02
δ=0
δ=0.2
δ=0
Wпогр/W₀
Wгар/W₀
Wпогр/W₀

Fig. 6

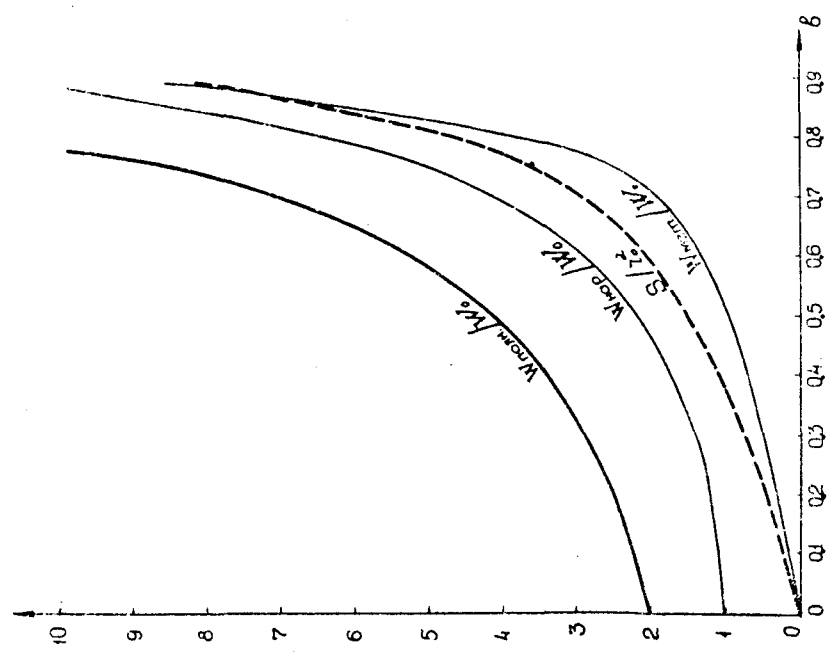
W/W0
W/W0 max
W/W0 min
W/W0 ср
0
0,1
0,2
0,3
0,4
0,5
0,6
0,7
0,8
0,9
1
2
3
4
5
6
7
8
9
10
β

Fig. 8

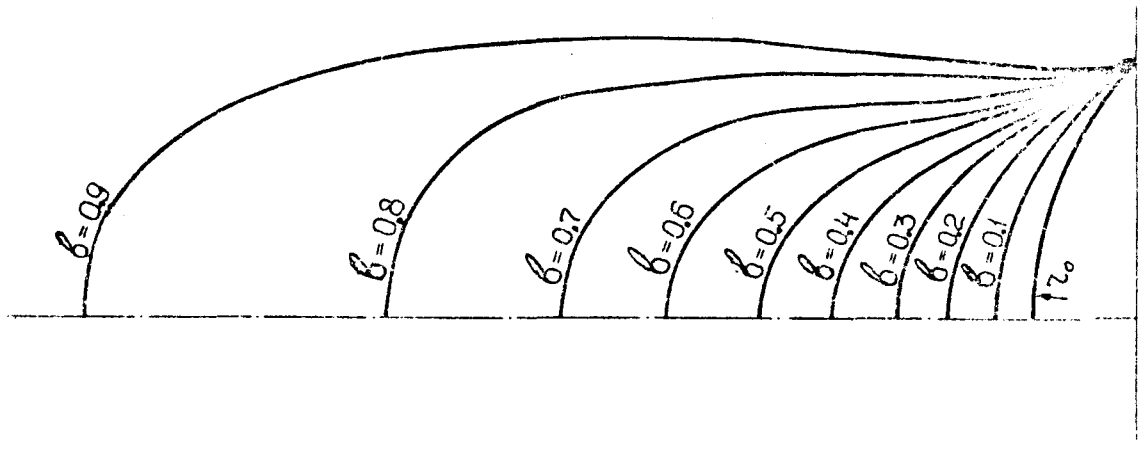
β=0,9
β=0,8
β=0,7
β=0,6
β=0,5
β=0,4
β=0,3
β=0,2
β=0,1
r₀

Fig. 7

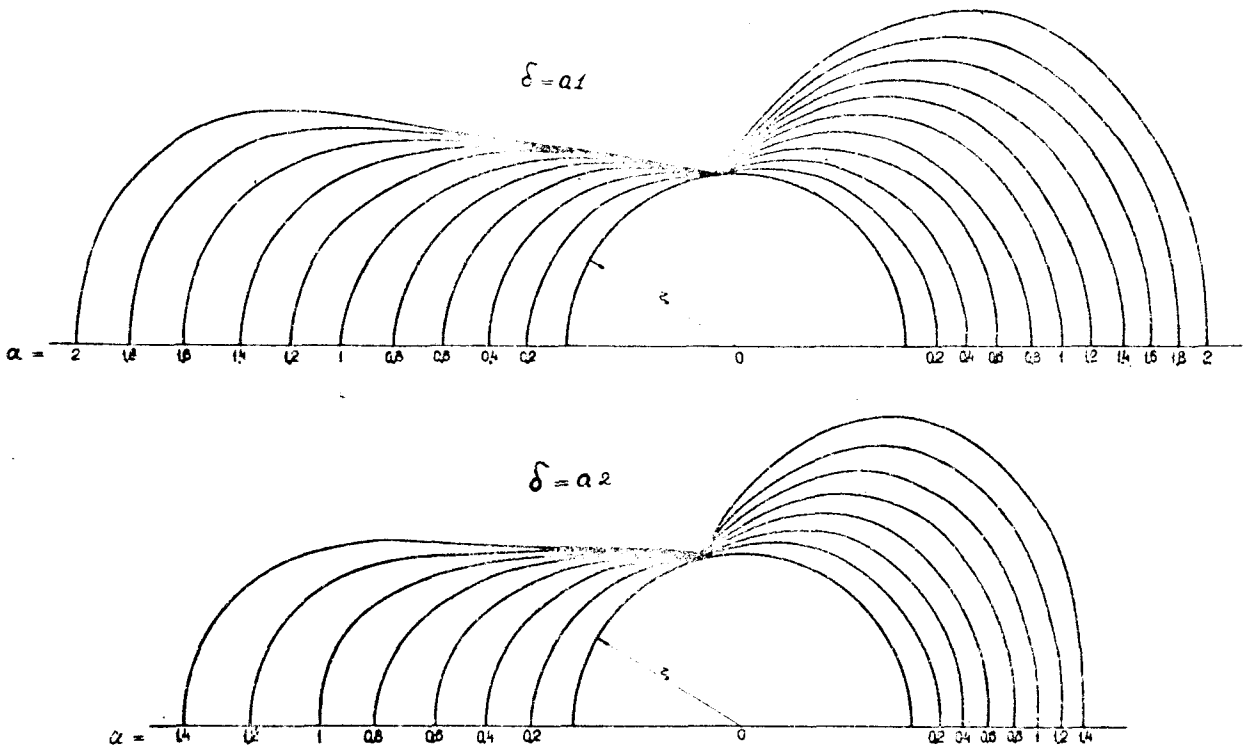
δ = a1
α =
2
1.8
1.6
1.4
1.2
1
0.8
0.6
0.4
0.2
0
0.2
0.4
0.6
0.8
1
1.2
1.4
1.5
1.8
2
δ = a2
α =
1.4
1.2
1
0.8
0.6
0.4
0.2
0
0.2
0.4
0.6
0.8
1
1.2
1.4

Fig. 9

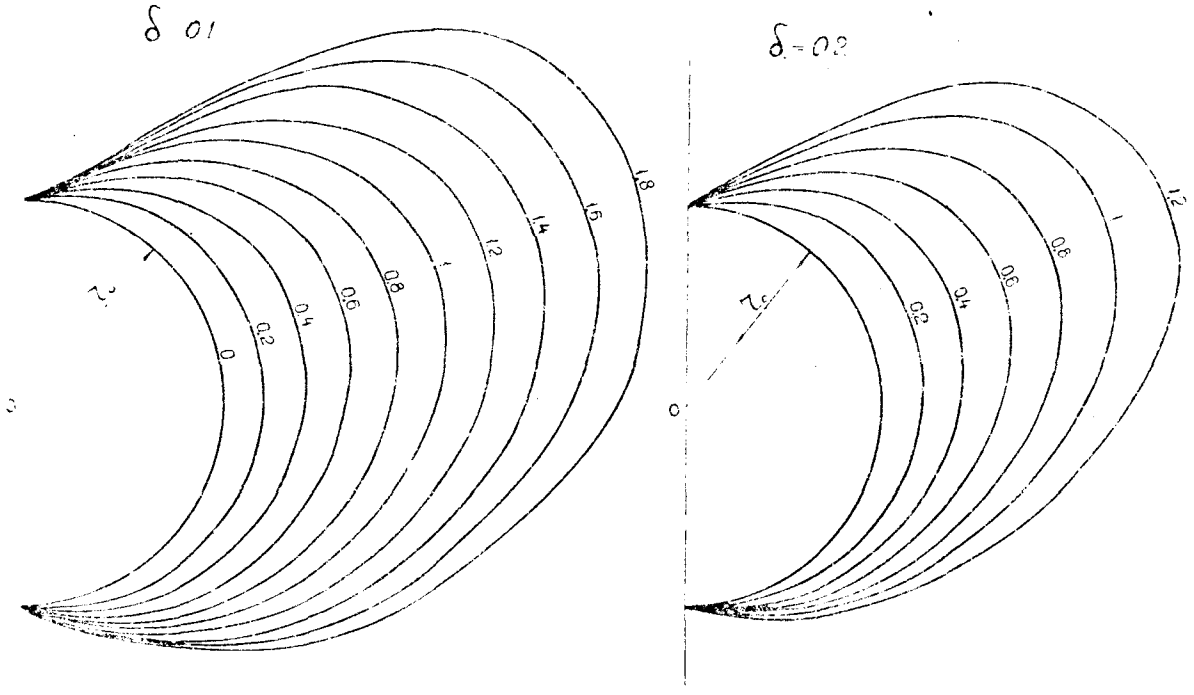
δ 01
δ=02
0
0.2
0.4
0.6
0.8
1
1.2
1.4
1.5
1.8

Fig. 10

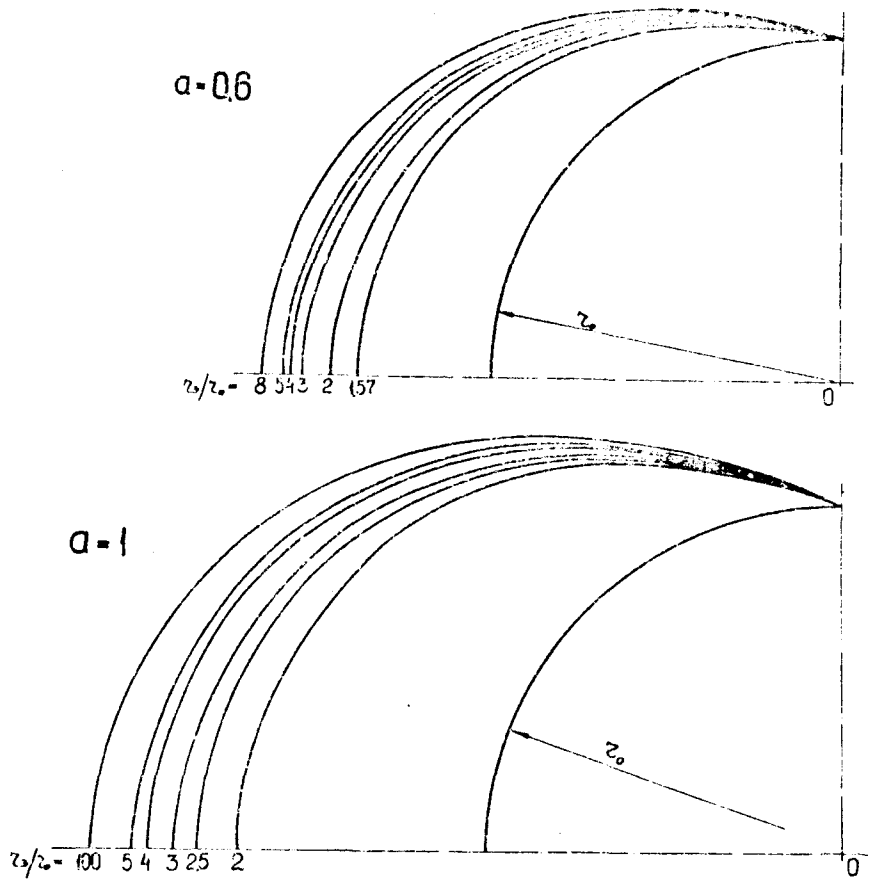

Fig. 11

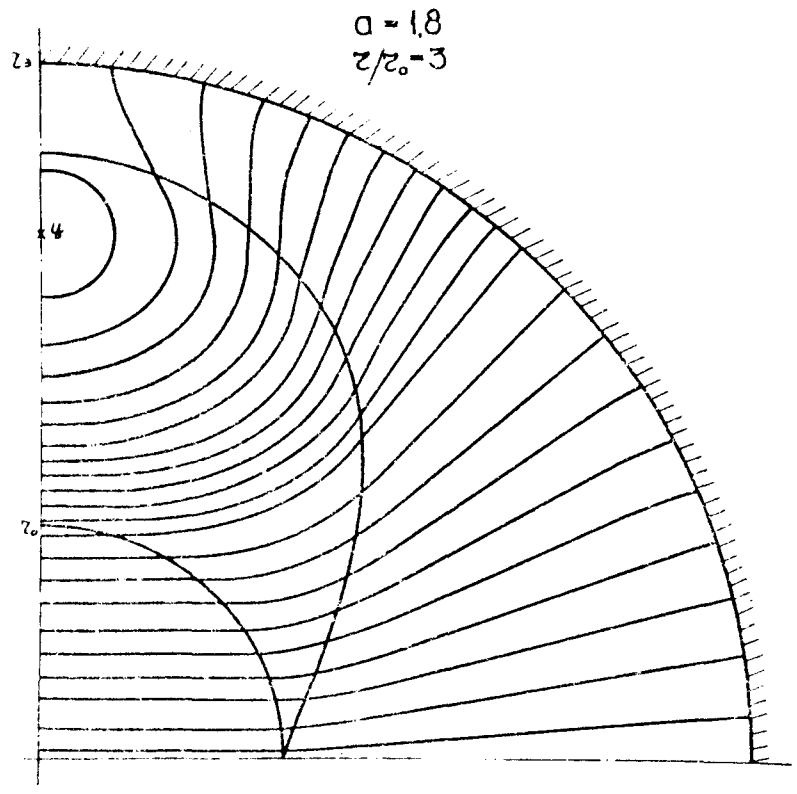

Fig. 12

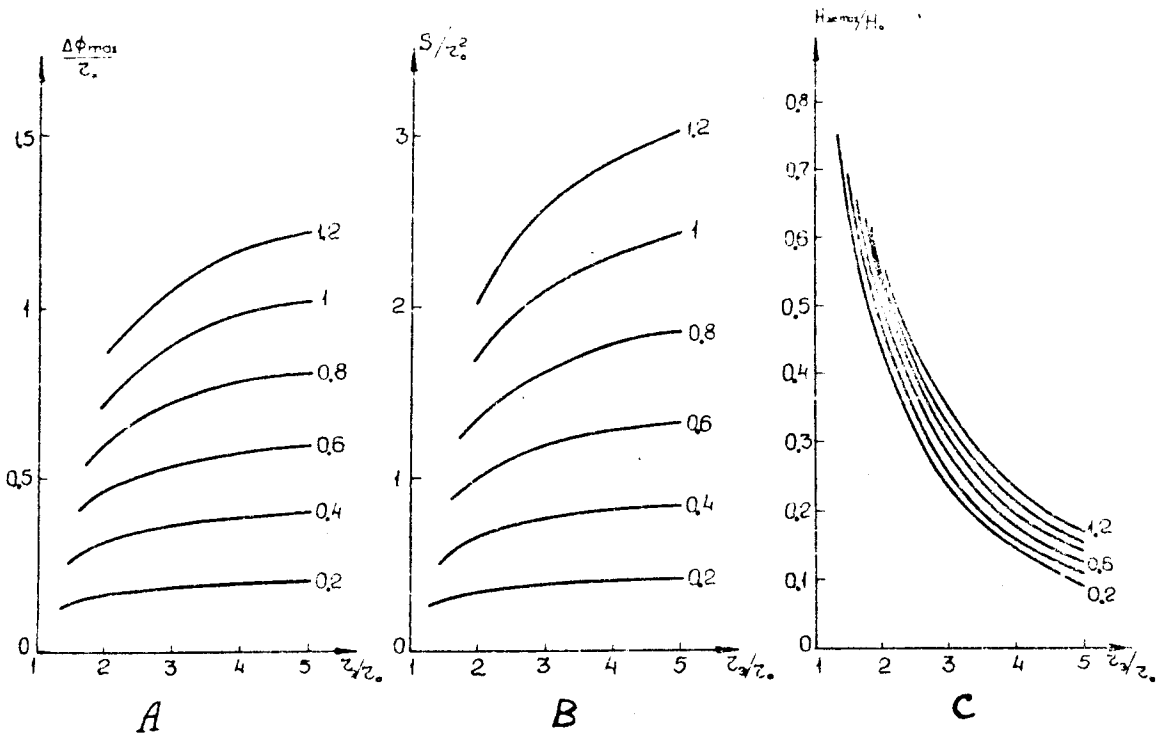

Fig. 13

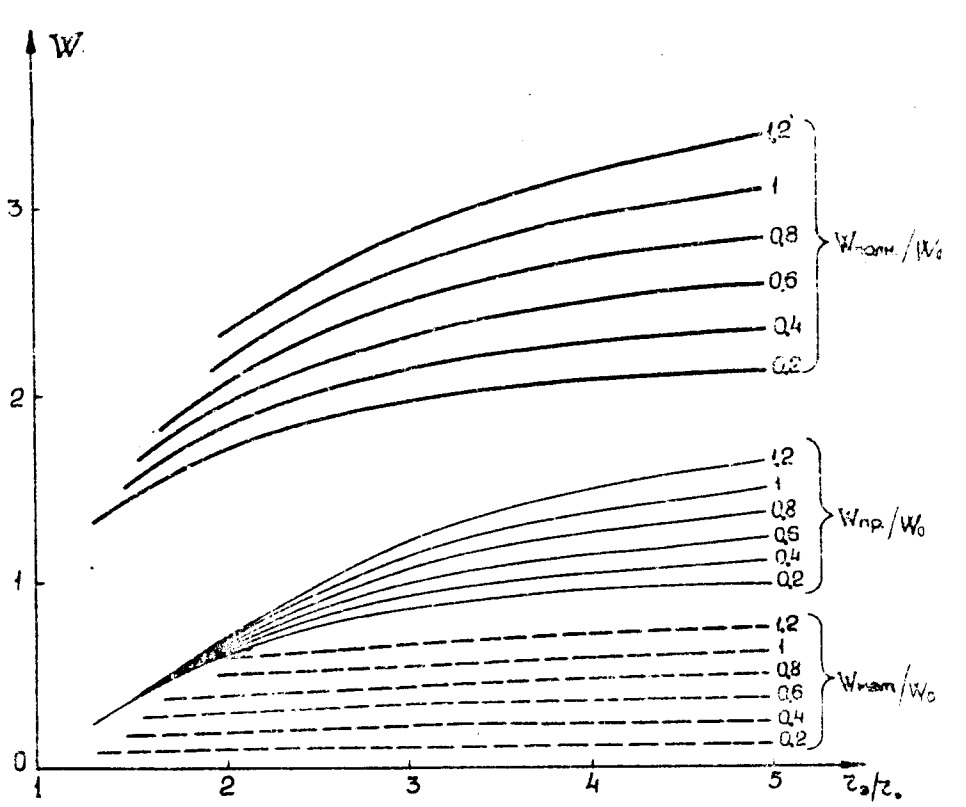

Fig. 14

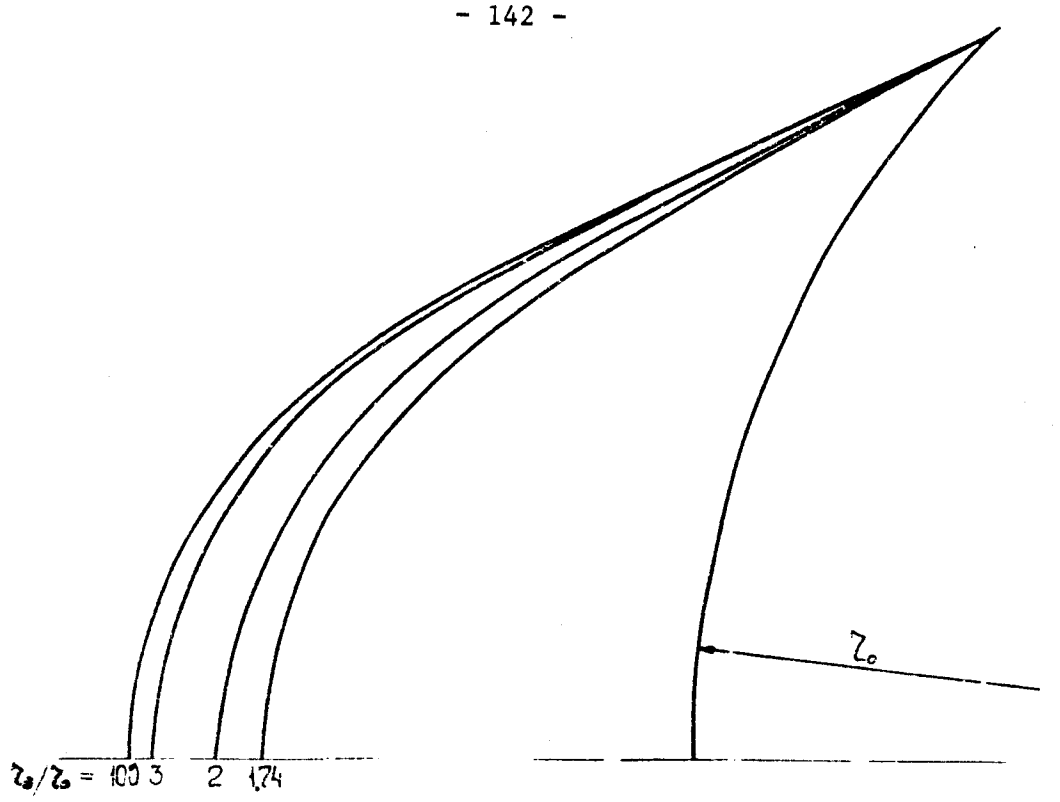
z_0
z_3/z_0 = 100 3 2 1,74

Fig. 15

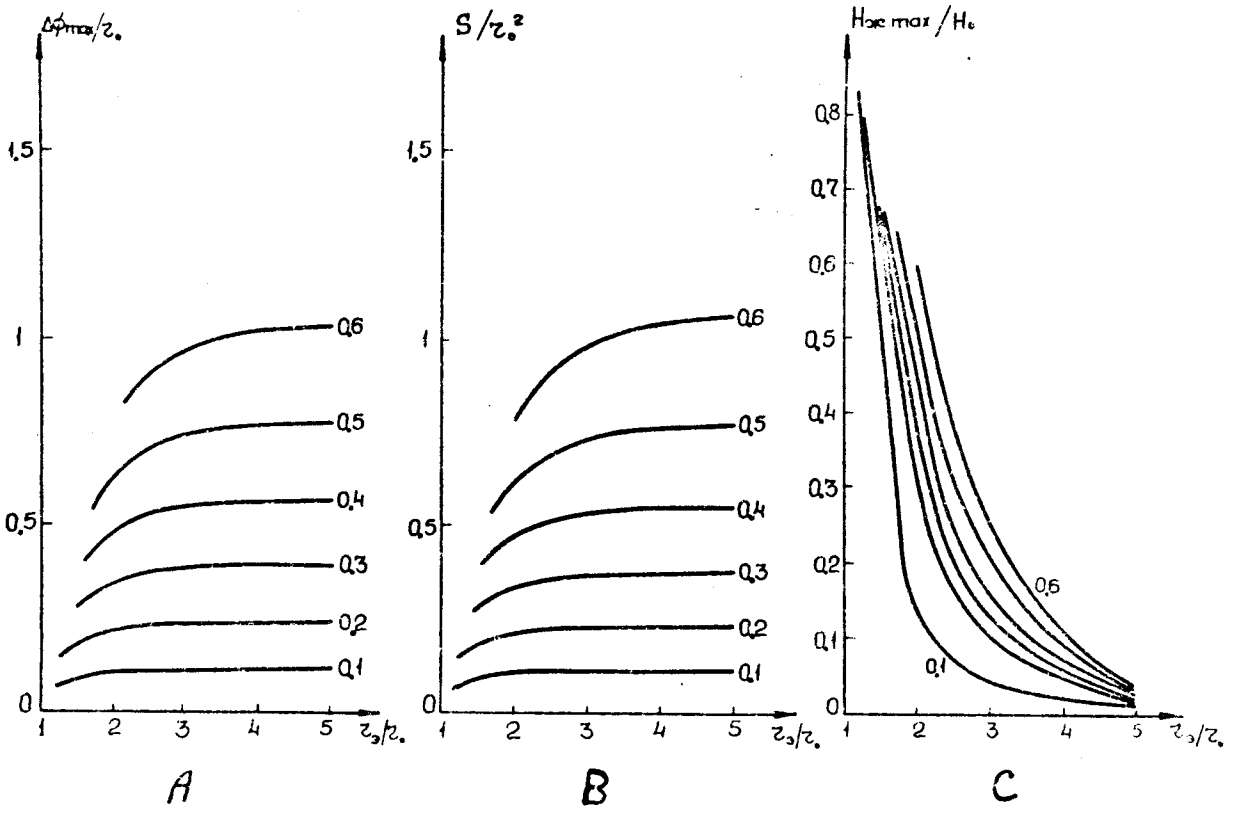
$\Delta\varphi_{max}/z_0$
S/z_0^2
$H_{oe\,max}/H_0$
1.5
1
0.5
0
0.6
0.5
0.4
0.3
0.2
0.1
0.8
0.7
0.6
0.5
0.4
0.3
0.2
0.1
1 2 3 4 5 z_3/z_0
A
B
C

Fig. 16

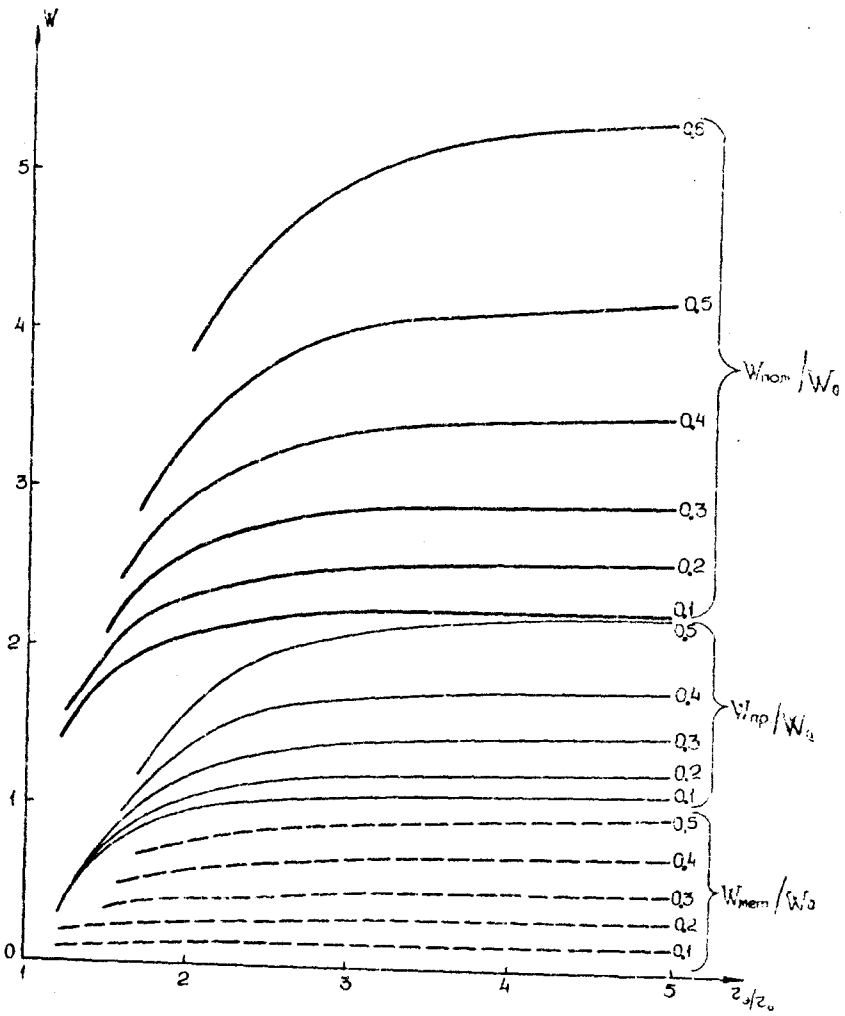
W
5
4
3
2
1
0
0,6
0,5
0,4
0,3
0,2
0,1
W_{nom}/W_0
0,5
0,4
0,3
0,2
0,1
$W_{пр}/W_0$
0,5
0,4
0,3
0,2
0,1
$W_{мем}/W_0$
1
2
3
4
5
z_1/z_0

Fig. 17

a - 06

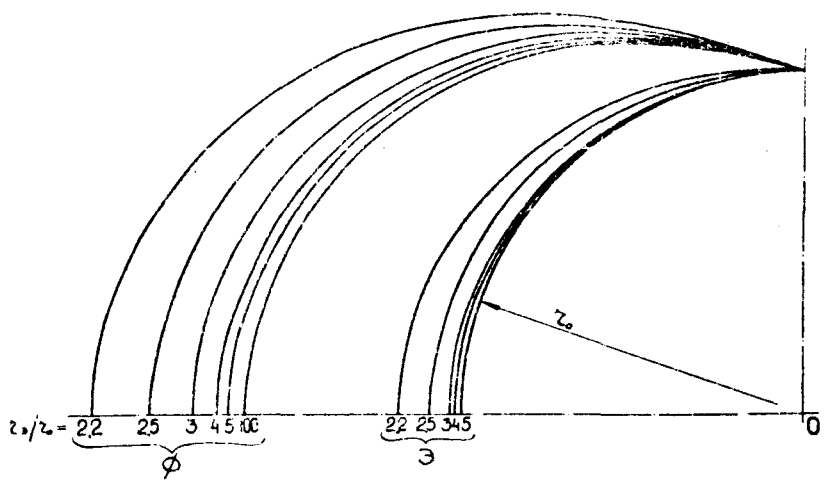

a - 1

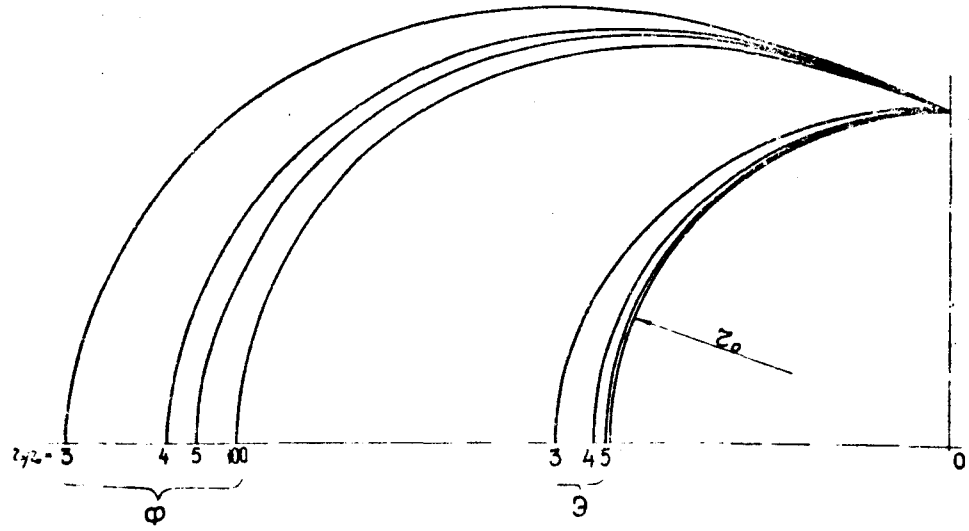

Fig. 18

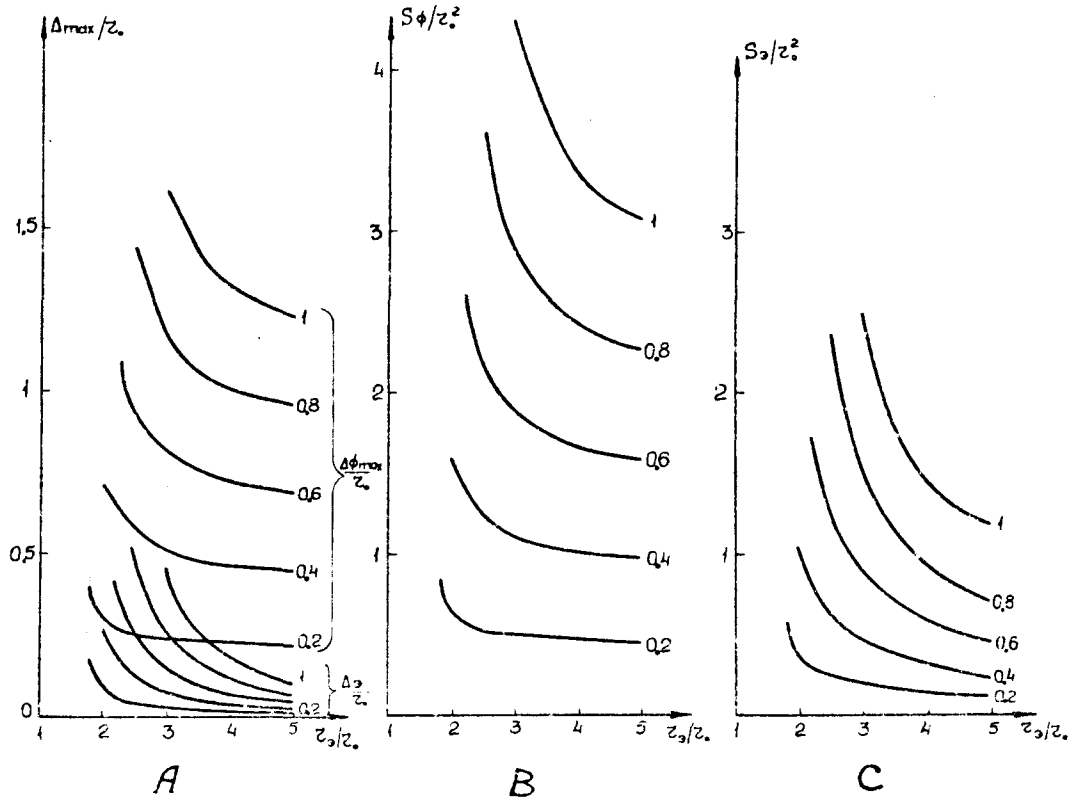
Δmax/z₀
1,5
1
0,5
0
1
0,8
0,6
0,4
0,2
Δφmax/z₀
Δэ/z₀
1
2
3
4
5
z_э/z₀
A
Sφ/z₀²
4
3
2
1
1
0,8
0,6
0,4
0,2
B
Sэ/z₀²
3
2
1
1
0,8
0,6
0,4
0,2
C

Fig. 19

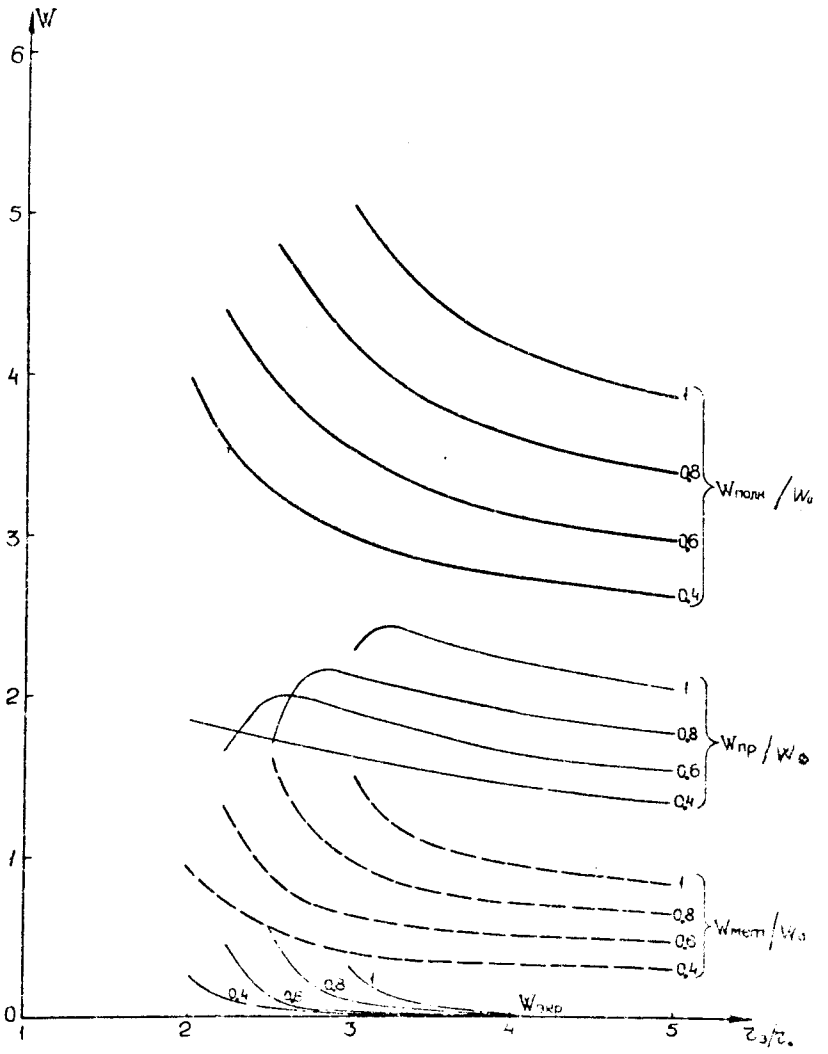

Fig. 20

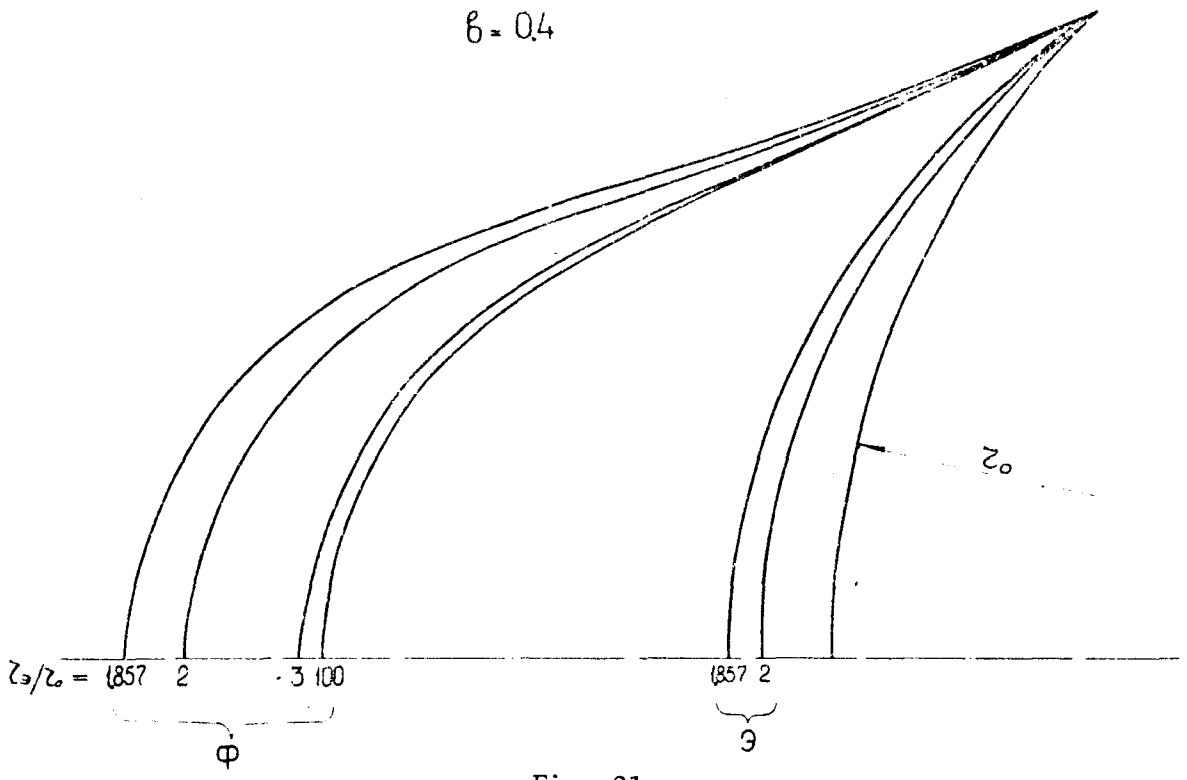
β = 0.4
z₀
z₃/z₀ = 1857 2 3 100
1857 2
Φ
Э

Fig. 21

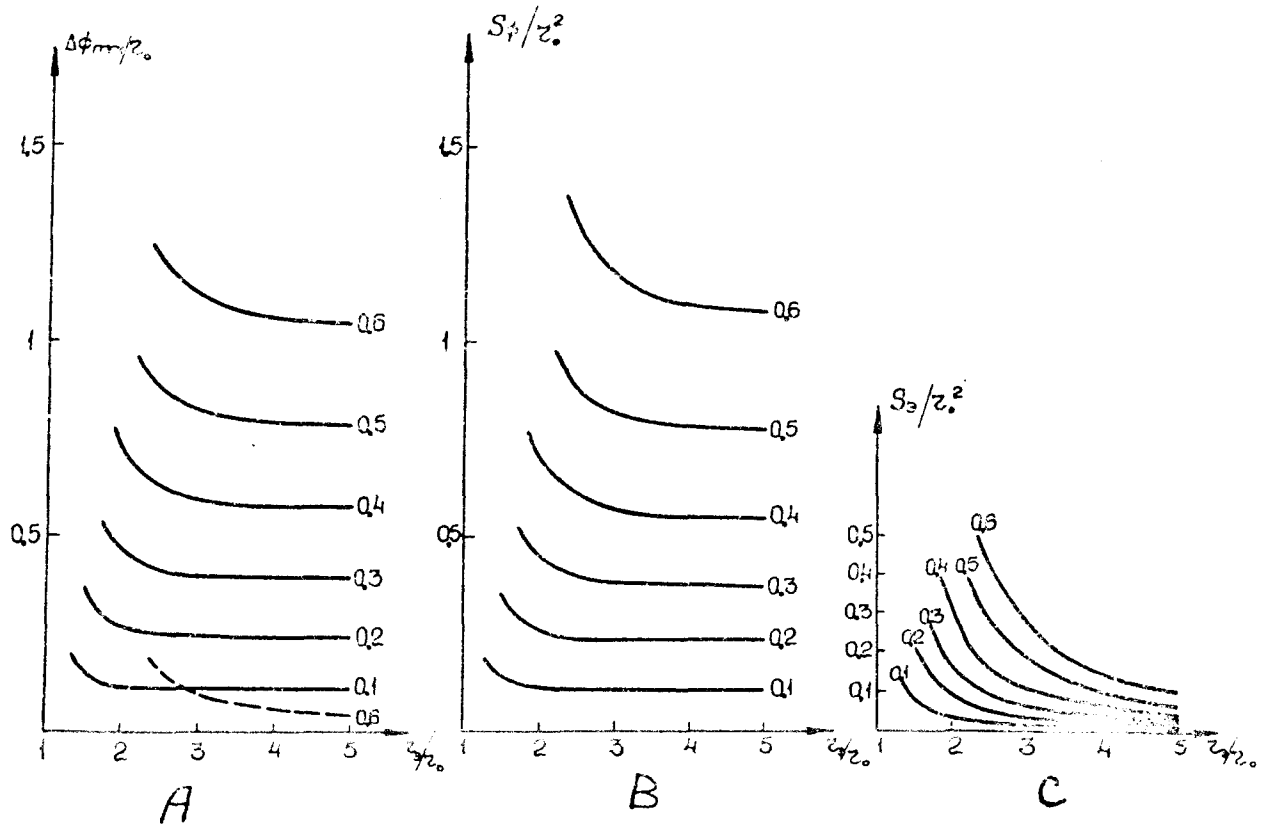
Δφmr/z₀
Sт/z₀²
Sэ/z₀²
0.6
0.5
0.4
0.3
0.2
0.1
A
B
C

Fig. 22

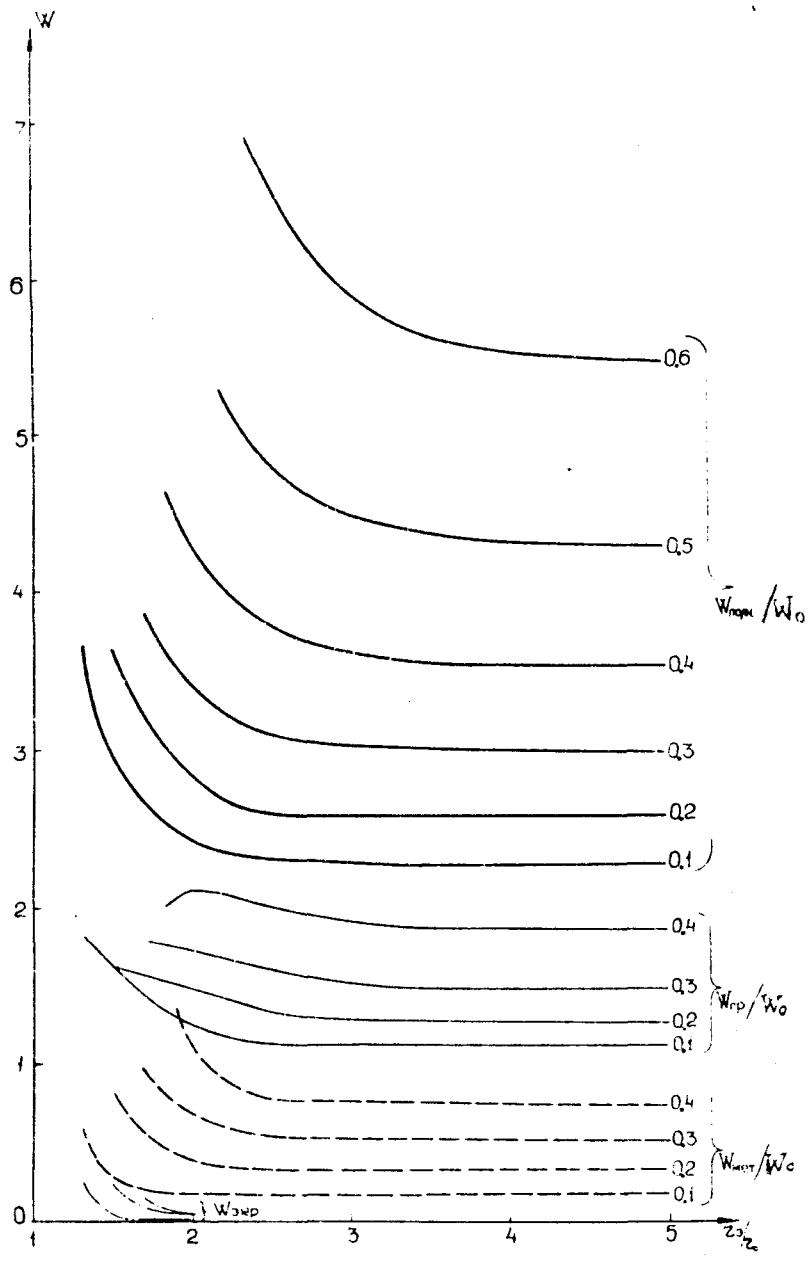

Fig. 23

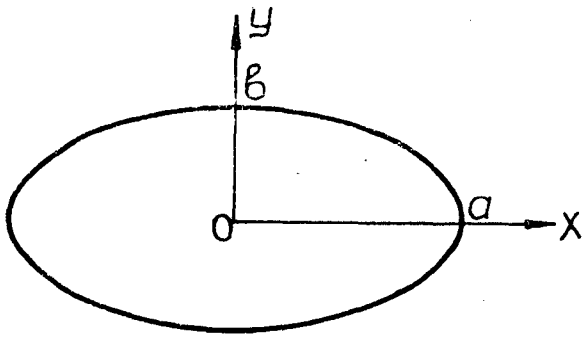

Fig. 24

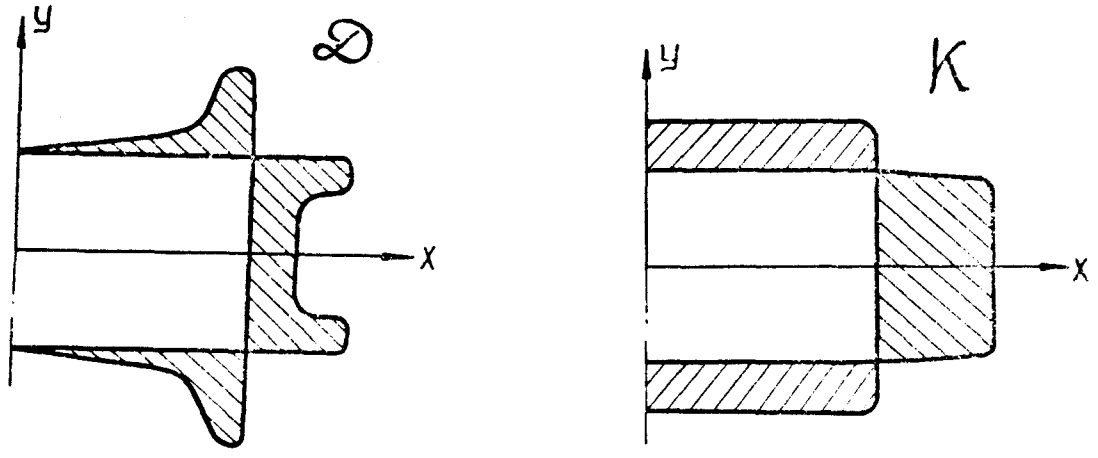

Fig. 25

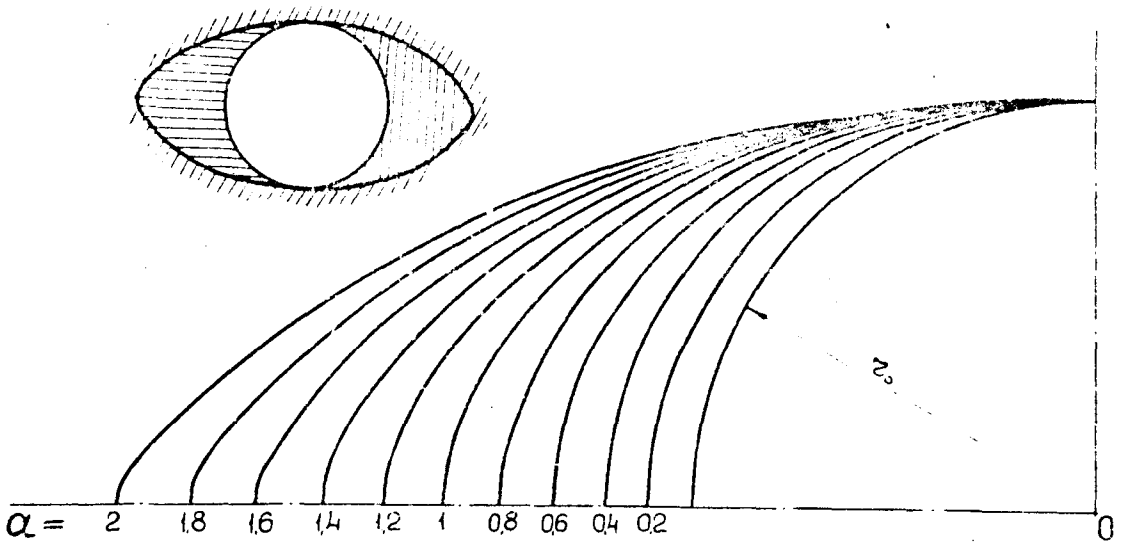

Fig. 26

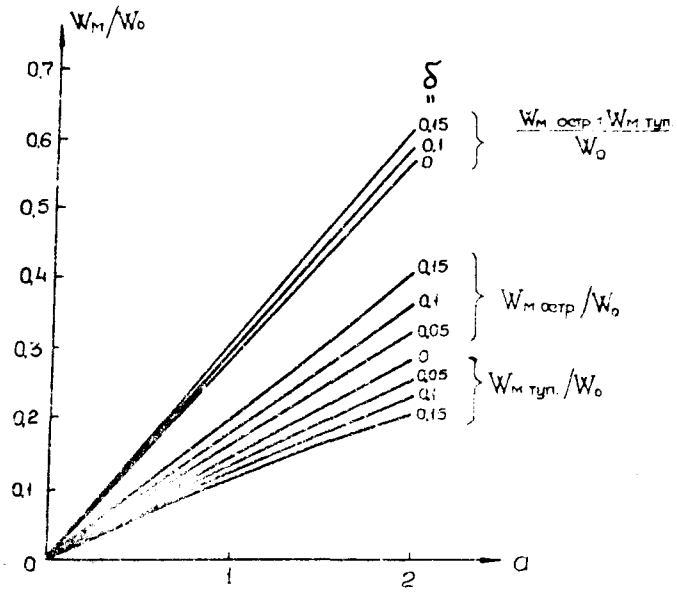
$W_м/W_0$
0,7
0,6
0,5
0,4
0,3
0,2
0,1
0
1
2
a
δ =
0,15
0,1
0
$\frac{W_{м\ остр} + W_{м\ туп}}{W_0}$
0,15
0,1
0,05
$W_{м\ остр}/W_0$
0
0,05
0,1
0,15
$W_{м\ туп.}/W_0$

Fig. 27

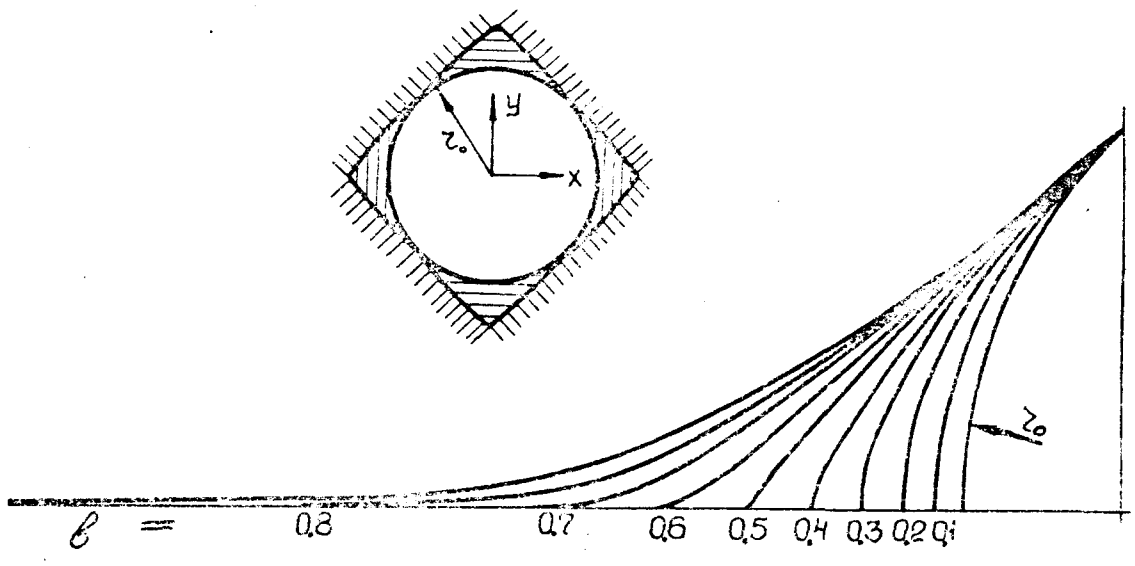
y
x
r_0
r_0
δ =
0,8
0,7
0,6
0,5
0,4
0,3
0,2
0,1

Fig. 28

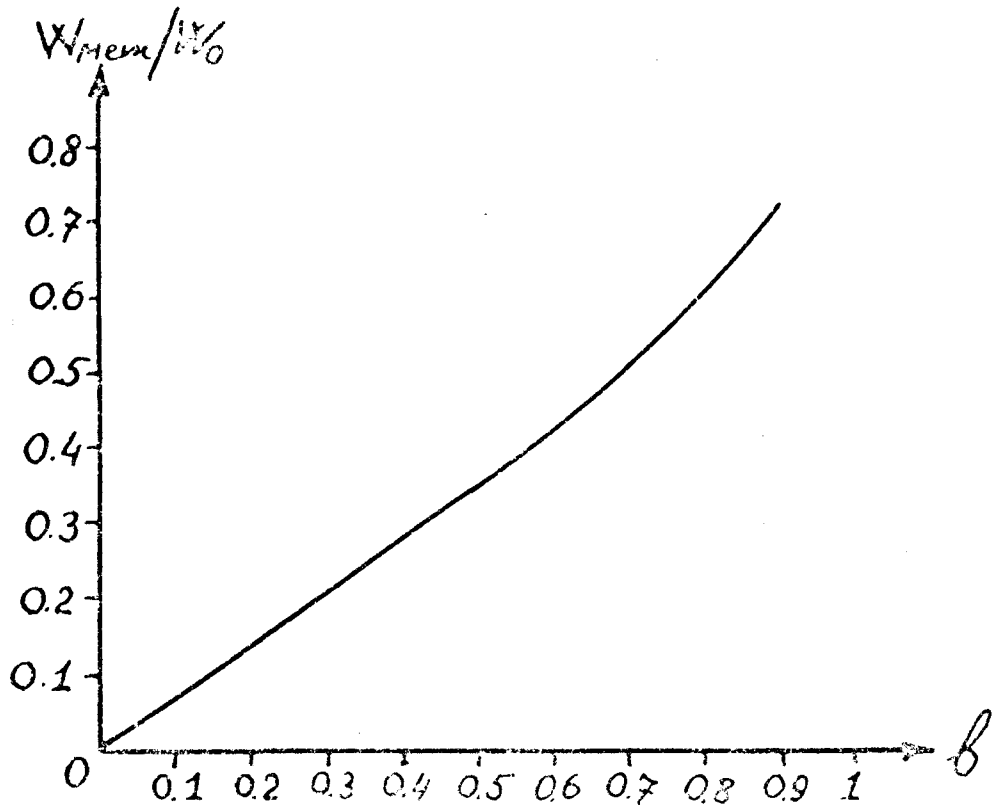

Fig. 29

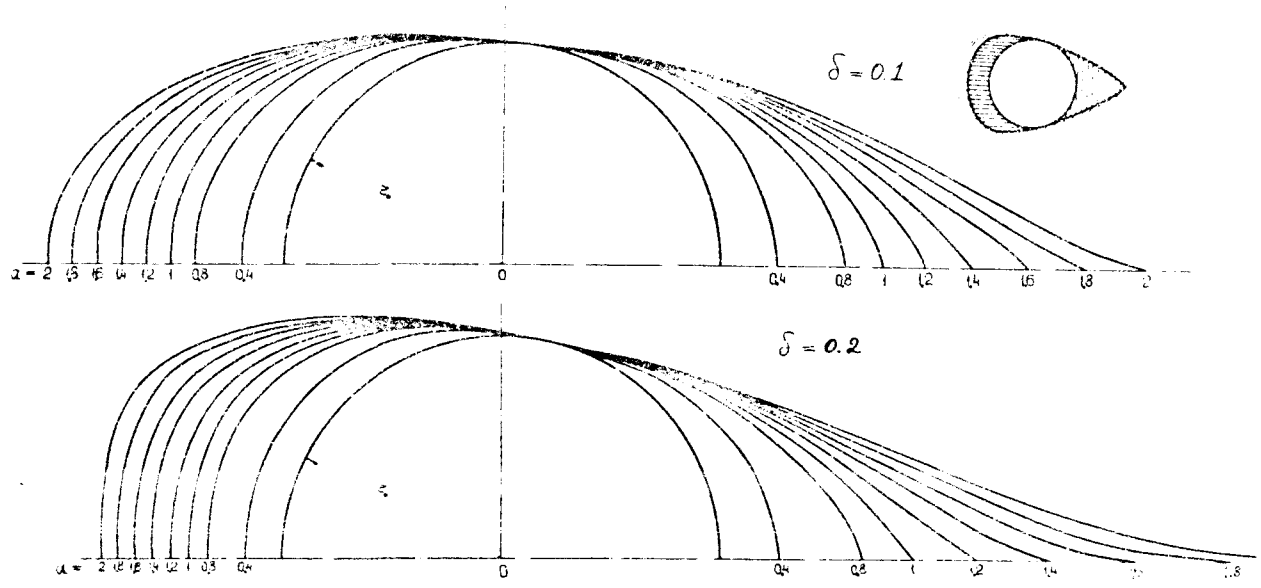

Fig. 30

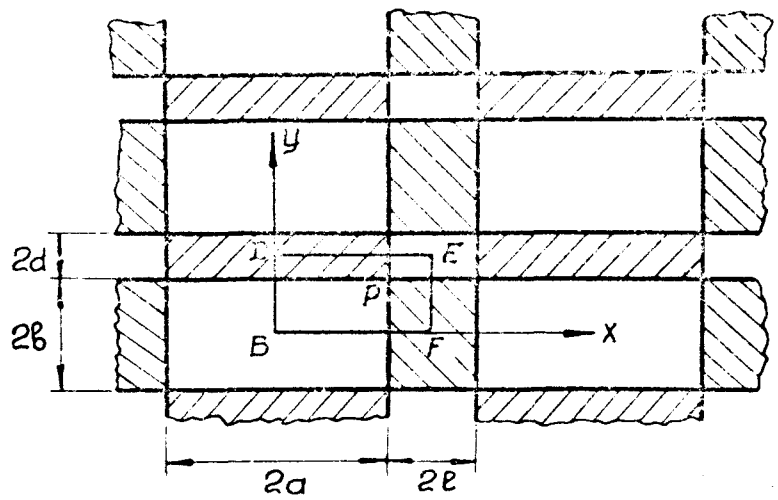

Fig. 31

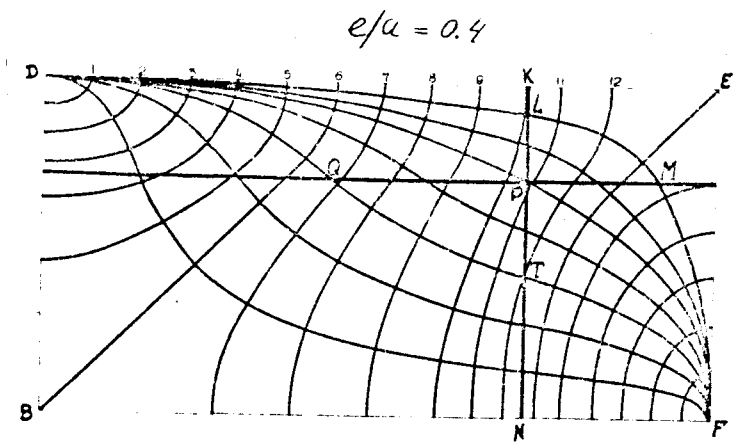

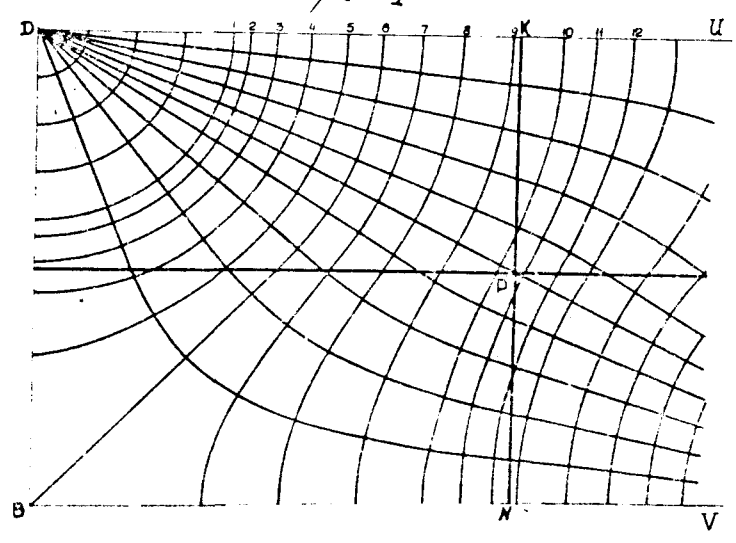

Fig. 32

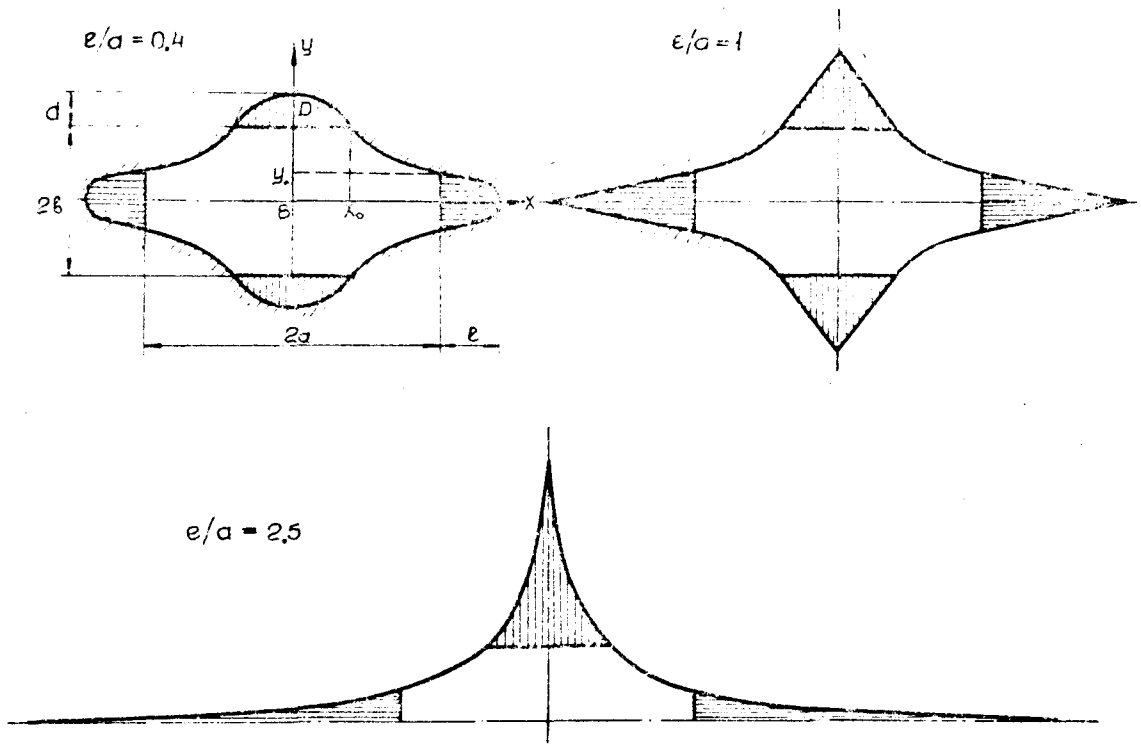
e/a = 0,4
y
d
D
y₀
2b
b
x₀
x
2a
e
ε/a = 1
e/a = 2,5

Fig. 33

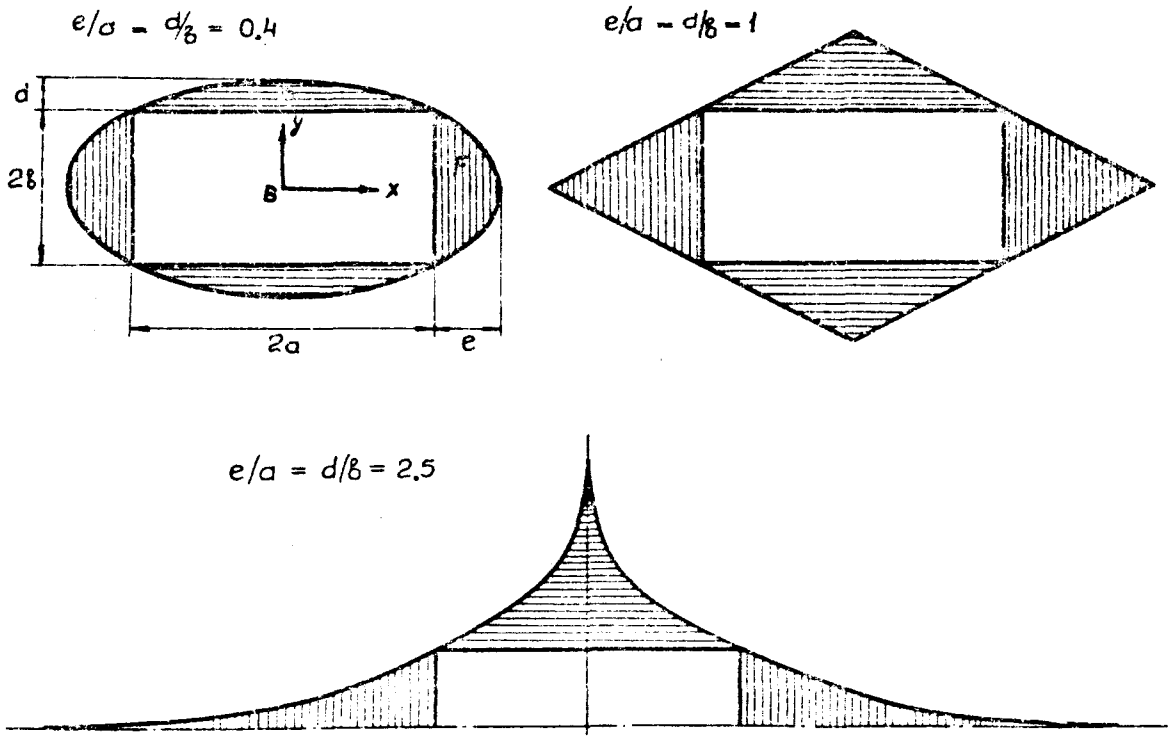
e/a = d/b = 0.4
d
2b
y
b
x
2a
e
e/a = d/b = 1
e/a = d/b = 2,5

Fig. 34

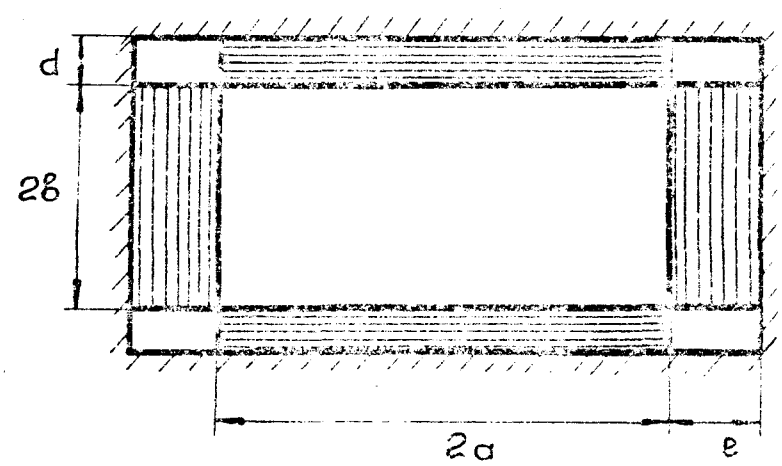

Fig. 35